IDENTIFICATION OF NOVEL SMALL MOLECULE INHIBITORS OF PROTEINS REQUIRED FOR GENOMIC MAINTENANCE AND STABILITY

Sarah C. Shuck

Submitted to the faculty of the University Graduate School
in partial fulfillment of the requirements
for the degree
Doctor of Philosophy
in the Department of Biochemistry and Molecular Biology,
Indiana University

June 2010

Accepted by the Faculty of Indiana University, in partial
fulfillment of the requirements for the degree of Doctor of Philosophy.

John J. Turchi, Ph.D., Chair

Mark R. Kelley, Ph.D.

Doctoral Committee

Thomas D. Hurley, Ph.D.

April 16, 2010

Frank A. Witzmann, Ph.D.

ACKNOWLEDGEMENTS

Foremost I would like to thank my thesis advisor Dr. John Turchi for his assistance, support and advice. He has gone above and beyond to provide me with wonderful advice, both professionally and scientifically. He has also been an amazing person to work for and with throughout my time here. I would also like to thank the other members of my committee, Dr. Mark Kelley, Dr. Tom Hurley and Dr. Frank Witzmann for their advice and help in earning my Ph.D. The members of the Turchi lab, especially Katie Pawelczak, have been a tremendous source of help, advice and friendship over the years. I would also like to specifically thank Brooke Andrews, Emily Short, John Montgomery and Victor Anciano for working closely with me on my project and really helping to keep it moving forward. I would also like to thank my family for supporting me throughout all of my higher education, it has been a very long road! My dad has given me so much wonderful advice about both work and life and his words will always stick with me. My mother has been a great friend and ear over the years. I would especially like to thank my brother and sister, Josh and Jodi, for all of their love and support throughout the years.

ABSTRACT

Sarah C. Shuck

Identification of novel small molecule inhibitors of proteins required for genomic maintenance and stability

Targeting uncontrolled cell proliferation and resistance to DNA damaging chemotherapeutics using small molecule inhibitors of proteins involved in these pathways has significant potential in cancer treatment. Several proteins involved in genomic maintenance and stability have been implicated both in the development of cancer and the response to chemotherapeutic treatment. Replication Protein A, RPA, the eukaryotic single-strand DNA binding protein, is essential for genomic maintenance and stability via roles in both DNA replication and repair. Xeroderma Pigmentosum Group A, XPA, is required for nucleotide excision repair, the main pathway cells employ to repair bulky DNA adducts. Both of these proteins have been implicated in tumor progression and chemotherapeutic response. We have identified a novel small molecule that inhibits the *in vitro* and cellular ssDNA binding activity of RPA, prevents cell cycle progression, induces cytotoxicity and increases the efficacy of chemotherapeutic DNA damaging agents. These results provide new insight into the mechanism of RPA-ssDNA interactions in chromosome maintenance and stability. We have also identified small molecules that prevent the XPA-DNA interaction, which are being investigated for cellular and tumor activity. These results demonstrate the first molecularly targeted eukaryotic DNA binding inhibitors and reveal the utility of targeting a protein-DNA interaction as a therapeutic strategy for cancer treatment.

John J. Turchi, Ph.D.

TABLE OF CONTENTS

LIST OF TABLES

LIST OF FIGURES

ABBREVIATIONS

8-oxo-G	8-oxo-Guanine
BER	Base Excision Repair
BrdU	5-Bromo-2'-deoxyuridine
CI	Combination Index
DAPI	4',6-diamidino-2-phenylindole
DBD	DNA binding domain
DNA-PK	DNA Dependent Protein Kinase
DNA-PKcs	DNA Dependent Protein Kinase Catalytic Subunit
DSB	Double-Strand Break
dsDNA	Double-Strand DNA
DMSO	Dimethylsulfoxide
DTT	Dithiothreitol
EMSAs	Electrophoretic Mobility Shift Assays
Exo	Exonuclease
FP	Fluorescence Polarization
HAP	Hydroxyapatite
HDR	Homology Directed Repair
HTS	High-Throughput Screen
IR	Ionizing Radiation
MMR	Mismatch Repair
NER	Nucleotide Excision Repair
NHEJ	Non-Homologous End Joining

NSCLC	Non-Small Cell Lung Cancer
NT	Nucleotide
OB	Oligonucleotide/Oligosaccharide Binding
PARP	Poly (ADP-ribose) Polymerase
PBMCs	Peripheral Blood Mononuclear Cells
PI	Propidium Iodide
Pol	Polymerase
Pt	Cisplatin
Q column	Quaternary Amine Column
ROS	Reactive Oxygen Species
RPA	Replication Protein A
SMIs	Small Molecule Inhibitors
SNPs	Single Nucleotide Polymorphisms
ssDNA	Single-Strand DNA
TopoI	Topoisomerase I
TopoII	Topoisomerase II
WT	Wildtype
XP	Xeroderma Pigmentosum
XPA	Xeroderma Pigmentosum Group A

1. Genomic Stability and Maintenance in Cancer

Cells rely on highly coordinated pathways and checkpoints to execute proper DNA replication and cell division (1). Dysregulation of these pathways from protein aberrations results in uncontrolled cell proliferation, which is a hallmark of the development of cancer (2). Many current chemotherapeutic agents exert their cytotoxic effect by inhibiting or counteracting the activity of mutated proteins that are no longer able to properly regulate cell growth. Cancer cells can acquire resistance to these drugs, which reduces the drug's effectiveness and presents a major hindrance regarding the treatment of cancer patients. Therefore, targeting essential regulatory proteins that are required for both normal cell proliferation and the response to chemotherapeutic treatment has the potential for widespread impact and utility for cancer therapy.

In order for cells to proliferate, they must progress through the cell cycle and efficiently replicate their DNA. Replication Protein A (RPA) is a eukaryotic single-strand DNA (ssDNA) binding protein that is involved in several DNA metabolic pathways including DNA replication (3). RPA is also essential in numerous DNA repair pathways including the nucleotide excision repair (NER) pathway, which is the main pathway cells employ to repair bulky DNA adducts (3). In addition to RPA, several other proteins are required for NER including Xeroderma Pigmentosum Group A (XPA), which has been implicated both in the development of cancer as well as in the response to chemotherapeutic treatment (4). Small molecule inhibitors of RPA and XPA have the potential for development into clinically significant treatments for a wide variety of malignancies with both single agent activity, in the case of RPA inhibition, and in combination therapy with chemotherapeutic agents that target genomic stability. The

small molecule inhibitors we have identified represent the first molecularly targeted eukaryotic DNA binding inhibitors and reveal the utility of targeting a protein-DNA interaction as a therapeutic strategy for cancer treatment.

1.1. Cancer Development

Cancer currently accounts for a quarter of all deaths in the United States and the rate of cancer deaths from 1991 to 2006 has decreased by only 16%, justifying the need for more effective cancer therapies (US Mortality Data 2006, National Center for Health Statistics, Centers for Disease Control and Prevention, 2009). Currently, lung cancer is the leading cause of cancer-related mortality, causing 30% of all cancer deaths in males and 26% in females (American Cancer Society, 2009). Standard therapy for lung cancer includes the use of chemotherapeutic agents combined with radiation therapy and surgery (5, 6). The development of lung cancer and its response to treatment is multi-factorial. Although the cellular genotype of each cancer cell is different, most cancers are believed to develop following the alteration of six essential regulatory mechanisms known as the hallmarks of cancer. These include an insensitivity to anti-growth signals, sustained angiogenesis, limitless replicative potential, tissue invasion and metastasis, evading apoptosis and self sufficiently in growth signals (2).

The dysregulation of cellular processes that contribute to the hallmarks of cancer can be attributed to changes at the molecular level. A series of acquired changes in the genomic sequence leading to improper protein expression and/or activity has the potential to lead to uncontrolled cell proliferation. Previous hypotheses have suggested a “two-hit” mechanism for tumor development in which a mutant allele is inherited from one parent and another later mutation is acquired throughout a person’s lifetime (7). These

mutations lead to altered protein expression and/or activity. Cellular pathways are in place to prevent mutations in the DNA sequence; however, DNA mutations do occur. This can lead to protein miscoding and loss of normal protein function or expression, which if the altered protein participates in the pathways identified by the six hallmarks of cancer, can lead to cancerous cell growth.

1.2. DNA Replication and Repair to Maintain Genomic Integrity

During normal cell division, cells go through four distinct stages of the cell cycle including G1, S, G2, and mitosis. These processes are tightly regulated by a number of checkpoints to ensure that each step is completed properly before the cell progresses on to the next. In order to propagate, cells must replicate their entire genome during S-phase so that during mitosis the daughter cells contain the entire unaltered genomic sequence, indicating the high fidelity that is required during DNA replication. Misincorporation of a base may or may not lead to a difference in the final protein amino acid sequence; however, if the altered base leads to a change in the amino acid, the structure, function and/or expression of the protein may be altered. If the expressed protein functions differently than the wild type protein, the overall cellular effect of the protein may become altered as well. This illustrates the importance of maintaining the genomic sequence in order to sustain normal cellular function.

When DNA is damaged or altered, the changes do not necessarily have an impact on the overall cell population. Phenotypic problems arise when DNA obtains a heritable change in the sequence, which is referred to as a mutation. These differences are then propagated on to daughter cells and eventually a large cell population exists containing the mutation. Mutations in the DNA contribute to cancer development, however,

changes are also evidenced in genetically transmitted diseases such as cystic fibrosis, phenylketonuria and Xeroderma Pigmentosum (XP) (8, 9, 9). These diseases are characterized by hereditary genetic mutations in the DNA that result in either individual protein mutations or a combination of mutations that result in strong phenotypic characteristics. These diseases are characterized by changes in protein function that result from genomic mutations. Further understanding of how DNA mutagenesis results in the development of diseases can give insight into the development and progression of cancer as well as how and why cancers respond to current chemotherapeutic treatments.

In addition to mutations in DNA that can occur as a product of faulty replication, other agents can induce damage to the DNA that can result in improper base pairing, gaps formed in the DNA, and bulky lesions that disrupt the Watson and Crick double-strand DNA (dsDNA) helix (10). One example of a chemical alteration in DNA is the formation of 8-oxoguanine (8-oxoG), which is produced as a result of a chemical reaction between guanine and a reactive oxygen species (ROS) (10). Typically, guanine (G) bases pairs with cytosines (C), however, 8-oxoG mispairs with adenine, leading to a change in the DNA sequence (10). The formation of 8-oxoG has the potential to be particularly mutagenic because cells are constantly exposed to ROS that can induce DNA damage and 8-oxoG is not always readily recognized by repair machinery (10). The mispairing between G and A has the potential to cause deleterious effects to the cell if the change in sequence leads to a mutant protein.

Mutations that are induced in somatic cells as opposed to germ cells do not necessarily lead to genetic changes that are passed onto offspring, but rather are heritable from one cell to another in the same organism. Therefore, mutations that accumulate in

somatic cells can lead to the development of diseases such as cancer and diabetes and also contribute to aging. In order to counteract the DNA damage induced by exogenous and endogenous agents, cellular regulatory systems are in place to recognize and repair DNA damage.

1.3. DNA Replication

In order to maintain the integrity of the genomic sequence, S-phase DNA replication is tightly regulated in order to ensure that replication occurs in a timely manner, but also to make certain that the genome is accurately replicated (11). For this to occur, the cell must coordinate the formation of multi-protein complexes at several origins of replication throughout the genome (12). The regulation of protein complex formation is initiated during the G1-phase of the cell cycle by the formation of the pre-replication complex (pre-RC), which assembles at origins of replication (12). The formation of pre-RCs occurs in a two-step mechanism which involves the binding of 2 helicase complexes (Mcm2-7) in opposite orientations by the activity of Cdc6 and Cdt1 in an ATP-dependent mechanism (Figure 1) (11). The loading of two Mcm2-7 complexes in opposite orientations at replication origins allows for bi-directional DNA replication that is characteristic of eukaryotic DNA replication (11). Once the initial pre-RC has been formed, the cell is licensed to proceed into S-phase, which is allowed by the inactivation of the anaphase promoting complex (APC) at the G1/S transition (Figure 1) (13, 14). Inactivation of the APC allows for the activation of kinases, including S-CDK

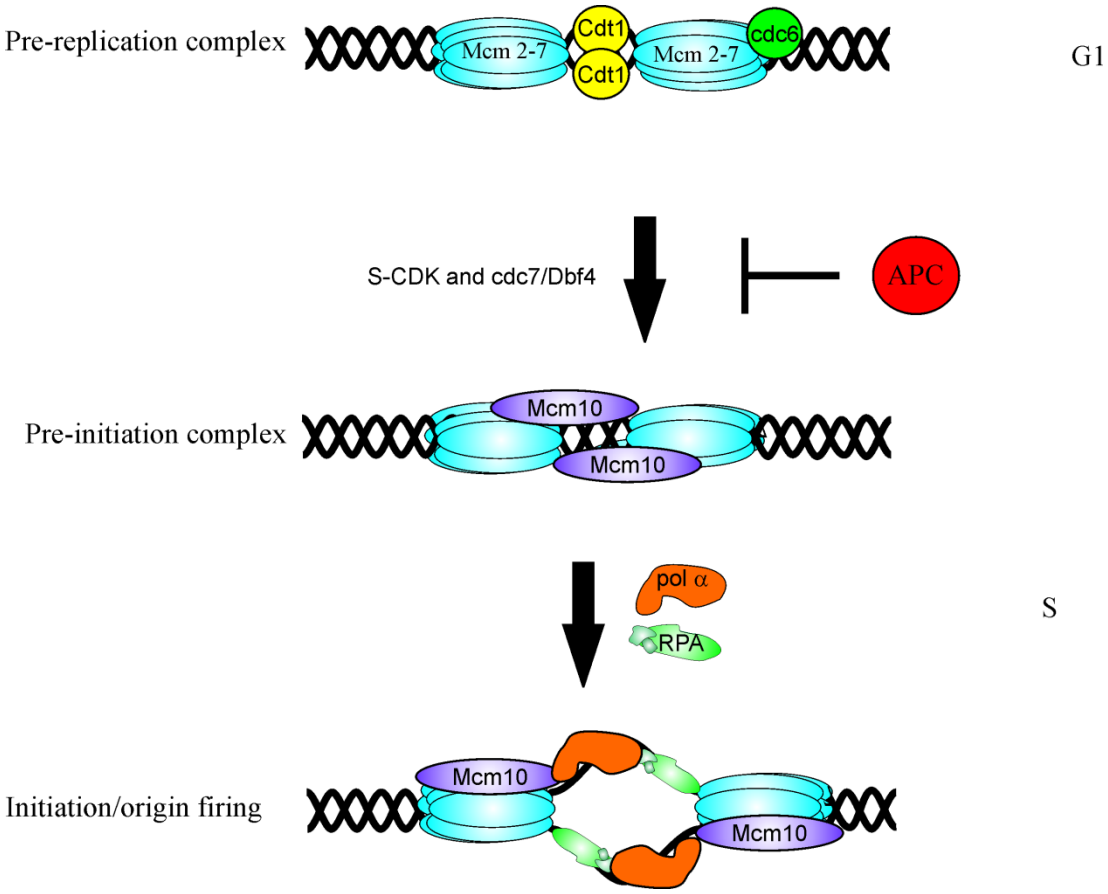

Figure 1. DNA replication. Formation of the pre-replication complex occurs during the G1 phase of the cell cycle and involves loading of two Mcm2-7 helicase complexes in opposite orientations from the origin of replication to allow for bi-directional DNA replication. This activity is coordinated by Cdt1 and cdc6. During the transition from G1 to early S, Mcm10 is recruited to the sites of replication. This occurs by inactivation of APC and activation of S-CDK and cdc7/Dbf4. Following this formation, the DNA around the origin of replication is unwound and polymerase alpha is recruited to begin replicating the DNA and RPA is recruited to bind to unannealed ssDNA to prevent reannealing. From this point, DNA replication proceeds to replicate the entire genome with the activity of other proteins not pictured including topoisomerases.

and Cdc7/Dbf4, that are important for permitting the cell to progress through the cell cycle (13). These proteins along with the activity of several others work to form the pre-initiation complex (pre-IC), which is in part responsible for ensuring that individual replication forks fire only once during S-phase (11). Cyclin-dependent kinases (CDKs) directly prevent the formation of the pre-RC, and therefore the formation of these complexes can only occur during G1, when the activity of CDKs is low (11). Mcm2-7 helicases that are bound at the origin of replication work to unwind dsDNA and lead to the formation of ssDNA, which is bound by RPA (Figure 1) (15). Upon DNA unwinding, DNA polymerase α is recruited to prime the template and to begin replicating the DNA (16). As the DNA replication machinery progresses along the length of DNA, regions downstream of the replication machinery that have not yet been replicated become positively supercoiled in relation to the DNA that has been unwound (17). In order to relieve the torsional stress induced upon the DNA, topoisomerase proteins are needed to produce breaks in the DNA backbone and then rejoin the DNA strand, allowing DNA replication to proceed (17, 18).

The overall mechanism of DNA replication has been conserved throughout all eukaryotes, however the intricacies of each pathway including the proteins involved and how they are regulated, can vary between organisms (19). The number of steps and checkpoints required to initiate DNA replication coupled with the energy the cell expends to carefully proofread the DNA indicate the inherent importance of maintaining genomic integrity. If DNA damage has been induced and is not repaired or if proteins involved in DNA replication have been dysregulated, the cell does not proceed further until the damage has been repaired or the proteins are correctly regulated (20). This response

involves the coordination and overlap between several different pathways in order to ultimately result with either accurate repair of DNA or the induction of apoptosis (20).

RPA is required for preventing the reannealing of dsDNA unwound by helicases following initiation of replication and it has also been shown to interact with and modulate the activity of several proteins involved in DNA metabolism including DNA polymerase α (21). RPA is important for both the initiation of replication when the Mcm2-7 helicases unwind dsDNA, as well as during elongation, when dsDNA is being unwound ahead of the replication fork. The role of RPA is thought to not only be in preventing DNA strand reannealing, but also to regulate proteins involved in DNA metabolism.

1.4. DNA Repair Pathways

In addition to the role of proteins involved in DNA replication for maintaining genomic integrity, several pathways within the cell regulate the removal and repair of induced DNA damage. While some signaling crosstalk occurs between these pathways, the mechanism of damage recognition distinguishes the pathways from each other and allows for the removal of almost every type of DNA lesion. The coordination of multiple proteins within each pathway allows for efficient repair of DNA to reduce the number of potential mutations and to prevent the development of disease.

1.4.1. Base Excision Repair

Base excision repair (BER) is the main pathway cells use to repair non-bulky DNA base damage induced by endogenous and exogenous sources. It is activated in response to damaged base residues and nucleotides as well as in response to abasic sites (22, 23). The main source of endogenous chemical changes in the DNA result from

reactive oxygen and nitrogen species that are produced from normal cellular metabolism, however BER also repairs damage from environmental/therapeutic alkylating agents, such as temozolomide (TMZ) and methylating agents including methyl methanesulfonate (MMS) (10, 23).

BER is an important pathway for repairing DNA damage that is constantly being induced, for example 8-oxo-G, and ensuring that the genomic sequence remains unaltered (24). The recognition of nonbulky DNA damage by the BER pathway is initiated by damage-specific DNA glycosylases that create abasic or apurinic/apyrimidinic (AP) sites, which can then be recognized by AP endonuclease 1 (APE 1) (22). APE 1 cleaves the phosphodiester backbone leaving a free 3′-hydroxyl group and a 5′-deoxyribose phosphate surrounding the nucleotide gap (22). Following this step, two subpathways, long patch BER and short patch BER, are available to further process the DNA resulting in polymerase addition of the correct base and ligation of the DNA strand (24). Although there are two distinct sub-pathways of BER, there is overlap between the two with both involving Poly (ADP-ribose) polymerase (PARP), which acts enzymatically to poly(ADP-ribos)ylate other proteins and to autoribosylate, which results in its release from DNA, allowing DNA repair to continue (23). PARP is currently being targeted for inhibition using chemical agents, the majority of which compete with NAD^+ to bind to the active site of PARP (22, 25). PARP -/- mouse fibroblasts have been shown to have increased sensitivity to methylating agents such as MMS, indicating the potential for combination therapy with alkylating/methylating agents in conjunction with inhibitors of the BER pathway (23).

1.4.2. Mismatch Repair

Chemical modification of bases is one manner in which DNA damage is induced, however, mispairing of bases during DNA replication can also compromise genomic integrity. DNA polymerases ensure correct base insertion during DNA replication by employing mechanisms including base discrimination during initial substrate binding and 3'-5'exonuclease (exo) proofreading activity, however these mechanisms are not infallible and mistakes can be made (26). Mismatch repair (MMR) is the pathway used to repair incorrect base insertions during DNA replication to prevent errors from becoming permanent in dividing cells (27). Proteins involved in both *E. coli* and human MMR have been described, however a complete description of all of the proteins involved and their function has not been thoroughly described for humans (27). Functional homology between proteins found in *E. coli* and humans has been described, allowing for identification of factors likely missing from human MMR (27). *E. coli* MutS (human hMutSα (MSH2-MSH6) and hMutSβ (MSH2-MSH3)) is a homodimer that is referred to as the "mismatch recognition" protein and is responsible for recognizing base-base mismatches and small insertion and deletion mispairs. MutS contains intrinsic ATPase activity that is required for MMR (27). MutL (human MutLα (MLH1-PMS2), hMutLβ (MLH1-PMS2) and hMutLγ (MLH1-MLH3)) functions as a homodimer with intrinsic ATPase activity that physically interacts with MutS to enhance recognition (27). MutL has been shown to interact with several proteins involved in MMR as well as DNA replication, including MutS and DNA polymerase III, respectively, indicating a role for MutL as a factor to increase functional MMR complex assembly and suggesting a mode of linking MMR to DNA replication (27). Hemi-methylated DNA serves as a marker for

discriminating between parental and daughter DNA strands in *E. coli* in which the daughter strand is unmethylated and the parental strand contains methylation at the N6 position of adenine (27). This differential methylation serves as the signal for *E. coli* MutH, which does not have a known human homolog, to recognize the parental DNA strand, which presumably contains the correct DNA sequence (27).

The combined activities of proteins involved in MMR with the actions of additional helicases and polymerase III result in removal of the base-base mismatch and resynthesis of the correct DNA sequence from the parental template (27). Using *in vitro* reconstitution experiments, RPA has been shown to have a role in human MMR and has been suggested to bind and protect ssDNA during this repair pathway (28). The importance of this pathway in maintaining genomic stability is evidenced by hereditary nonpolyposis colon cancer (HNPCC) in which patients have mutations in the gene encoding the human homologs of MutS and MutL (29). hMSH2 is within the chromosome locus to which HNPCC genetic defects have been mapped and was the first mismatch repair protein to be identified to be linked to HNPCC (30, 31). Since that time, additional mutations in proteins in the MMR pathway including hMLH1 and PMS2, have been identified and correlated with HNPCC (32). Mutations in these proteins lead to deficient MMR, resulting in microsatellite instability and incorrect insertion of bases (27). Microsatellite instability is characterized by nucleotide insertions and deletions that result in miscoded proteins that can lead to neoplastic growth (33). Regions of genomic instability typically occur at particular sites known as “hotspots” and microsatellite polymorphisms are used as a both a prognostic and diagnostic tool in disease states (27, 33).

MMR-deficient cells have been shown to be resistant to certain chemotherapeutic treatments such as TMZ and cisplatin, which presents opportunities for using MMR status both as a predictive marker for cancer development and as a means of predicting tumor response to chemotherapy (27). Another interesting aspect of MMR in response to chemotherapy is that many cancers acquire mutations in MMR genes following treatment, causing cytotoxicity in non-cancerous, rapidly dividing MMR-proficient cells (27). In addition, cancer cells that are MMR-proficient may be killed by chemotherapy, however, the treatment may induce mutations in MMR genes in other cells, leading to the development of secondary cancers (27). These characteristics of MMR-proficient and deficient cells have important implications in cancer therapy both in the treatment and screening of cancer patients, and more needs to be elucidated about the human MMR pathway to allow it to be further exploited for therapeutic benefit (27).

1.4.3. Nucleotide Excision Repair

As evidenced in the case of MMR, cellular ability to repair DNA damage is required to maintain genomic integrity. The nucleotide excision repair (NER) pathway removes bulky DNA adducts caused by exogenous and endogenous sources including UV irradiation and chemical mutagens (4). The repair of bulky DNA damage is initiated by a damage recognition step and assembly of a pre-incision complex, followed by excision of the damaged strand and gap-filling DNA synthesis (4). There are two subpathways of NER, global genomic repair (GG-NER), which recognizes DNA damage by proteins in the NER pathway and repairs DNA damage found throughout the genome, and transcription-coupled repair (TC-NER), which is activated by stalling of RNA polymerase II to repair damage on actively transcribed genes (4). Once initial

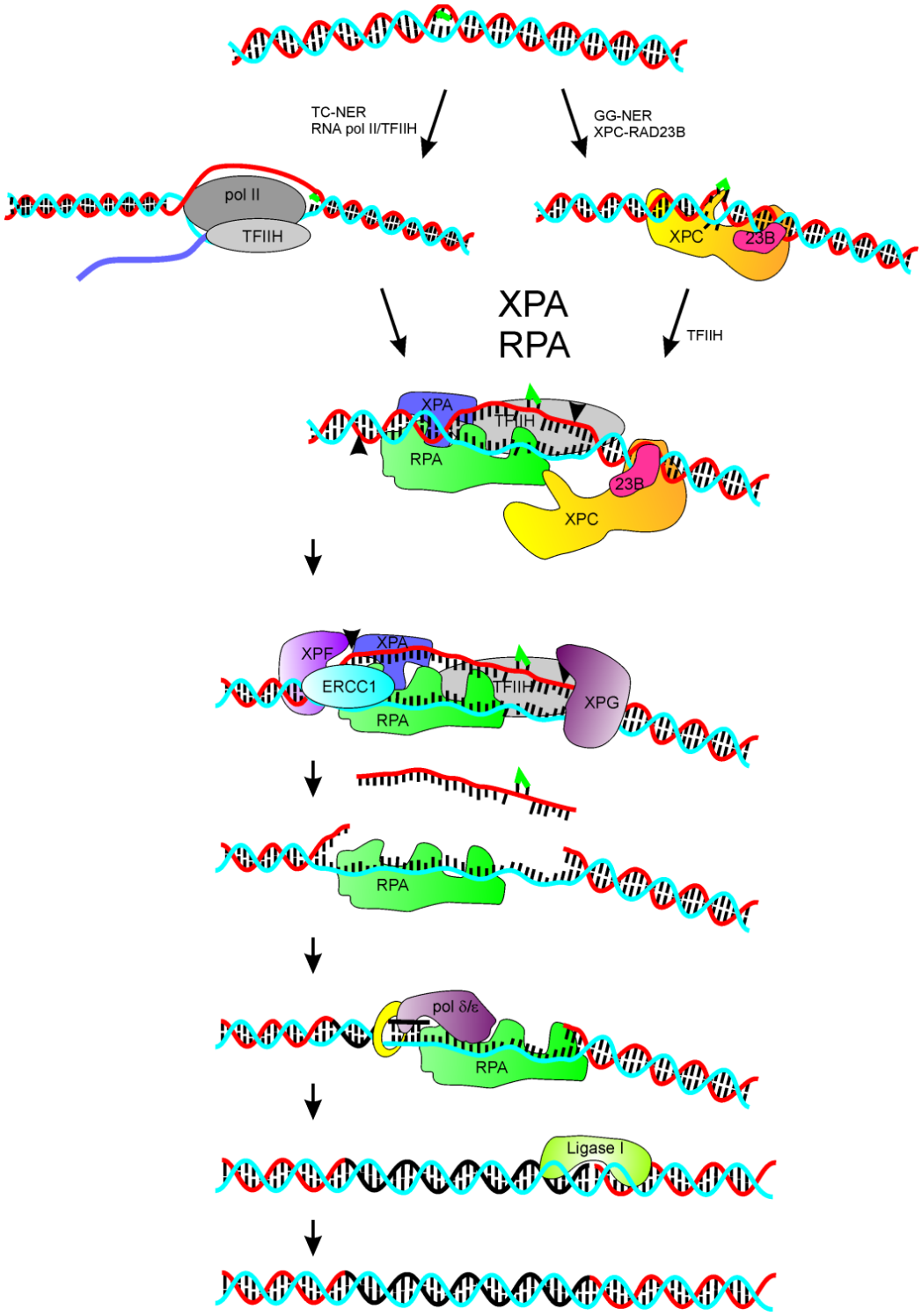
TC-NER
RNA pol II/TFIIH
GG-NER
XPC-RAD23B
pol II
TFIIH
XPC
23B
XPA
RPA
TFIIH
XPA
TFIIH
RPA
23B
XPC
XPF
XPA
ERCC1
TFIIH
XPG
RPA
RPA
pol δ/ε
RPA
Ligase I

Figure 2. Eukaryotic Nucleotide Excision Repair. Nuleotide excision repair is iniated by either pauing of RNA pol II during transcription (TC-NER) or by recognition of damage by XPC/RAD23B (GG-NER). From this point the pathways converge and additional proteins including RPA, XPA and TFIIH are recruited to the site of damage. As these proteins are recruited, XPC/RAD23B becomes dissociated from the DNA (in GG-NER) and the endonucleases XPF and XPF are recruited to make 5′ and 3′ incisions around the site of damage as indicated by the black arrows. Following incision, the damaged piece of DNA is removed and RPA remains bound to the single-strand region of DNA. Polymerase δ or ε are recruited to the DNA along with PCNA and the excised region of DNA is filled in. Ligase I is then recruited to seal the nick in the DNA resulting in repaired, double-strand DNA.

Table 1. NER factors

Factor	subunits/associations	Activity	PTM
XPA	p36	damage verification	phosphorylation
XPB	TFIIH	helicase	
XPC	RAD23B	damage recognition	ubiquitylation
	centrin-2		sumoylation
XPD	TFIIH	helicase	
XPE	DDB1, DDB2	damage recognition E3-ligase	ubiquitylation
XPF	ERCC1	incision	
XPG		incision	
RPA	p70/p34/p14	damage recognition resynthesis	phosphorylation
Pol epsilon/DNA ligase I		Gap-filling/ligation	
Pol delta/ XRCC1-DNA ligase IIIα		Gap-filling/ligation	

recognition has occurred, the pathways converge for the excision and gap filling steps (Figure 2).

The six core factors involved in the damage recognition and dual incision steps of GG-NER are the XPC-RAD23B complex, transcription factor IIH (TFIIH), XPA, RPA, XPG, and XPF-ERCC1 (Table 1) (34). Following damage recognition, the 9 subunit transcription factor IIH (TFIIH) complex is recruited to the site of damage. TFIIH has helicase activity (via XPB and XPD) that unwinds DNA around the site of damage to allow further processing, but it also interactions with other proteins in the pathway, including XPA. After TFIIH is recruited and the pre-incision complex with XPA and RPA has formed, XPG and XPF-ERCC1 are recruited to the site of damage to make the 3′ and 5′ incisions, respectively, around the lesion to form an excision product of 27-29 nucleotides (35). Upon excision of the damaged DNA, DNA polymerase ε or δ, PCNA and RFC are used to fill in the gap and DNA ligase is used to seal the nick (Figure 2).

Xeroderma Pigmentosum, XP, is an autosomal recessive disease with 7 complementation groups and a single variant that is categorized by extreme sensitivity to sunlight and a predisposition to cancer, predominantly skin cancer (9). The clinical manifestations of this disease result from decreased DNA repair capacity resulting from mutations in proteins required in the NER pathway. In 1968, a direct link was found between DNA repair and carcinogenesis following the observation that cells derived from XP patients were unable to repair ultraviolet (UV) induced DNA damage, leading to a predisposition to cancer (36). The analysis of XP allowed the delineation of the NER pathway with each complementation group, XPA through XPG, corresponding to an essential protein in the pathway (Table 1). Over the past decade, there have been major

advancements in the understanding of XP and its relationship to DNA repair, further clarifying numerous aspects of the NER pathway. This work has allowed for further understanding of how variations in NER proteins, including expression level, mutations and single nucleotide polymorphisms (SNPs), can increase an individual's susceptibility to cancer as well as predict the response to chemotherapeutic treatments.

Proteins important for NER have been implicated in the development of cancer, such as in the case of XP, but they have also been linked to chemotherapeutic response. Testicular cancer presents a 90% cure rate with combination cisplatin treatment (37). The dramatic response of testicular cancer to cisplatin has been thought to be correlated to cellular DNA repair capacity. Previous work has shown a correlation between NER protein levels (XPA, ERCC1, and XPF) and the ability of cells to repair cisplatin lesions, for example, testis tumor cell lines have decreased levels of NER proteins and decreased cisplatin repair capacity (38, 39). A decrease in cisplatin repair can lead to persistent DNA lesions which, if left unrepaired, can increase cytotoxicity, the mechanism thought to contribute to the sensitivity of testicular cancer to cisplatin treatment. This presents the possibility of inhibiting DNA repair capacity to increase cellular sensitivity to DNA damaging agents that are repaired by the NER pathway. Small molecule inhibitors of proteins required for NER, including XPA and RPA, would be predicted to increase cellular sensitivity to cisplatin, in much the same way that decreased levels of these proteins result in increased cellular sensitivity to cisplatin treatment.

1.4.4. Double-Strand DNA Break Repair

Double-strand DNA breaks (DSBs) occur when endogenous and/or exogenous agents induce a break in the DNA backbone (40). The breaks induced in the phosphodiester backbone of the DNA can result from ROS produced from either cellular metabolism or from ionizing radiation (IR) (41). Following a dsDNA break, chromosomes become unstable and fragments can move and insert themselves indiscriminately or can be separated unequally between progeny cells (40). These types of lesions can be repaired, however if cellular mechanisms do not accurately respond to these lesions, deletion or insertion of chromosome fragments can activate oncogenes and/or inactivate tumor suppressors, leading to carcinogenesis (40). Several mechanisms are in place to lead to repair of DNA strand breaks that are activated by cell cycle checkpoints that arrest cell cycle progression in order to allow repair of the DSB (40).

Two distinctive pathways have been identified in mammalian cells that are responsible for repairing DSBs, homology directed repair (HDR) and non-homologous end joining (NHEJ) (40). NHEJ is also the cellular mechanism for introducing diversity into immune cells during V(D)J recombination (40). HDR and NHEJ vary in the proteins involved and in the accuracy of repair. HDR is very accurate because a sister chromatid serves as the template for repair of the parental strand while NHEJ involves the joining of non-compatible ends, which can lead to mutations in the DNA sequence in addition to loss of DNA sequence and genomic instability (40). How each pathway is activated in the cell is unknown, however, the requirement of HDR for a sister chromatid indicates a cell cycle component in the regulation of these pathways in which HDR is the primary pathway used during S and G2 (40).

Repair of DSBs by NHEJ requires several steps to result in reformation of an intact DNA strand. Like most DNA repair pathways, proteins required for NHEJ bind and recognize the DSB and lead to the recruitment of other proteins that coordinate their activities to result in a repaired piece of DNA (40). The first proteins to bind are those that make up the DNA-PK (DNA-dependent protein kinase) heterotrimer, including the Ku70/80 heterodimer and DNA-PKcs (catalytic subunit) (40). Following this step, DNA ends are processed by nucleases and polymerases including Artemis and XLF/Cernunnos and the ligase IV/XRCC4 complex ligates the DNA ends to reform the duplex DNA structure (40). The intricacies of this process have let to be elucidated, but the basic mechanism of NHEJ has been delineated.

HDR is initiated by degradation of one strand on either side of a dsDNA break by nucleases followed by coating of the ssDNA region by RPA, which is known as DNA resectioning (42). From this point, most of the subpathways involve invasion by the ssDNA region into regions of homology found elsewhere within the DNA, which is used as a template to synthesize DNA (42). The DNA resynthesis step is accomplished by core resection machinery a component of which is the Mre11 complex, which is composed of Mre11, Rad50, and Nbs1 (42). BRCA1, a tumor suppressor, functions as an ubiquitin ligase that polyubiquitinates CtIP, a ssDNA nuclease (42). Both of these proteins are involved in HDR and are thought to play a role in mediating the DSB repair pathway choice of cells (43).

IR is widely used in the treatment of various cancers both as a single agent and in combination with other chemotherapies, including cisplatin (44). Increased cellular sensitivity to IR following treatment with cisplatin has been described and is believed to

occur through decreased NHEJ (45). Deficiencies in DNA-PKcs have been shown to lead to increased radiosensitivity in both cellular and mouse models (41, 46). Also, cells with deficiencies in Rad52 (the yeast homolog of Rad50) show increased DSBs and cytotoxicity following exposure to ionizing radiation (41). PARP, in addition to its role in BER, also plays a role in the recognition and repair of single-strand breaks, presenting the potential to increase cellular sensitivity to IR by PARP inhibition (47).

Defects in DNA repair pathways are frequently observed in cancer cells, which can be a factor in cancer development but also has the potential to be exploited therapeutically. For instance, defects in BRCA1 and BRCA2 lead to decreased HDR and have been shown to increase sensitivity to PARP inhibition (48). This scenario, referred to as "synthetic lethality" addresses the observed lethality that is induced by having a defect in two proteins, while a defect in either by itself does not induce lethality (48). Mutations in the BRCA1 gene have been shown to be a reliable predictive indicator of breast cancer development with carriers incurring a lifetime risk of 39-54% of development of epithelial ovarian cancer (EOC) (49). BRCA1 has also been implicated in the progression of breast cancer as well as the response of these cancers to DNA crosslinking chemotherapeutic agents such as cisplatin, however resistance to these drugs continues to be a major limitation in disease treatment (50). Determining the expression profile of tumor cells and correlating this to the response to various treatments is an ongoing endeavor in cancer treatment research. For example, PARP inhibitors are currently being analyzed in the context of BRCA1 status, in order to induce an optimal cytotoxic effect. This allows the possibility to increase patient response to chemotherapeutic treatment. Inhibitors of other proteins such as DNA-PKcs have also

been developed and increase cellular sensitivity to IR both *in vitro* and *in vivo* and the potential exists that these studies will be expanded into the clinical setting to increase tumor sensitivity to IR (51).

1.5. Inhibition of Proteins Required for Genomic Maintenance and Stability

As described in previous sections, maintaining genomic stability is essential to prevent mutations and eventual disease acquisition. A paradigm exists in which inhibition or disruption of the maintenance of genomic stability has deleterious consequences as seen in the acquisition of mutations and eventual development of disease; however inhibition of genomic stability in carcinogenic cells that have acquired uncontrolled growth potential could lead to decreased cell and tumor growth. Several proteins involved in DNA repair and replication have already been targeted by small molecule inhibitors including PARP and topoisomerase II, however the long-term benefits of drugging these targets has yet to be realized, possibly due to the redundancy of function, leading to incomplete abrogation of cellular activity. We hypothesize that targeting RPA and XPA presents a non-redundant mode of inhibition, as evidenced by the cellular effects of inhibiting these proteins as seen with siRNA and in disease states.

1.5.1. Replication Protein A (RPA)

Replication protein A (RPA) is a heterotrimeric single-stranded DNA (ssDNA) binding protein made up of 70, 34, and 14 kDa subunits (3). RPA's ssDNA binding activity is achieved though high-affinity interactions between oligonucleotide/oligosaccharide (OB) folds with DNA (52, 53). Six OB-folds are found throughout the 3 subunits, four within p70, and one each in p32 and p14, however the

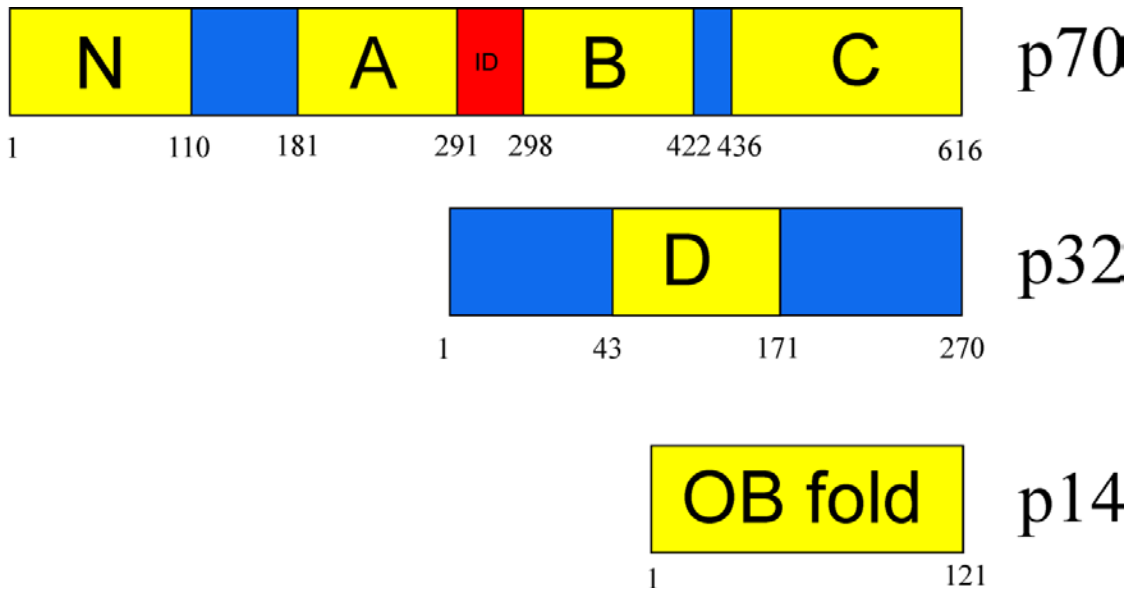

Figure 3. Replication Protein A. The three subunits of RPA are depicted. OB folds are shown in yellow and the interdomain region of p70 is illustrated in red.

role of each of these OB-folds in binding to DNA has not been completely elucidated (Figure 3) (53). The ssDNA binding activity of RPA is required for several DNA metabolic pathways including DNA replication, recombination and repair (3). OB-folds in DNA binding domains A and B (DBD-A and DBD-B) in the central region of the p70 subunit contribute most of the binding energy for RPA-ssDNA interactions (Figure 3) (52). OB-folds contact DNA in two primary ways, through hydrophobic stacking of the bases with aromatic amino acids and by hydrogen bonding between side chains of the amino acids and the phosphate backbone (3). These structural features make OB-folds an attractive target for the development of small molecule inhibitors (SMIs) of DNA binding activity.

Crystal structure analysis of DBD-A and DBD-B within RPA p70 bound to DNA revealed a conformational change in RPA when bound to an 8-nucleotide (nt) DNA substrate (Figure 4) (54). However, the DNA binding activity of RPA is thought to extend beyond the central OB-folds of p70 because of the observation that there is a 50-fold difference in the affinity of RPA for 30-nt vs. 10-nt DNA structures, despite the crystal structure indicating that the 8-nt DNA structure occupies almost the entire space of this domain (Figure 4) (3). This implicates additional regions of RPA as being important for changing the dynamics of RPA-DNA interactions and there is some evidence of a contribution from DBD-D (within the p32 subunit) on RPA's binding activity on longer substrates (3, 55, 55). This was evidenced by a decrease in DNA-binding activity when comparing WT RPA to RPA containing a missing DBD-D domain on DNA substrates 40-nt or longer (55). However, studies looking at the ability of RPA p32 and p14 to bind DNA alone do not show significant DNA binding activity,

A

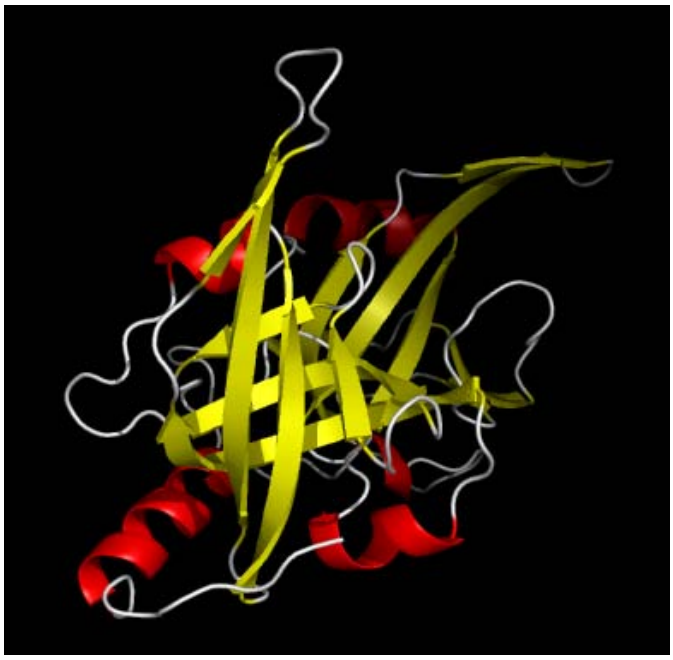

B

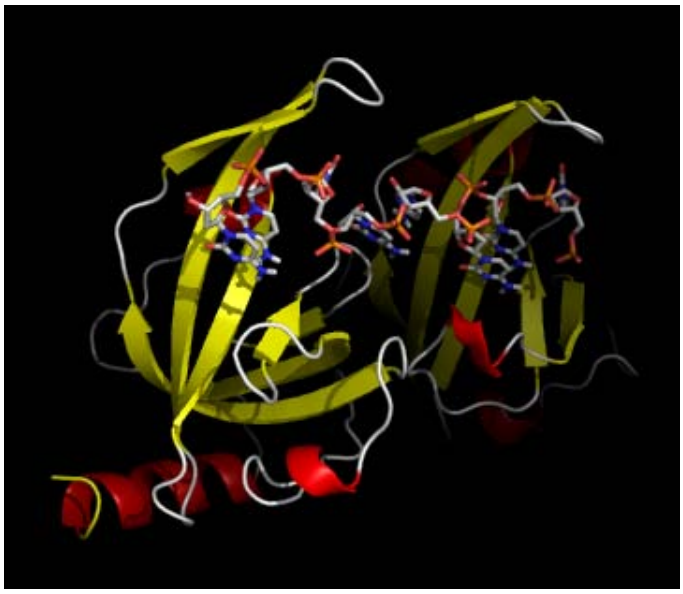

Figure 4. Structure of RPA. The crystal structure of RPA p70 from residues 181-422 is represented in the absence (1A) or presence (1B) of a $(dC)_8$ DNA substrate. The structure was analyzed using PYMOL analysis of the PBD file 1FGU. 4A represents RPA in the open conformation in which it is unbound to DNA. 4B depicts RPA bound to the $(dC)_8$ DNA substrate.

suggesting that the role of these subunits is structural in nature as opposed to contributing to DNA-protein interactions (56).

RPA has been shown to interact with different types of DNA, although it displays the highest affinity interaction with ssDNA (3). RPA has also been shown to have DNA unwinding activity on oligonucleotides in which it is able to separate dsDNA into ssDNA (57). This activity has been suggested to reside within the p70 subunit of RPA (58). RPA was first shown to interact with cisplatin-damaged DNA by Clugston and colleagues in 1992 and the involvement of RPA in the repair of cisplatin induced DNA damage was expanded upon the discovery that RPA preferentially binds to cisplatin damaged DNA compared to undamaged (59, 60). RPA has also been shown to bind to UV-damaged DNA (3). These interactions suggest that RPA is involved in discriminating damaged from undamaged DNA and implicates RPA in the damage recognition step of NER, in addition to suggesting that RPA is a potential factor in recognizing DNA damage during DNA replication.

RPA interacts with several proteins required for NER including XPA, XPG and XPF/ERCC1 (61, 61-64). RPA has been shown to affect the activities of these proteins *in vitro,* for example, RPA increases the DNA binding activity of XPA as well as the endonuclease activity of XPG and XPF/ERCC1 (63, 64). RPA has also been suggested to regulate the polarity of DNA strand binding by XPG 3' to the site of damage and XPF/ERCC1 5' to the site of damage (65). These characteristics indicate that RPA does not only have a role in DNA binding, but also influences the activity of other proteins involved in NER, although how RPA is increasing this activity is not fully understood.

The potential exists that RPA acts as a scaffold to bring other proteins into close proximity to DNA or that RPA is affecting the activity of proteins directly.

RPA also interacts with proteins involved in DNA replication including DNA polymerase α (66). Again, it is not clear what role these interactions play in replication, but it is possible that RPA binding to ssDNA acts as a scaffold to recruit proteins to the sight of replication and to participate in the formation of replication foci, allowing DNA replication to proceed (3). *In vitro* studies demonstrate that RPA can influence the activity of both helicases and polymerases and may play a role in regulating polymerase fidelity during DNA replication (3). Inhibition of the ssDNA binding activity of RPA has the potential to increase our understanding of the role of RPA in various pathways and to further elucidate the relationship between DNA binding activity and RPA's role in regulating protein function. In addition, targeting specific OB-folds found within RPA would allow the identification of the role each OB-fold is playing in RPA function.

Cancer cells are continuously progressing through the cell cycle, replicating their DNA and producing progeny cells. The essential role of RPA in DNA replication can be exploited to specifically target highly proliferative cancer cells. A molecularly targeted agent designed to inhibit the DNA binding activity of RPA would directly prevent its involvement in DNA replication and lead to reduced progression through S-phase and could ultimately result in the loss of cell viability. In addition, inhibition of RPA has the potential to potentiate the effects observed with DNA damaging chemotherapeutic agents by inhibiting the repair of the damage, leading to persistent DNA damage that can potentially increase cytotoxicity.

1.5.2. Xeroderma Pigmentosum Group A

XPA is a 36 kDa zinc metalloprotein that appears to be exclusively involved in the NER pathway (Figure 5). XPA participates in the initial steps in both GG-NER and TC-NER and is thought to play a role in recognizing bulky DNA damage due to its increased affinity for UV-damaged or cisplatin damaged duplex DNA compared to undamaged (67, 68). The ability of XPA to interact with and recognize damaged DNA is thought to occur by deformation and local changes in the electrostatic potential of DNA that contains a bulky DNA lesion (69).

XPA is able to directly interact with several proteins in the NER pathway including RPA, ERCC1, and TFIIH and may play a role recruiting and stabilizing NER proteins. The N-terminal portion of XPA (residues 4-97) has been shown to interact with the RPA p32 subunit and ERCC1 (70). The C-terminal portion of XPA (residues 226-273) has been shown to interact with TFIIH and the central domain (residues 98-219) represents the minimal DNA binding domain (MBD) and interacts with RPA p70 (70). The MBD domain also contains a zinc-binding domain which contains the sequence Cys-X-X-Cys-$(X)_{17}$-Cys-X-X-Cys which are Cys105, Cys108, Cys126, and Cys129, and is different from other typical zinc-binding DNA binding domains (70, 71). The C-terminal domain contains several positively charged residues including Lys 141, Lys 145, Lys 151, Lys 179, Lys 204 and Arg 207 (70). This positively charged region has the potential to interact with the negatively charged DNA backbone. Several glutamic and aspartic acid residues are also found within the central domain, which also have the potential to interact with the negative charged DNA backbone (70). Although the crystal structure of XPA has not been resolved, the solution structure provides valuable information on

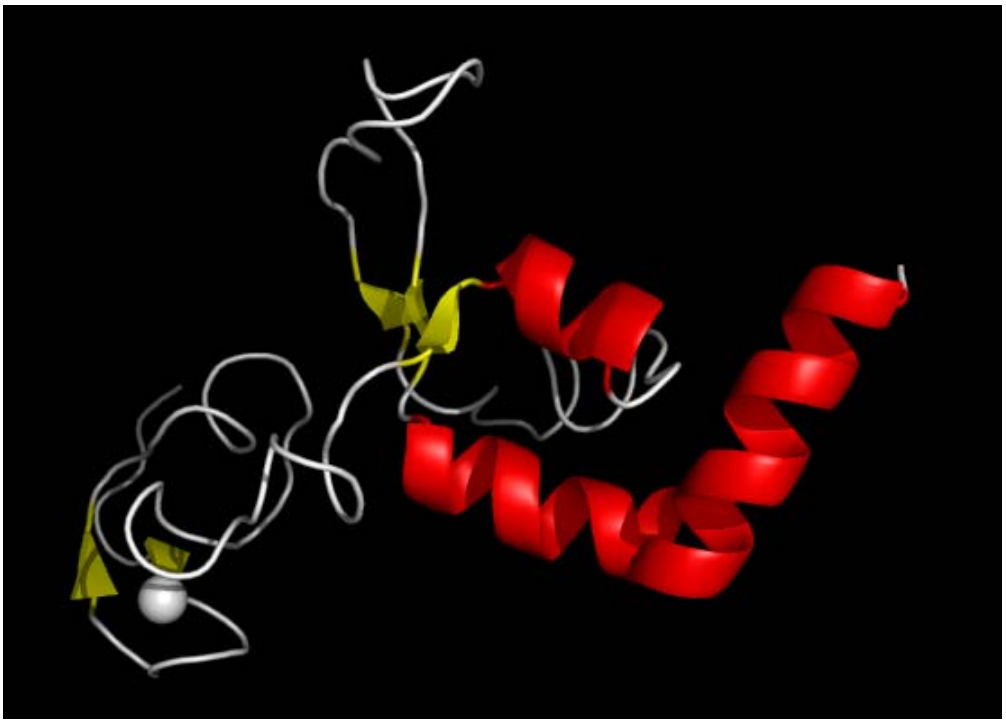

Figure 5. NMR structure of XPA. The solution structure of XPA (PDB code 1XPA) was visualized using PyMol. Beta sheets are depicted in yellow, alpha helices are depicted in red and loop regions are depicted in white. A zinc ion is represented by a white sphere.

XPA's structure and potential interactions between XPA and DNA. Further work has demonstrated that mutation of two conserved lysines, 141 and 179, to glutamate decreased cellular repair of UV-induced DNA lesions and decreased *in vitro* DNA binding activity (72). Interestingly, mutation of residues that were not required for cellular repair of UV-induced lesions did inhibit XPA's DNA binding activity, indicating that DNA binding alone is not responsible for NER of UV-induced DNA damage (72). *In vitro* analysis of XPA activity has also demonstrated that it can interact with both strands of a duplex cisplatin-damaged substrate and that it inhibits RPA-dependent DNA unwinding (73, 74). These observations provide further insight into mechanistic roles for XPA in regulating NER.

Interactions between XPA and other proteins required for NER show a potential role for XPA in stabilizing and regulating NER proteins. Inhibiting the DNA binding activity of XPA using small molecules is hypothesized to prevent XPA from participating in NER, leading to persistent DNA damage and resulting in increased cytotoxicity. As previously discussed, the repair of cisplatin lesions by NER is thought to contribute to cellular sensitivity to this agent and by inhibiting proteins required for NER, the cytotoxic effect of cisplatin can potentially be increased. Because XPA has not been demonstrated to play a role in cellular pathways beyond NER, inhibition of its DNA binding activity is expected not to possess single-agent activity and presents an opportunity to increase the cytotoxic activity of cisplatin without toxic effects from single-agent treatment.

1.6. Chemotherapeutic Drugs

1.6.1. Alkylating Agents

Nitrogen mustards are one of the earliest identified reagents to induce DNA interstrand crosslinks, which were recognized as a potential anti-cancer therapy due to their high reactivity with DNA (75). Nitrogen mustards exert their cytotoxic and mutagenic effect by forming interstrand DNA crosslinks between guanine residues at the N7 atoms (75). Because of the low specificity of these agents, their benefits as anti-cancer treatments are limited. Highly reactive molecules such as these are able to not only cause modification on the DNA, but may also form adducts on proteins, leading to deleterious cellular effects that may result in increased mutagenesis and the development of secondary cancers (75). Despite these limitations however, nitrogen mustards have played a very important role in cancer treatment over the past decade (75).

Temozolimide (TMZ) is an alkylating agent used in the treatment of cancers, particularly glioblastomas, that works by methylating adenine and guanine residues, causing them to mispair during DNA replication (76). Typically the cell can repair the most cytotoxic lesion induced, 0^6 –methyl guanine, by direct reversal by 0^6 – methylguanine methyltransferase (MGMT), and tumor response to TMZ treatment is correlated with the expression of MGMT (76). However, if MGMT is underexpressed or inactive, cells can repair methylated residues using the BER pathway, indicating the importance in this pathway in cellular sensitivity to TMZ (23, 76). Current studies examining the effect of PARP inhibition on TMZ sensitivity have been conducted and it was observed that PARP inhibition increases the anti-proliferative effect of TMZ,

indicating the importance of BER to repair lesions induced by TMZ, as well as the chemotherapeutic benefit of BER inhibition (77).

1.6.2 Topoisomerase Inhibitors

Because of the essential role of DNA replication in cell proliferation, several chemotherapeutics have been developed to impede this pathway. Topoisomerase I (topoI) has been the target of several chemotherapeutic drugs including camptothecin (CPT) and topotecan (78). Topoisomerase II (topoII) has also been the target of inhibition by chemotherapeutic drugs including doxorubicin and etoposide (78). Etoposide induces its cytotoxic effect by interfering with the breakage and rejoining reaction that topo II uses to relieve DNA supercoiling during replication (79). Etoposide interacts with topo II and traps a covalent reaction intermediate called the cleavable complex, which is believed to prevent the progression of DNA replication and ultimately induce apoptosis (79). Although it is an effective chemotherapeutic agent, etoposide has very undesirable secondary effects manifested by the development of secondary cancers, including leukemia (80).

The mechanism of action by topo poisons is thought to be manifested not by direct inhibition of protein activity, but rather the stabilization of a covalent-DNA intermediate complex that blocks DNA replication from occurring but may also signal for repair (78, 79). The repair of these lesions is thought to occur by the endonucleolytic activity of Flap-endonucleases including Mre11/Rad50 and XPF/ERCC1 due to the increased sensitivity to yeast strains to CPT when mutations in these proteins are made (78). However, the exact repair mechanism of these lesions has not been elucidated and inhibition of DNA repair in general with, for example, RPA inhibitors, has the potential

to increase the cytotoxic activity of topoI and II poisons. In addition, inhibition of RPA has the potential to potentiate the cytotoxic effects induced by etoposide due to dual inhibition of replication, both in initiation and elongation.

1.6.3. Cisplatin

The effect of platinum on cell survival was first observed by Dr. Barnett Rosenberg and colleagues in 1965 in which he observed elongation of *E. coli* cells, indicating an inability to divide, following exposure to an electric field (81). Further analysis indicated that it was the platinum containing electrode that was responsible for this effect, as well as components of the buffer used to inoculate the bacteria, which included chloride and ammonia (81). These studies were the first to characterize a cellular effect by platinum containing compounds and studies analyzing the effect of these compounds in cancer cells soon followed (82, 83).

Cisplatin, or *cis*-diamminedichloroplatinum (II), was one of the platinum containing compounds identified by these studies to have an anti-proliferative effect on tumor cells (83). Cisplatin is composed of a central platinum ion that is coordinated with two *cis*-amine ligands as well as two *cis*-chloride ligands in a planar configuration (84). Intracellularly, a decreased chloride ion concentration favors hydration of the cisplatin molecule to form an aquated, more reactive form of cisplatin, $[Pt(NH_3)_2Cl(OH_2)]+$ (84). Once aquated, cisplatin reacts with intracellular targets including both proteins and DNA, but its primary cellular target is thought to be DNA in which it binds covalently to guanine and adenine bases to form bulky adducts including 1,2 dGpG (65%), 1,2 dApG (25%) and 1,3 dGpNpG (5-10%) in addition to interstrand crosslinks (85, 86). The formation of a cisplatin-DNA adduct induces a kink that disrupts normal DNA metabolic

processes including replication and transcription (86). This disruption leads to activation of cellular processes that can result in removal of the cisplatin adduct and restoration of the DNA sequence, or, if the adduct is left unrepaired, the cell may undergo apoptosis. Since the first identification of cisplatin, several other derivatives of this compound have been analyzed for their antitumor activity, including oxaliplatin, carboplatin, and *trans*-diamminedichloroplatinum(II), each of which varies in toxicity and activity (85, 87).

Currently platinum containing drugs containing are integrated into treatment regimens for late stage lung cancer patients (5, 88). Although cisplatin is a front line therapy in the treatment of several cancers, efficacy varies significantly between patients causing a spectrum of responses. The high mortality rate associated with lung cancer is indicative of the inadequate response of patients to chemotherapeutic treatment. Differences in the metabolism and uptake of cisplatin as well as the repair of cisplatin-DNA lesions represent a few of the factors thought to influence cisplatin sensitivity. Several groups are currently examining the genotypic and proteomic differences between patients to determine if there are links between protein expression and response to chemotherapy.

2. Small Molecule Inhibition of RPA and its Effect on DNA Replication and Repair

2.1. Introduction

The identification of small molecule inhibitors of proteins is a rapidly growing field in which researchers have undertaken screening small molecule libraries to identify compounds that display inhibition of protein activity. These SMIs have the potential to decrease tumorigenic growth and impact numerous diseases. The identification of proteins that are correlated with cancer development and response to treatment, such as the ras family of proteins, has led to the identification of many small molecules that inhibit protein activity, however successful integration of these molecules in a clinical setting has not always transpired (89, 90). This is due to a number of factors including rapid adaptability of cancer cells as well as redundancy between pathways, leading to cellular compensation of protein inhibition. The wide range of mutations incurred in different cancers along with the heterogeneous cellular population found within a single tumor contributes to tumor response to protein inhibition. The effect of tumor diversity is becoming more apparent as SMIs of proteins known to be misregulated in cancer often do not have the desired effect on tumor development and response to chemotherapeutic treatment (89). Recent hypotheses on the development of anti-cancer agents has lead to the suggestion that inhibiting proteins important for maintaining genomic stability may be an effective way to perturb tumorigenic growth (91). Although all tumors are distinguished by differences in protein mutations, all cancers are defined by having some deficiency in maintaining genomic stability (91). Inhibition of proteins essential for this process may prove to be a means of globally preventing cancer development and proliferation and has the potential for widespread utility in cancer treatment.

The essential requirement of RPA for DNA replication and repair suggests the effect of inhibiting this protein will be a reduction of the ability of any rapidly dividing cell to proliferate and to repair DNA damage that requires RPA. This presents the opportunity for single-agent activity of inhibition of RPA in addition to the potential utility of combination therapy integrating RPA inhibition in conjunction with DNA damaging chemotherapeutics. Using a novel high-throughput screen, we have identified a class of SMIs of RPA and present the characterization of one of these compounds, TDRL-505, which shows *in vitro* inhibitory activity of RPA's DNA binding activity in addition to single agent cytotoxic activity in NSCLC cell lines. TDRL-505 shows synergistic cellular activity with cisplatin and etoposide and presents the first identification of a small molecule that inhibits the DNA-binding activity of a protein.

2.2. Materials and Methods

2.2.1. Materials

Oligonucleotides were purchased from Integrated DNA Technologies, Inc. (Coralville, IA). Vybrant Apoptosis Assay Kit was purchased from Invitrogen. Cisplatin, etoposide, aphidicolin, propidium iodide (PI) and 5-bromo-2'-deoxyuridine (BrdU) were obtained from Sigma Chemical Co. and nocodazole was obtained from Calbiochem. RPMI 1640 containing L-glutamine (Mediatech) was supplemented with 10% fetal bovine serum (FBS) and 1% penicillin/streptomycin. H460 and A549 cells are from ATCC and maintained in RPMI. All small molecule inhibitors were obtained from ChemDiv (San Diegeo, CA) and resuspended in 100% dimethylsulfoxide (DMSO) at a final concentration of 10 mM and stored at -20°C. Dulbecco's phosphate buffered saline (PBS) was obtained from Gibco. α-RPA primary antibody was obtained from

NeoMarkers and goat α-mouse secondary antibody was obtained from Santa Cruz Biotechnology.

2.2.2. Chemicals

Cisplatin was prepared at a concentration of 1 mM by dissolving into dH_2O and stirring for 1 hour. The solution was then sonicated for 10 minutes at 60% power after which 1 mL aliquots were stored at -20°C. BrdU was prepared at a concentration of 20 mM in dH_2O and stored at -20°C. Etoposide was dissolved in DMSO at a final concentration of 50 mM and stored at -20°C. Nocodazole was resuspended in DMSO to a final concentration of 5 mg/mL and stored at room temperature. Aphidicolin was resuspended in 100% EtOH and stored at 4°C. PBS-ethylenediaminetetraacetic acid (EDTA) was prepared at 9.6 mg/mL PBS with 0.8 mM EDTA. PI was dissolved at a final concentration of 1mg/mL in dH_2O and stored at 4°C.

2.2.3. DNA Substrates

All ssDNA substrates were gel purified on preparative 12% denaturing polyacrylamide gels. Briefly, DNA was electrophoresed at 280 volts for 3 hours and visualized by UV-shadowing. Bands were cut from the gel and eluted overnight with rotation at 4°C in 3 mL of elution buffer (0.3M NaOAc, 1 mM EDTA and 0.1% SDS). The DNA was then EtOH precipitated with 9 mL of -20°C 100% EtOH, 0.3 M NaOAc, and 1 µg/mL glycogen with incubation at -80°C for one hour. DNA was then sedimented at 7800 x *g* for 45 minutes, the pellet resuspended in dH_2O and concentration determined by absorbance reading at 260 nm. For specific DNA sequence information, see Appendix A.

2.2.4. RPA Purification

Heterotrimeric RPA was purified by transforming BL21 (DE3) competent cells with p11-tRPA plasmid DNA provided by Dr. Marc Wold (56). Cells were incubated overnight at room temperature without shaking and then at 37°C with shaking until cells gave an absorbance reading of 0.8 at A_{600}. Protein expression was then induced with IPTG with shaking and incubation at 37°C for two hours. Cells were then harvested by centrifugation at 700 x *g* for 30 minutes at 4°C. The pellet was resuspended in 10 mL H1 buffer (30 mM Hepes, 1 mM DTT, 0.25% myo-inositol, and 0.1% NP-40, with a protease inhibitor mix (containing 1µg/mL phenylmethanesulfonylfluoride (PMSF), aprotinin, leupeptin, and pepstatin)) and sonicated at 60% power 3 x 30 seconds with 30 second pauses between pulses. The lysate was then sedimented at 11,200 x *g* for 30 minutes at 4°C. The supernatant was loaded over a 20 mL Blue Sepharose column, which was washed in 0.1 M NaOH and 1 M NaCl and then equilibrated with H1 buffer with 0.1 M KCl, at 1 mL/min. Following loading of the column, it was washed with H1 buffer with 0.1 M KCl, H1 Buffer with 0.8 M KCl, and H1 buffer with 0.5 M NaSCN at 1 mL/min. After washing, the protein was eluted into 10 mL fractions with H1 Buffer containing 1.5 M NaSCN. Protein containing fractions were identified using Bradford analysis, pooled and loaded directly onto a 5 mL hydroxyapatite (HAP) column equilibrated in H1 buffer. The sample was loaded at 2 mL/min and the column was washed with H1 buffer. H1 Buffer with 0.1 M KPi was used to elute the protein off of the column in 5 mL fractions. Protein containing fractions were identified using Bradford analysis, pooled, and loaded onto a 5 mL Q-sepharose column, equilibrated in 0.1 M KCl, at 2 mL/min. The column was washed with H1 buffer with 0.1 M KCl and protein was eluted using a gradient from

0.1 M to 1 M KCl and fractions containing RPA were identified using Bradford and SDS-PAGE analysis, pooled and dialyzed overnight at 4°C in H1 buffer (Figure 8A).

2.2.5. High-Throughput Screening

A small molecule library of compounds from ChemDiv was screened as described in Turchi et al. (92). Briefly, 60 nM RPA and 10 nM fdT_{12} DNA were mixed in binding buffer (20 mM Hepes, 1 mM DTT and 0.01% NP-40) and then aliquoted into 384 well plates containing 10 μM of each compound in a final volume of 50 μL. Fluorescence anisotropy was used to determine inhibition of RPA binding to DNA as described in section 2.2.7. Positive hits that significantly inhibited RPA-DNA interactions were identified and obtained from ChemDiv.

2.2.6. Electrophoretic Mobility Shift Assays (EMSAs)

EMSAs were performed in 20 μL reactions, unless otherwise indicated, containing 5′ [P32] labeled DNA and protein as indicated in the Figure legend. EMSAs examining protein binding to DNA were performed by incubating protein and DNA for 5 minutes at room temperature in RSSE buffer (20 mM Hepes, 1 mM DTT and 0.01% NP-40). For EMSAs examining compound inhibition of protein binding to DNA, protein was pre-incubated with compound in RSSE buffer for 5 minutes at room temperature. Compounds were diluted from 10 mM stocks in 100% DMSO to 0.5 mM in 10 μM Hepes and 10% DMSO. Following pre-incubation, DNA, RSSE buffer and agarose dye (10% glycerol, 10 mM EDTA, 0.01% xylene cyanol and 0.01% bromophenol blue) were added to the reactions which were incubated for an additional 5 minutes at room temperature. Samples were loaded onto a 6% native polyacrylamide gel and electrophoresed at 170 volts for 1 hour. Gels were then dried and exposed to a

PhosphoImager screen (Molecular Dynamics) for 30 minutes. The screen was then scanned using a Storm 820 (Amersham Biosciences) and quantified using ImageQuant software (Molecular Dynamics). The results presented indicate the average and standard deviation from at least 3 individual experiments. The IC_{50} values were calculated using Sigma Plot with fitting to the appropriate decay curve.

2.2.7. Fluorescence Anisotropy

Anisotropy based binding assays were performed in a volume of 500 µL in RSSE buffer containing protein and 5′ fluorescein-labeled DNA as indicated in the Figure legend. 10 nM DNA was mixed with buffer in each reaction and fluorescence read using a Cary Eclipse fluorescence spectrophotometer. Fluorescence was read at 515 nm following excitation at 495 nm with vertical and horizontal polarizers. Slit widths were each set at 5 nm and voltage was typically 800 volts. For reactions containing TDRL-505 and protein, reactions were pre-incubated with binding buffer in a final volume of 500 µL for 2 minutes after which precipitate was removed by spinning at 9300 x *g* for 10 minutes. The supernatant was then mixed with DNA and fluorescence was read. The final concentration of DMSO in each 500 µL reaction was 0.5%. The fluorescence anisotropy values (r) were calculated using the equation (r) = Iv-Ih/Iv + 2Ih (equation 2.1). The results indicate the average and standard deviation from at least 3 individual experiments. The IC_{50} value was calculated using Sigma Plot with fitting to the appropriate decay curve.

2.2.8. Crystal Violet Cell Viability Assays

Cell viability assays were performed using a modified version of the protocol described (Van SS, Mol. Cancer Ther, 2006). H460 NSCLC cells were seeded at 1 x 10^4

cells/cm^2 in 6-well plates. Cells were incubated for 24 hours at 37°C and then treated with increasing concentrations of TDRL-505 (in a final concentration of 1% DMSO) or vehicle (1% DMSO) for 48 hours at 37°C. After treatment, cells were trypsinized and resuspended in 1 mL media. 10 µL of resuspension was replated onto a 24-well plate in triplicate and grown for 5 days at 37°C. Wells were then washed with PBS and stained with crystal violet solution (0.75% Crystal Violet in 50% EtOH with 0.125% NaCl and 0.88% Formaldehyde) for 10 minutes. Following staining, cells were washed in dH_2O and the dye resolubilized with 1% SDS in PBS. Absorbance was read at 595 nm using a SpectraMax M5 spectrophotometer (Molecular Devices). The results are presented as the average and standard deviation from at least 3 individual experiments and the IC_{50} value was calculated using Sigma Plot with fitting the appropriate decay curve.

2.2.9. Cell Cycle Analysis

H460 NSCLC cells were plated at a density of 1 x 10^4 cells/cm^2 for 24 hours and then treated with increasing concentrations of TDRL-505 (at a final DMSO concentration of 1%) or vehicle (1% DMSO) for 48 hours as indicated. Following plating and treatment of H460 cells, adherent and non-adherent cells were collected and sedimented by spinning at 170 x *g* for 5 minutes and then washed twice with 1% bovine serum albumin (BSA) in PBS-EDTA. Cells were fixed in 70% EtOH at -20°C followed by incubation on ice for 30 minutes following which cells were pelleted at 170 x *g* for five minutes and stained with 1 µg/mL propidium iodide (PI) and 25 µg/mL RNaseA for 1.5 hours. PI stained cells were then analyzed on a Becton Dickinson FACScan flow cytometer (BD Bioscience, San Jose, CA). Cells were gated and analyzed on a histogram with events plotted against the FL2-A parameter. Cell cycle distribution was analyzed

using ModFit software (Verity Software House, Topsham, ME). To determine the effect of TDRL-505 on entry into S-phase, G2 arrest was induced by treatment with 0.8 μg/mL nocodazole for 12 hours (93). Cells were then washed with PBS and treated with either vehicle or TDRL-505 (100 μM) for various times as indicated. Cells were harvested and analyzed for cell cycle distribution as described above. The results presented indicate the average of at least 3 individual experiments.

2.2.10. Analysis of BrdU Incorporation

To analyze incorporation of 5-Bromo-2′-deoxyuridine (BrdU) into cellular DNA, H460 NSCLC cells were plated at a density of 1×10^4 cells/cm^2 for 24 hours and then treated with 0.8 μg/mL nocodazole for 12 hours to induce a G2 cell cycle arrest (93). Following induction of G2 arrest, cells were treated with vehicle or 100 μM TDRL-505 for 8 or 12 hours as indicated in the Figure legend. Two hours prior to harvesting, cells were labeled with 10 μM BrdU after which adherent cells were trypsinized and pelleted at 170 x *g* for 5 minutes. Cells were then washed with PBS-EDTA, pelleted at 170 x *g* for 5 minutes and fixed in 1 mL 70% EtOH (-20°C) while vortexing. Following fixation, DNA was denatured with 0.5 mL 2 M HCl for 20 minutes at room temperature, washed with wash buffer (PBS with 0.5% BSA) and pelleted at 170 x *g* for 5 minutes. The HCl was then neutralized with 0.5 mL 0.5 M sodium borate for 2 minutes to which 1 mL wash buffer was added and cells were pelleted at 170 x *g* for 5 minutes. Cells were then incubated with 50 μL mouse anti-BrdU antibody (CalBiochem) diluted 1:500 in dilution buffer (PBS with 0.5% Tween-20 and 0.5% BSA) for 20 minutes at room temperature, washed with wash buffer, pelleted and then incubated with 50 μL AlexaFluor 488 goat anti-mouse secondary antibody (Invitrogen) (1:500 in dilution buffer) for 20 minutes at

room temperature. Following antibody incubation, cells were washed, pelleted and then incubated in 1 μg/mL PI in PBS-EDTA for at least 30 minutes at 4°C. Cells were then analyzed using flow cytometry (as described in 2.2.9) for cell cycle and BrdU staining using FLA and FL1 parameters, respectively.

2.2.11. Annexin V/PI Staining

H460 cells were plated at a density of 1 x 10^4 cells/cm^2 for 24 hours and treated for 48 hours with increasing concentration of TDRL-505. Following treatment, cells were analyzed for apoptosis using an Annexin V-FITC/PI Vybrant Apoptosis Assay Kit (Invitrogen), according to manufacturer's instructions. Briefly, adherent and non-adherent cells were collected and pelleted at 170 x *g* for 5 minutes. Cells were then washed with PBS-EDTA and resuspensded in 100 μL of 1x Annexin V binding buffer (10 mM Hepes, 140 mM NaCl, 2.5 mM $CaCl_2$, pH 7.4). PI was added to a final concentration of 1 μg/mL along with 5 μL of the Annexin V conjugate dye. Cells were then incubated for 15 minutes at room temperature after which 400 μL of 1x Annexin V binding buffer was added. A minimum of 1 x 10^4 cells were analyzed for each sample on a BD FACScan flow cytometer using FL1 and FL2 parameters. Data was analyzed using WinMDI version 2.8 software (http://facs.scripps.edu/software.html, 1-19-00). A549 cells were plated and treated as described for H460 cells. The results indicate the average and standard deviation of at least 3 individual experiments (H460s). IC_{50} values were determined using Sigma Plot with fitting to the appropriate decay curve.

PBMCs were isolated from whole blood using a Ficoll purification protocol. Whole blood was collected and diluted with an equal volume of PBS and then applied to a 15 mL conical tube containing ~4 mL of ficoll being careful not to mix the two. The

sample was then sedimented at 400 x *g* for 35 minutes at -20°C with no brake and no acceleration. Following sedimentation, red and polynuclear cells were retained in the ficoll layer and PBMCs were confined to the interface between the blood layer and ficoll layer. The interface layer containing PBMCs was removed and diluted with 10x volume of PBS and sedimented at 300 x *g* for 10 minutes. The cells were then resuspended in 10 mL of media and plated onto 10 cm dishes. Cells were then treated immediately as described for H460s and harvested and analyzed by flow cytometry at 24 and 48 hour time points as described for H460 cells.

2.2.12. Indirect Immunofluorescence

H460 cells were plated on chamber slides (LabTek) at a concentration of 40 cells/μL in 500 μL and allowed to adhere for 24 hours. Cells were then treated for 3 hours with either 50 μM TDRL-505 or vehicle as indicated in the Figure legend. To determine the effect of etoposide on RPA foci formation, cells were treated for 4 hours with either 50 μM TDRL-505 or vehicle, as indicated, in the presence or absence of 25 μM etoposide. Following treatment, cells were fixed in 4% paraformaldehyde at 25°C for 3 minutes followed by incubation with 0.2% Triton X-100 for 2 minutes at 4°C. The slides were then blocked in blocking buffer A (15% FBS in PBS-EDTA) for 1 hour at 25°C and then incubated with mouse anti-RPA p34 primary antibody (Neomarkers) (1:500) in blocking buffer A for 1 hour. Slides were then washed 3 x 10 minutes with blocking buffer A and incubated with Alexa Fluor-594 goat-anti-mouse secondary antibody (Invitrogen) (1:300) in blocking buffer A for 1 hour. Slides were again washed with blocking buffer A and stained with 300 nM DAPI diluted in PBS-EDTA for five minutes. Slides were then mounted and images captured using a Zeiss fluorescent

microscope using filters for Texas Red to visualize RPA staining and 4′,6-diamidino-2-phenylindole (DAPI) for visualizing DNA. Slides were visualized and images analyzed and quantified using ImageJ software (http://rsb.info.nih.gov/ij/index.html, 2-12-10).

2.2.13. Western Blot Analysis

H460 cells were plated at a density of 1 x 10^4 cells/cm^2 in 10 cm dishes for 24 hours then treated with either vehicle (1% DMSO) or increasing concentrations of TDRL-505 for 8 hours as indicated in the Figure legend. Following treatment, adherent cells were scraped with 100 μL RIPA buffer (150 mM NaCl, 10 mM Tris pH 7.2, 0.1% SDS, 1% Triton X-100, 1% deoxycholate, 5 mM EDTA and 1 μg/mL PMSF, aprotinin and pepstatin) and incubated on ice for 10 minutes with vortexing at 2 minute intervals. Samples were then spun at 10,000 x *g* for 10 minutes at 4°C and supernatant removed. Protein concentration was determined using Bradford analysis and ~45 μg of total protein was electrophoresed on a 12% Bis-Tris SDS-PAGE gel (Invitrogen) in 2-(N-Morpholino)ethanesulfonic acid (MES) buffer at 200 volts for 1 hour. The gel was then transferred to a PVDF membrane activated with methanol at 30 volts for 1 hour in NuPage transfer buffer (Invitrogen) and then blocked in blocking buffer B (2% BSA-TBS-Tween (0.5% Tween-20, 20 mM Tris, pH 7.5, and 0.17 M NaCl)) for 1 hour. RPA was detected with a mouse anti-RPA p34 antibody (Neomarkers) diluted to 1:3000 in blocking buffer B for 1 hour. The blot was then washed 3 x 5 minutes in TBS-Tween followed by a goat anti-mouse secondary antibody (Santa Cruz Biotechnologies) diluted to 1:5000 in blocking buffer B. The blot was then washed 3 x 5 minutes in TBS-Tween and protein was visualized using chemiluminescence reagent (0.1 M Tris, pH 8.5, 1.25

mM Luminol, 0.18 mM *p*-coumaric acid and 0.03% H_2O_2) followed by exposure using a Fuji LAS-3000 system (Tokyo, Japan).

2.3. Results

Identification of Small Molecule Inhibitors from High-Throughput Screen

In order to identify novel small molecule inhibitors of RPA, an *in vitro* high-throughput screen of a small molecule library of compounds from ChemDiv was conducted. A fluorescence-based high-throughput assay was employed, measuring inhibition of RPA binding to fluorescein-labeled DNA. Our assay yielded a z-score of 0.8 (92). Initial screening of approximately 42,000 compounds identified 54 that inhibited RPA from binding to DNA (92). In order to confirm the inhibitory activity of compounds identified from the primary screen, we used non-spectroscopic EMSA assays to minimize false positives due to the spectral characteristics associated with many of the compounds. Secondary screening analysis revealed two compounds that displayed significant inhibition of RPA-DNA binding activity *in vitro* (compounds 3 and 5) (Figure 6A). Compound 3 consists of a tri-substituted pyrazole ring with an oxo-butanoic acid at N1, a p-methyl benzene ring at the C3 position, and a 7-ethoxyquinolin-2(1H)-one at the

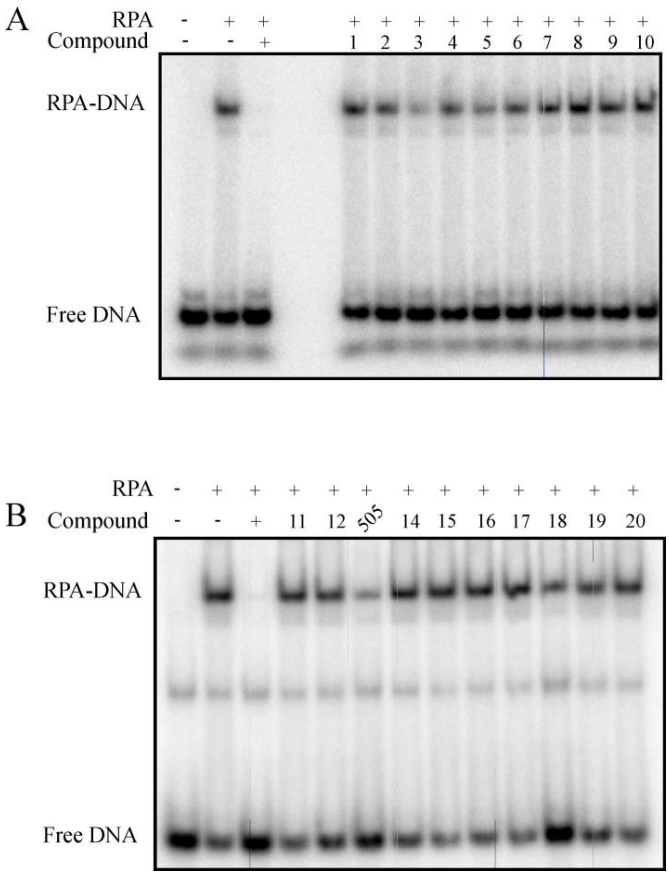

Figure 6. Identification of SMIs of RPA. 6A. EMSA analysis of compounds identified from the high-throughput screen performed for RPA. 25 nM RPA was incubated with 100 µM of each compound for five minutes to which 25 nM SJC 1.5 Xba (34-nt) DNA was added and incubated an additional 10 minutes. Samples were then electrophoresed on polyacrylamide native gels as described in section 2.2.6. 6B. EMSA analysis of compound 3 like small molecules. Reactions were performed and analyzed as described in 6A.

C5 position (Figure 7A). Compound 5 consists of a benzoic acid containing a 6-methoxy cyclopenta[c]quinoline at the C4 position (Figure 7B).

As *in vivo* inhibition of RPA using siRNA has been shown to be cytotoxic due to its critical role in DNA metabolic processes, we analyzed the effect of compounds 3 and 5 on NSCLC cell viability (94). While no cellular effect was seen with compound 5, limited cellular activity of compound 3 was observed, however these analyses were hampered by poor solubility. Considering the high level of *in vitro* inhibition observed with compound 3, we retained a core structure consisting of a substituted dihydropyrazole with a 4-oxo-butanoic acid at N1 and a phenyl substituent at C3 to initiate analysis of structure activity relationships (SAR) and identify compounds with cellular activity (Figure 7C).

Structure-Activity Relationship Studies of Compound 3 like Molecules

Structure-activity relationship (SAR) studies were performed by retaining the core structure described in Figure 7C and searching the ChemDiv library to identify small molecules containing this core structure. Eighty-one analogs were identified and obtained from ChemDiv with differing substitutions off the phenyl ring (R2) and varying substituents at position C5 on the dihydropyrazole ring (R1) (Figure 7C). These derivatives were analyzed for *in vitro* RPA inhibitory activity using EMSAs (Figure 6B and data not shown). A subset of these compounds that showed the ability to inhibit RPA's DNA binding activity were further characterized to determine how the structure of each contributes to inhibition of DNA binding activity. Using EMSA analysis, titrations of each compound were performed and the IC_{50} of each was determined. Among the

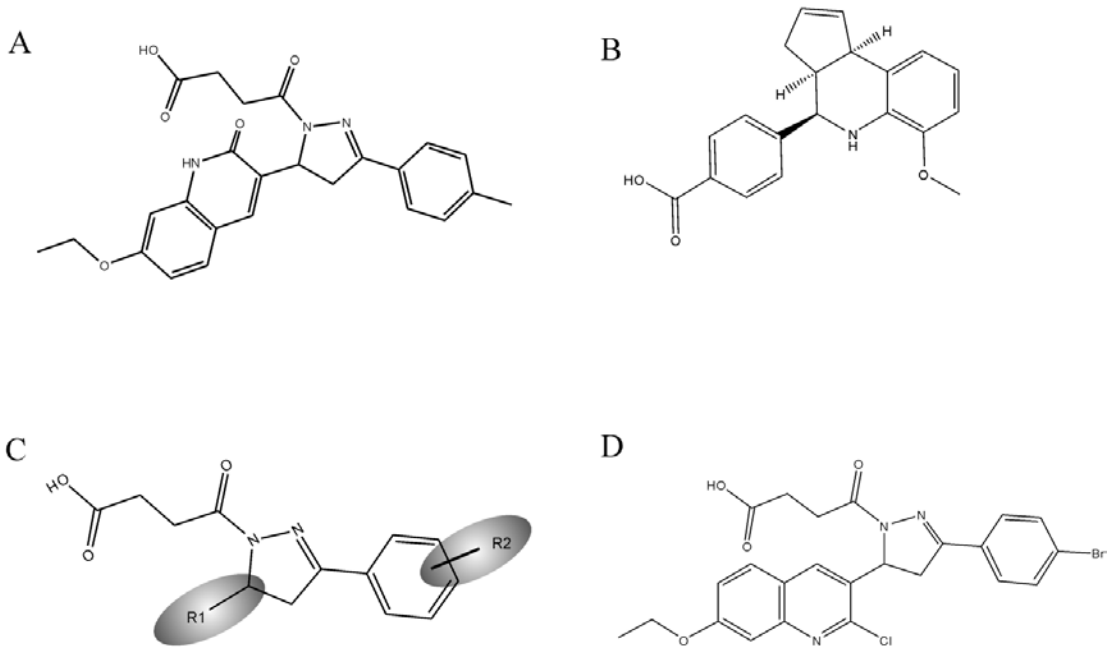

Figure 7. Structures of SMIs of RPA. 7A. Structure of compound 3, identified from the HTS for SMIs of RPA. 7B. Structure of compound 5, also identified from the HTS for SMIs of RPA. 7C. The core structure of compound 3 retained for searching the ChemDiv library. 7D. Structure of TDRL-505.

compounds analyzed, TDRL-505, consisting of a methoxy quinolone at the R2 position and bromine at the R1 position, was the most potent inhibitor with an IC_{50} of 13 μM (Figure 7D and Table 2). TDRL-520-523 also contain a bulky substituent at the R1 position, however, these compounds contain a di-substituted pyrazole ring and show varying capacities for inhibiting RPA-ssDNA interactions (Table 2). Interestingly, TDRL-518, which does not inhibit RPA's DNA binding activity *in vitro,* retained the initial core structure associated with compound 3; however it contains a diethyl amine group at the R1 position that has the potential to be positively charged at neutral pH. This group is not expected to interact with the positively charged arginines and lysines found in the RPA OB-folds that are responsible for interaction with negatively charged DNA, which is a potential explanation for the lack of inhibition observed with this compound. Compound 523 also did not display inhibition of RPA-DNA interactions and contains a di-substituted pyrazole with a methoxy group at the C3 position of the benzene ring. Compounds 518 and 523 do not show significant *in vitro* activity, however, how the structures of these compounds influence this activity is not known. As the quinoline substitution had the most potent *in vitro* activity, we analyzed the structures of all compounds obtained in the analogy search with this substituent. Three additional compounds were identified; however, their analysis was hampered by similar insolubility issues as observed for compound 3.

We then analyzed cellular activity of the 6 compound 3 like molecules shown in Table 2 in H460 cells and calculated IC_{50} values for each compound following a 48 hour exposure using Sigma Plot with fitting to the appropriate decay curve. A correlation between *in vitro* and cellular activity, consistent with cellular inhibition of RPA was

Table 2.

Structure activity relationships of small molecule RPA inhibitors

Name	**Structure**	**IC_{50} (μM)**	
		In vitro	*Cellular*
TDRL-505	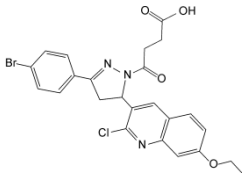	12.9 ± 1.3	30.8±1.7
TDRL-518	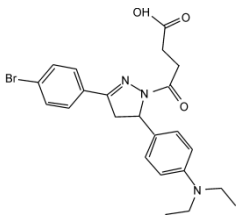	>100*	NA
TDRL-520	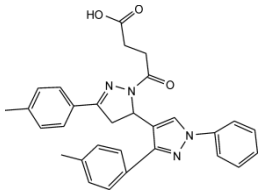	20.3±10.7	49.9±2.5
TDRL-521	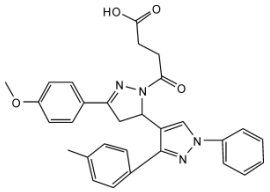	71.7±33.9	56.9±6.7
TDRL-522	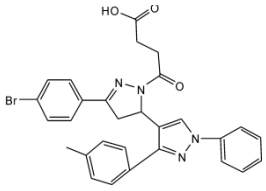	56.1±6.7	38±32***
TDRL-523	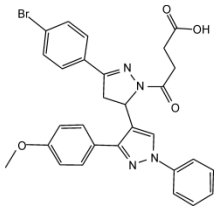	>100**	31.0±5.2

Table 2. *In vitro* and Cellular IC50 values for Compound 3 like small molecules.

The *in vitro* IC_{50} was determined by EMSA analysis as described in Figure 6A. Cellular IC_{50} was determined by treating H460 cells and analyzing annexinV/PI staining as described in section 2.2.6. The *in vitro* and cellular data was analyzed using standard 4 parameter logistic curves. The IC_{50} values and standard error of the fit were determined from this analysis using Sigma Plot with fitting to the appropriate decay curve.

*inhibition at the highest concentration tested (100 μM) was 9%

**inhibition at the highest concentration tested (100 μM) was 36%

*** Maximum observed cytotoxicity was 80% of control

observed. Interestingly, compound 523, which showed minimal inhibition of RPA *in vitro*, did display modest cellular activity, which could be attributed to metabolism or other cellular effects. After analysis of the cellular and *in vitro* inhibitory activity of compound 3 analogs, TDRL-505 displayed the lowest *in vitro* IC_{50} and was the most potent compound of those examined in cells. We therefore selected this compound to further investigate its mechanism of action and the cellular effects that result from inhibition of RPA-ssDNA interactions using a comprehensive series of *in vitro* and cell based assays.

In vitro Analysis of TDRL-505

RPA binding to synthetic oligonucleotide substrates has been well characterized with respect to structural features and kinetics of binding (54, 74, 95, 96). In order to determine the potential mode of binding and inhibitory activity of TDRL-505, inhibition of RPA by TDRL-505 was examined on various DNA substrates. A 34-base purine rich substrate (SJC 1.5 Xba, Appendix A) was used to examine inhibition of RPA-DNA interactions using EMSA analysis. The purine-rich substrate allows for a true equilibrium between free RPA and RPA-DNA complex to be achieved, which is essential when examining a competitive binding reaction. Pyrimidine-rich sequences of this length display an extremely slow rate of dissociation from RPA which limits their utility in competitive binding reactions (96). This length of DNA is also capable of extending beyond DBD-A and DBD-D OB folds of RPA p70 to allow interactions with the other OB-folds within p70 as well as the p34 and p14 subunit. This analysis has the potential to provide information about where the compound interacts with RPA. TDRL-505 was titrated with 25 nM RPA in the presence of 5′-[^{32}P]-labeled 34-base purine-rich ssDNA.

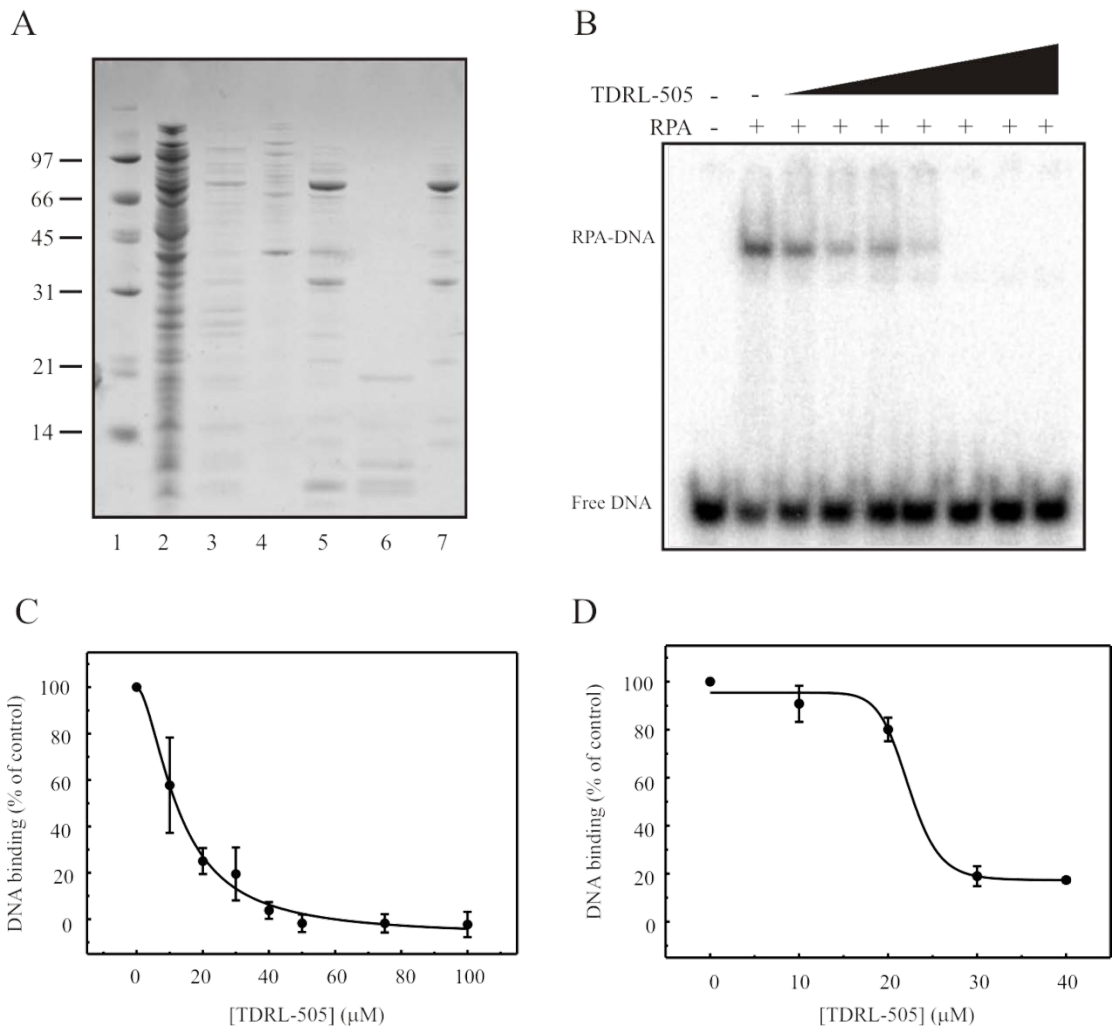

Figure 8. ***In Vitro*** **Analysis of TDRL-505.** 8A. Wild-type RPA purification SDS-gel. RPA was purified as described in section 2.2.4. The lanes represent as follows: 1-Low molecular weight marker, 2-Whole cell extract, 3-Pooled fractions, blue sepharose column, 4-Flow through, blue sepharose column, 5-Pooled fractions, HAP column, 6-Flow through, HAP column, 7-Pooled fractions, Q column. 8B. Analysis of TDRL-505 on RPA DNA binding activity. 25 nM RPA was incubated with increasing concentrations of TDRL-505 for five minutes at room temperature to which 25 nM SJC 1.5 Xba (34-nt) DNA was added for an additional five minutes. Samples were electrophoresed on a native polyacrylamide gel as described in section 2.2.6. 8C. Quantification of 8B. The data was fit to a standard 4 parameter logistic curve with an n=4. 8D. Anisotropy analysis of RPA binding to a dT_{12} DNA substrate. The data was fit to a standard 4 parameter logistic curve with an n=3.

Analysis of binding in an EMSA using the 34-base purine-rich sequence revealed a concentration dependent decrease in binding with an IC_{50} of 13 μM, as determined by Sigma Plot analysis (Figure 8B and 8C).

To further define the mechanism of inhibitory action of TDRL-505, we assessed binding to poly-T ssDNA 12 bases in length (dT_{12}). The length of this DNA substrate largely restricts binding to DBDs A and B, which has been shown in the co-crystal structure of RPA p70 (amino acids 183-420) with a short oligonucleotide, to interact with DNA (54). The sequence was modified to be pyrimidine-rich (dT_{12}) because of a relatively fast off rate of RPA for a substrate of this length. The faster on-rates of RPA for pyrimidine-rich DNA can compensate for the decrease in affinity associated with the shorter length to allow detection (96). A fluorescence polarization (FP) based anisotropy assay was used in the analysis of the dT_{12} substrate as the lengthy electrophoretic separation associated with EMSA analysis is detrimental to accurately analyze inhibition of binding to this substrate. RPA binding to a 34-base purine-rich sequence does not display the same high rate of dissociation that is seen with dT_{12}, which allows this substrate to be used in EMSA analysis. Titration of TDRL-505 resulted in a concentration dependent decrease in RPA binding and an IC_{50} value of 20.4 μM (Figure 8D). The fact that TDRL-505 still displays robust inhibition on the short 12 base substrate strongly suggests that the compound is targeting the central p70 OB-folds (DBD-A and -B).

TDRL-505 induces cytotoxicity in a NSCLC cell model

Having determined the *in vitro* inhibitory activity of TDRL-505 on RPA-DNA interactions, we sought to determine the mechanism of cellular activity of this compound. The effect on cell viability was determined using two independent assays presented in Figure 9. The induction of apoptosis was assessed via a flow cytometric based assay measuring propidium iodide (PI) uptake, which is a DNA intercalating agent that indicates a loss of membrane integrity, and annexin V staining of extracellular membrane bound phosphotidylserine, an early step in the initiation of apoptosis (Figure 9A). H460 NSCLC cells were treated with increasing concentrations of TDRL-505 for 48 hours, after which annexin V/PI staining was performed. The results demonstrate minimal annexin V staining suggesting that classical apoptosis was not occurring as a result of treatment (97). Interestingly, a concentration dependent increase in PI staining was observed, indicating a general loss of membrane integrity. Quantification of the viable cells (annexin V negative/PI negative) resulted in an IC_{50} of 30.8 μM as determined by Sigma Plot analysis (Figure 9B). The PI positivity in the absence of annexin V positivity is suggestive of necrotic cell death which has been observed in other cell models (98). As an independent measure of the effect of TDRL-505 on cell viability, we employed a crystal violet based assay modified from a previously published protocol (99). H460 cells were treated with increasing concentrations of TDRL-505 or vehicle for 48 hours, trypsinized and replated in the absence of compound. Cultures were then grown for five days and stained with crystal violet, washed, solubilized and quantified by measuring absorbance at 595 nm. Treated cultures were compared to a mock treated control and results presented as the percent of viable control cells. The data obtained reveal a

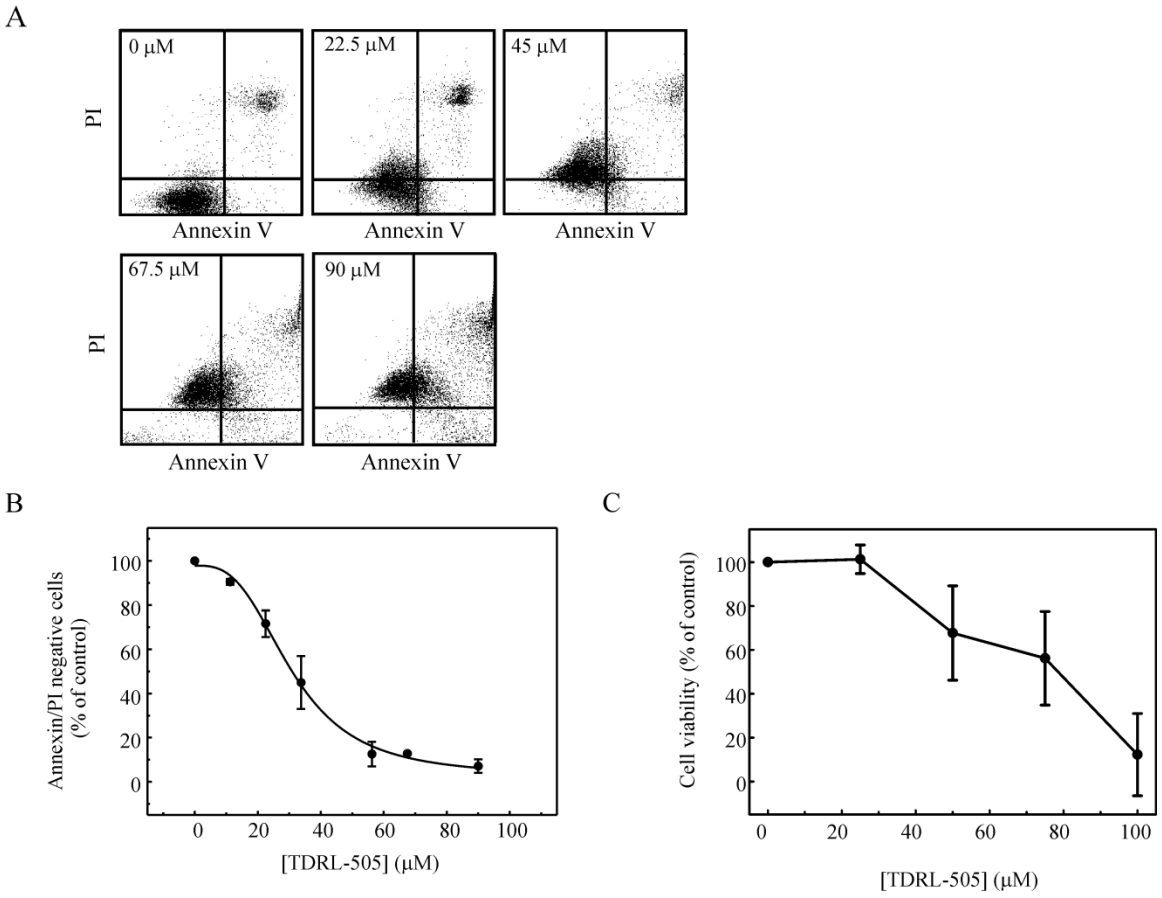

Figure 9. Cellular analysis of TDRL-505. 9A. H460 cells were treated for 48 hours with increasing concentrations of TDRL-505 as indicated in the Figure. Cells were then analyzed for Annexin V and PI content, represented by the x- and y-axis, respectively, using flow cytometry. Viable cells (Annexin V-/PI-) were determined to be those present in the lower left quadrant. 9B. The data from 3A was quantified and the percentage of untreated cells that did not stain with either dye (present in the lower left quadrant), indicating live cells, calculated. The average and standard deviation from 4 replicates are presented and the data fit to a 4-parameter logistic curve. The average IC_{50} of TDRL-505 in this treatment was determined to be 30.8 µM. 9C. H460 cells were analyzed for cell viability using crystal violet assays as described in section 2.2.8. The results represent the averages from 3 independent experiments that were fit to a 4-parameter logistic curve and are presented as the percentage of vehicle treated control cells.

significant reduction in cell viability with an estimated IC_{50} of 64 μM (Figure 9C). The similarity of cellular activity observed in the crystal violet analysis compared to that seen with the annexin V/PI staining suggests that the extent of PI staining is indicative of a true loss of cellular viability following treatment with TDRL-505. A similar result was also observed following treatment of A549 NSCLC cells with TDRL-505 (Figure 10). To determine if TDRL-505 displays selectivity for cancer cells, its effect was examined on a culture of freshly isolated non-cancerous peripheral blood mononuclear cells (PBMCs). After 24 hours of treatment, the cells showed a modest sensitivity to the compound compared to H460 cells with cell viability decreased by 50% at 100 μM of TDRL-505 compared to a greater than 90% loss of viability seen with H460 cells after 24 hours of treatment (Figure 11). Analysis of the 48 hour time point was not possible as a result of the inherent loss of PBMC viability with extended culture times. Therefore, TDRL-505 has shown significant cytotoxic effects in NSCLC cell lines while showing only modest activity in non-cancerous cells, supporting the possibility that a therapeutic treatment window may be achievable.

In order to determine the effect on cellular levels of RPA, we prepared cell extracts from H460 cells treated for 8 hours with increasing concentrations of TDRL-505 and analyzed the levels of RPA p34 and p70 using western blot analysis. As shown in Figure 12B, the levels of the p70 and p34 subunits of RPA did not change following treatment with TDRL-505. Indirect immunofluorescence was also used to determine the effect on RPA levels as well as its cellular distribution. Using triton washing to dissociate proteins not tightly bound to DNA, we observed a decrease in the level of RPA staining following a 3 hour treatment with 50 μM TDRL-505, indicating a potential

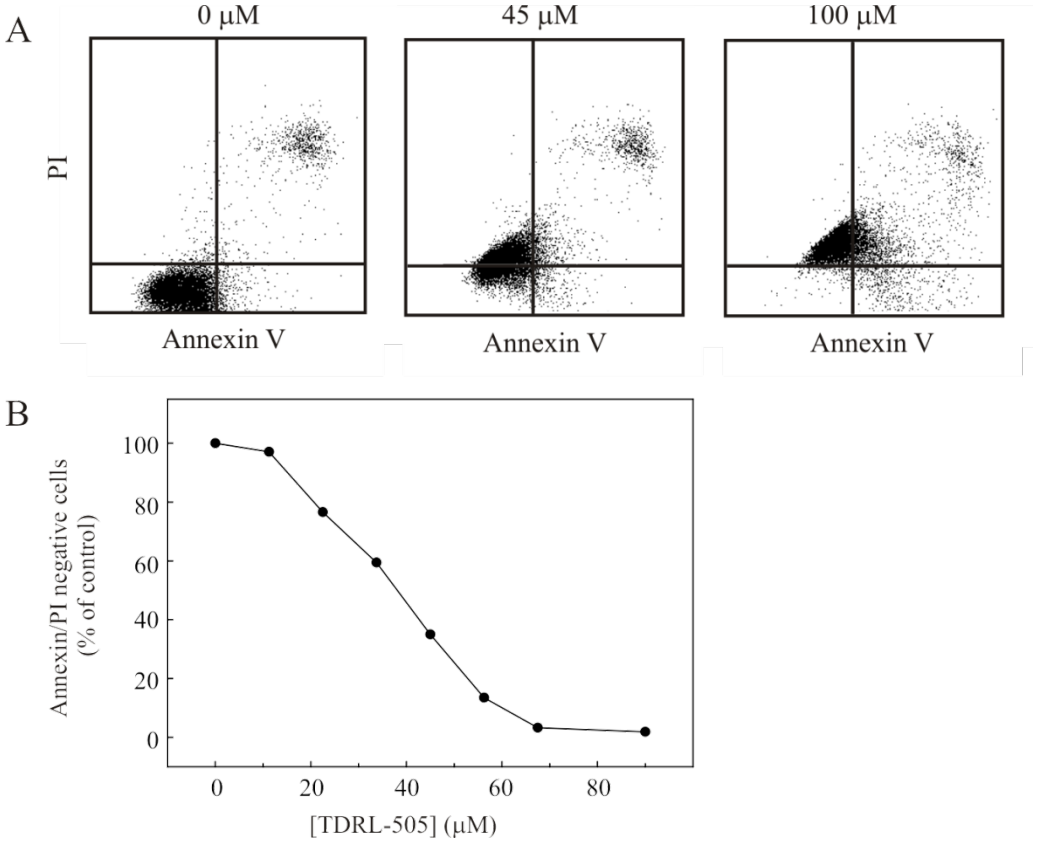

Figure 10. Effect of TDRL-505 on A549 NSCLC cells. 10A. A549 cells were treated for 48 hours with increasing concentrations of TDRL-505 as indicated in the Figure. Cells were then analyzed for PI and Annexin V staining using flow cytometry. PI and Annexin V staining are represented by the y- and x-axis, respectively. 10B. Quantification of 10A. Duplicate samples were analyzed for Annexin V/PI staining following treatment with TDRL-505 and presented as the percentage of cells with no staining, indicative of live cells. The IC_{50} of TDRL-505 in this treatment is ~38 μM.

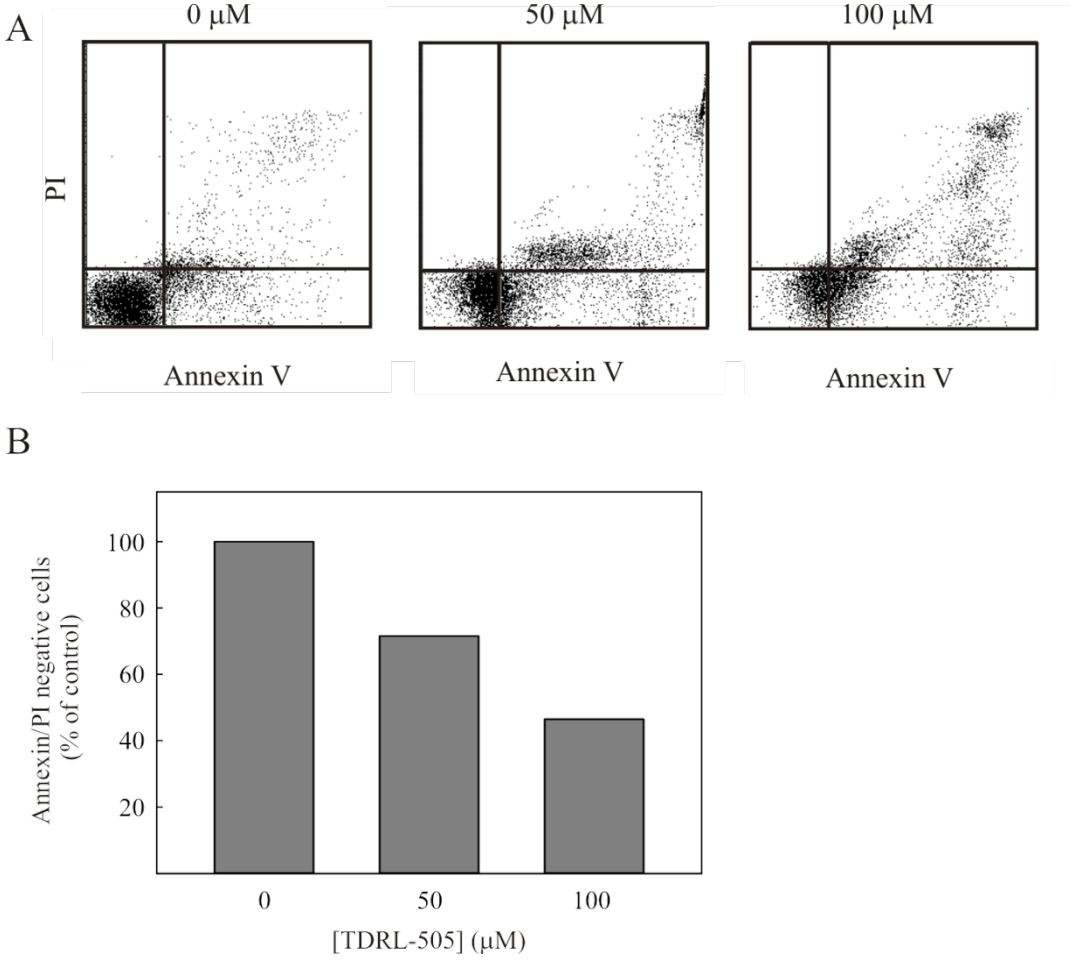

Figure 11. Effect of TDRL-505 on PBMCs. 11A. PBMCs were harvested as described in section 2.2.11. Cells were plated and treated with increasing concentrations of TDRL-505 as indicated for 24 hours. Cells were then processed for Annexin V/PI staining using flow cytometry. PI and Annexin V staining are represented by the y- and x-axis, respectively. 11B. Quantification of the percentage of viable, untreated cells (Annexin V/PI negative) from duplicate samples. The IC_{50} of TDRL-505 in PBMCs is estimated to be ≥ 100 μM.

decreased association of RPA with DNA following treatment with TDRL-505 without an overall decrease in protein level (Figure 12A). This data coupled with the western blot analysis indicates that RPA is not being degraded by TDRL-505, but its association with DNA is decreased, which indicates a potential mechanism of action of TDRL-505 in H460 NSCLC cells.

TDRL-505 prevents cellular entry into S-phase

The impact of TDRL-505 on differential nuclear distribution of RPA and its induction of cytotoxcity indicates that inhibition of RPA binding to DNA is exerting an anti-proliferative effect that is being manifested by an inability of RPA to interact with the DNA. RPA's essential role in replication in a highly proliferative cell and its inhibition in this process would cause an inability to initiate DNA replication, leading to an accumulation of cells in the G1/S phase of the cell cycle and eventual cell death (100). Therefore we assessed the effect of TDRL-505 treatment on H460 cell cycle progression and observed an increase in the proportion of cells in the G1-phase of the cell cycle in response to treatment (Figure 13). To determine if S-phase entry is inhibited in TDRL-505 treated cells, cells were synchronized in G2/M with nocodazole and then released from G2 arrest and re-fed complete medium supplemented with either vehicle or 100 μM TDRL-505. Both vehicle and TDRL-505 treated cells rapidly progressed through mitosis into G1 after removal of nocodazole (Figure 14A). Cells that were treated with vehicle alone entered into G1, as seen at the 4 hour time point and progression into S-phase is apparent after 8 hours with progression into G2 evident at 12 hours (Figure 14A). Cells that were treated with 100 μM TDRL-505 after release from nocodazole progressed into G1 but did not enter S-phase, even 12 hours post release. Interestingly, when TDRL-505

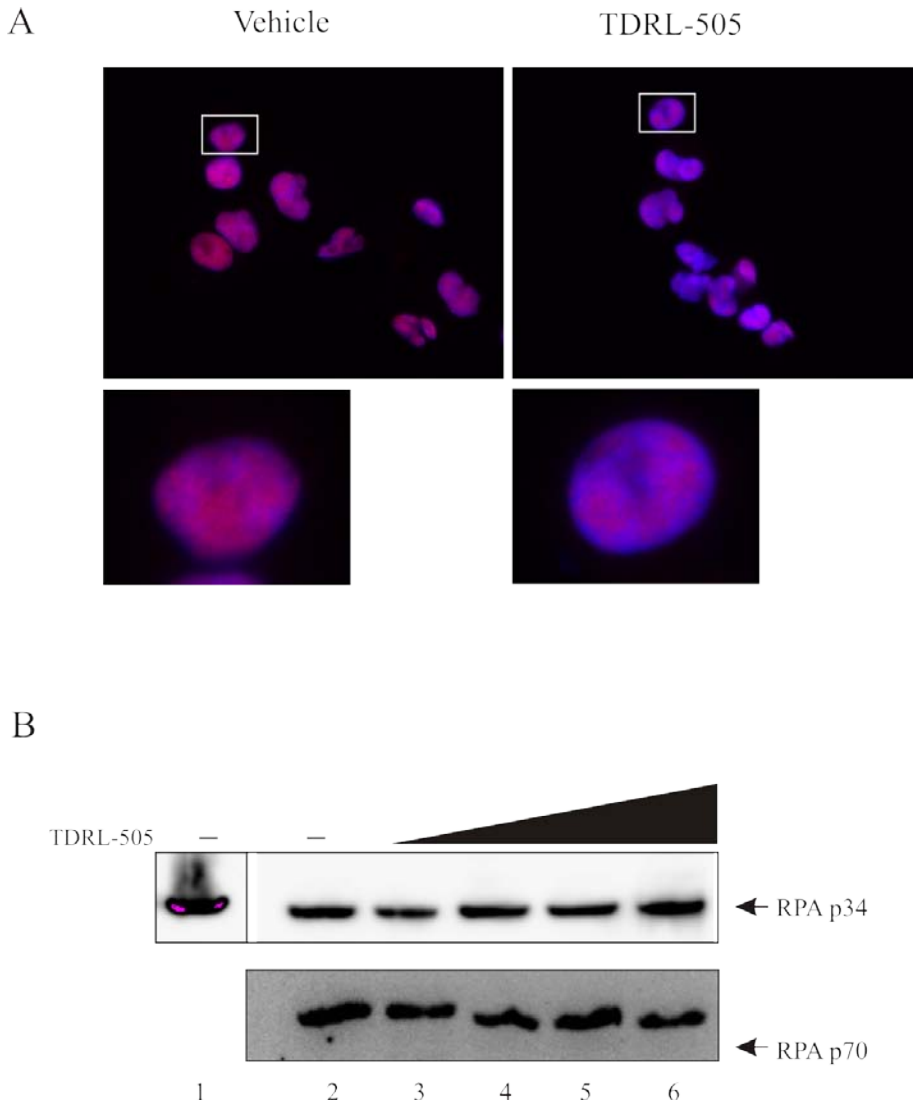

Figure 12. Cellular effect of TDRL-505 on RPA levels. 12A. H460 cells were treated with 50 µM TDRL-505 or vehicle for 3 hours and analyzed for RPA expression and localization by indirect immunofluorescence using an Alexa Fluor594 secondary antibody (red). Slides were counter stained with DAPI (blue) and images merged. Magnification of the boxed cells is presented below the lower magnification images. 12B. H460 cells were treated with increasing concentrations of TDRL-505 or vehicle for 8 hours and RPA expression was assessed via western blot analysis probing for the p70 and p34 subunit as indicated. Lane 2 is a vehicle treated control and Lanes 3-6 correspond to treatment with 25, 50, 75 and 100 µM TDRL-505, respectively. The positions of RPA p34 and p70 are indicated by the arrows.

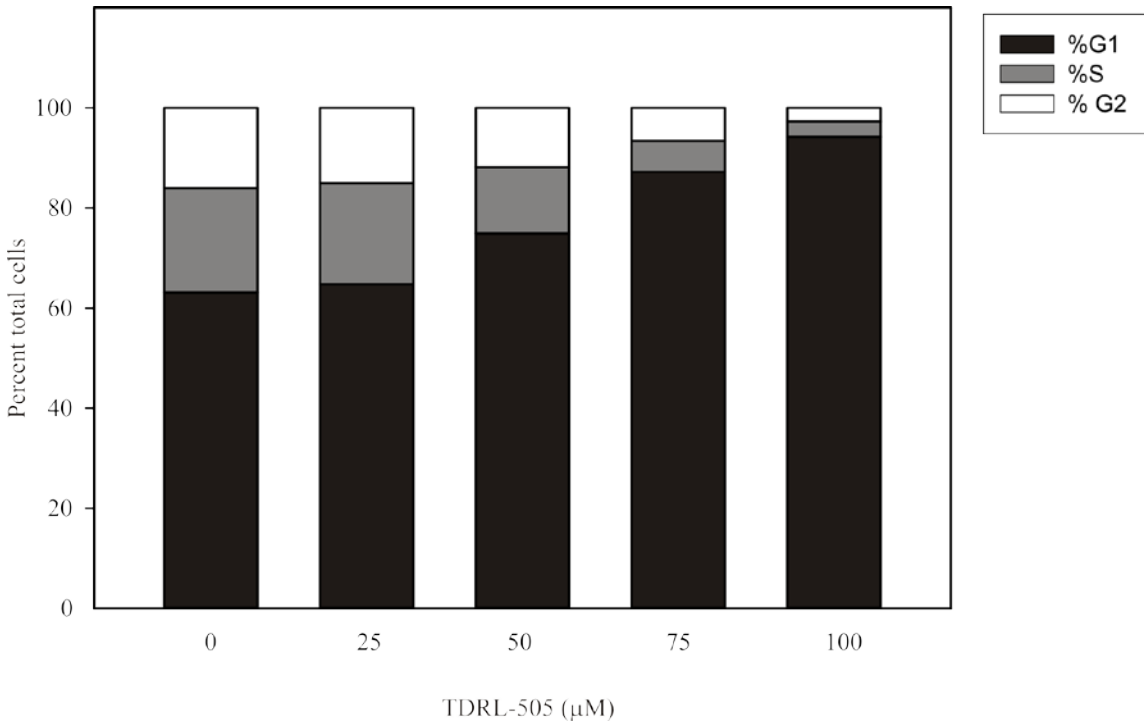

Figure 13. TDRL-505 induces a G1 arrest in H460 cells. H460 cells were treated for 48 hours with increasing concentrations of TDRL-505 as indicated. DNA content was assessed using PI staining and analysis by flow cytometry. The results presented are the average from 3 independent experiments.

was removed and cells were re-fed complete medium, they were able to reinitiate the cell cycle and proceed into S-phase (Figure 15). However, cells that were re-fed with 100 μM TDRL-505 showed prolonged G1 arrest and an increased sub-G1 population, typically indicative of cell death (Figure 15).

To increase the resolution of the biochemical steps in the transition from G1 to S phase, we assessed BrdU incorporation using the same treatment protocol to analyze for cell cycle. Following release of nocodazole arrested cells, 10 μM BrdU was added 2 hours prior to collection and cells were analyzed by flow cytometry for BrdU incorporation. In the presence of TDRL-505, no BrdU incorporation was observed while vehicle controls showed incorporation and progression through the cell cycle (Figure 14A). To determine the acute effect of TDRL-505 on DNA replication, asynchronous cells were treated with TDRL-505 for a short period of time (3 hours) and small but distinct differences in BrdU incorporation were observed (Figure 14B). Cells treated with TDRL-505 appear to display a lengthening of S-phase and fewer cells that have incorporated BrdU progressing through the cell cycle into G2 (Figure 14B). Therefore TDRL-505 influences the ability of H460 NSCLC cells to enter S-phase and induces a G1 arrest in these cells.

TDRL-505 acts synergistically with cisplatin and etoposide in a NSCLC cell model

In addition to its essential role in DNA replication, RPA is involved in several DNA repair pathways including the repair of bulky DNA adducts as well as DNA breaks induced by various types of exogenous and endogenous agents. The association of RPA with ssDNA is a significant feature of all of these pathways, indicating that inhibition of

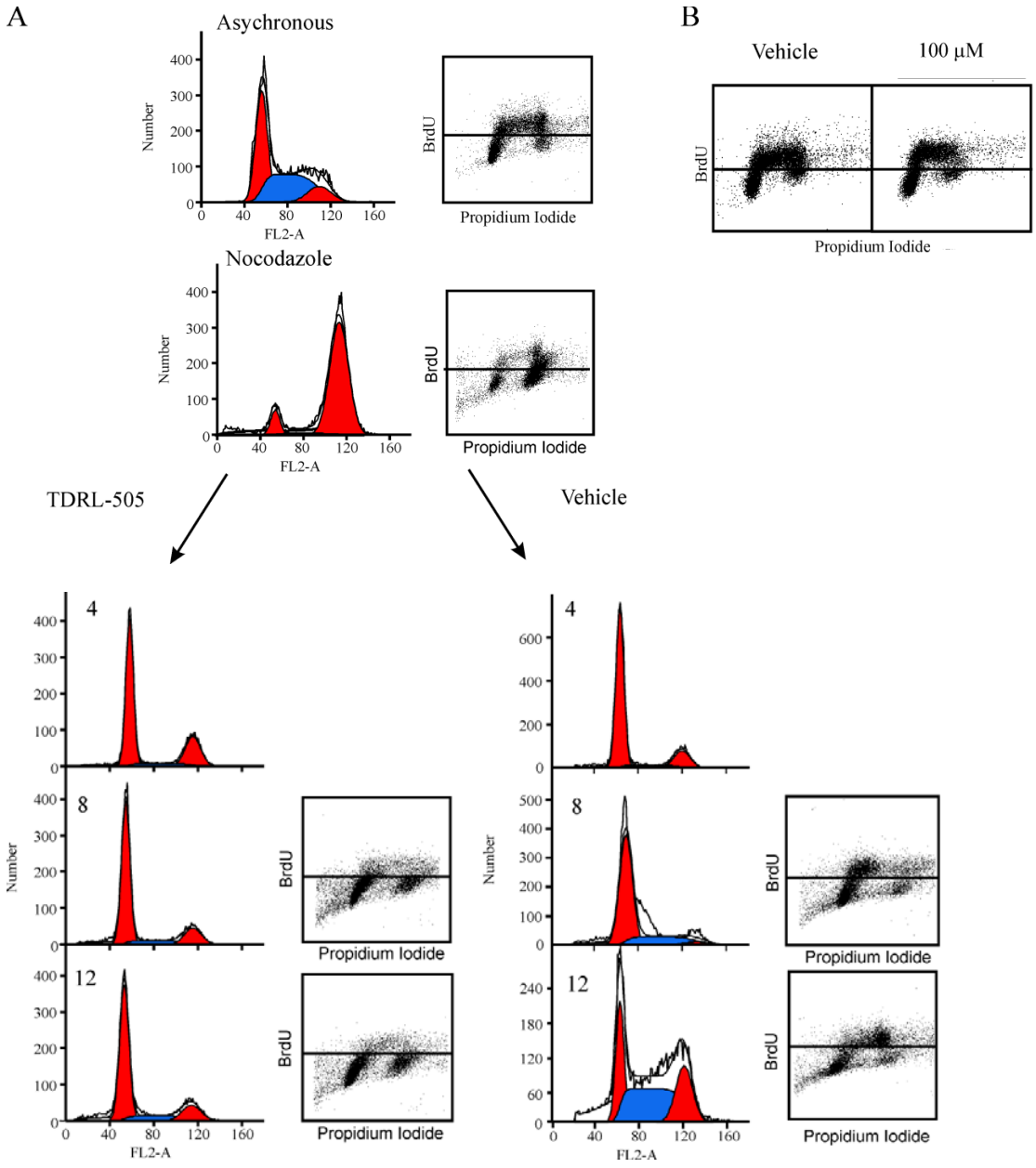

Figure 14. TDRL-505 prevents entry into S-phase. 14A. H460 cells were treated with 0.8 µg/mL nocodazole for 12 hours, washed then treated with either vehicle or 100 µM 505 for 4, 8 and 12 hours. BrdU (10 µM) was added during the final 2 hours of treatment. Cells were then harvested and analyzed using flow cytometry for cell cycle distribution and BrdU incorporation. 14B. Asynchronous cells were treated for 3 hours with either vehicle or TDRL-505. BrdU (10 µM) was added during the final hour of treatment and representative dot plots of the flow cytometry data are presented.

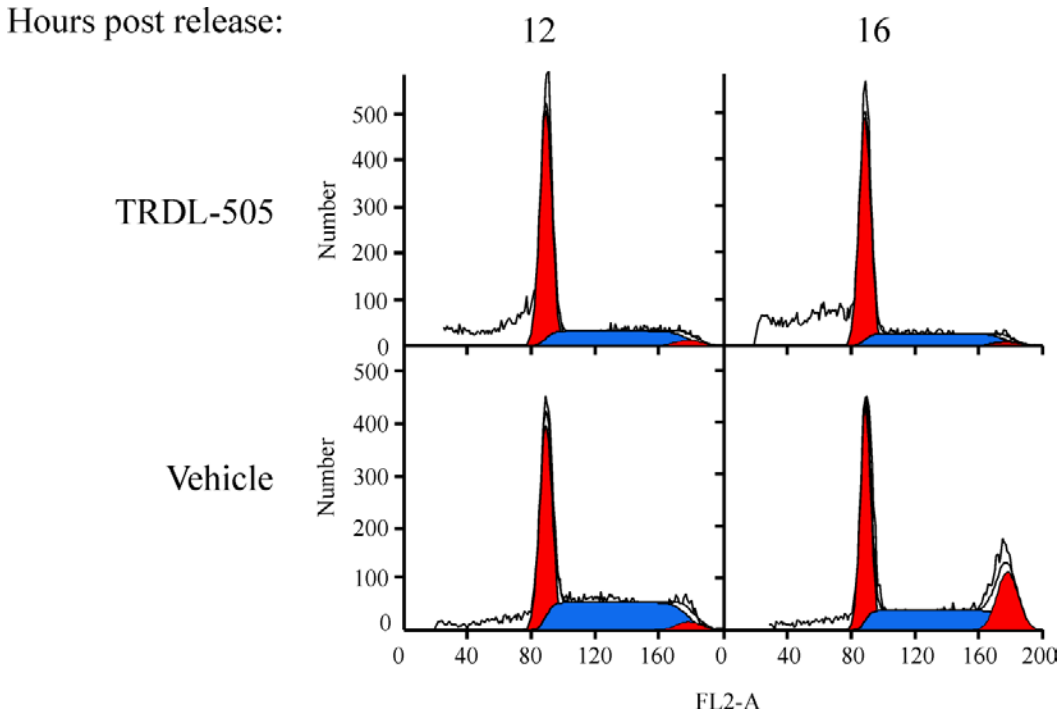

Figure 15. Removal of TDRL-505 results in progression through the cell cycle. H460 cells were treated with 0.8 µg/mL nocodazole for 12 hours to induce a G2 arrest, as seen in Figure XA. Following treatment, cells were washed and treated with 100 µM TDRL-505 for 12 hours after which cells were washed (vehicle) or compound was not removed (TDRL-505). Cells were then grown for an additional 12 or 16 hours, as indicated. Following the appropriate incubation period, cells were harvested and cell cycle distribution determined by PI staining and analysis with flow cytometry.

this activity would increase the cytotoxic effects induced by DNA damage. In order to analyze the synergistic activity of TDRL-505 with DNA damaging agents, we measured the combination index (CI), a measure of the interaction of two cytotoxic agents. We treated concurrently with increasing concentrations of cisplatin or etoposide along with increasing concentrations of TDRL-505. Combination index analyses using the Chou-Talalay method were performed with CI values greater than one indicative of an antagonistic effect, equal to one an additive effect, and less than one a synergistic effect (101). H460 cells were treated independently with cisplatin, etoposide and TDRL-505 and IC_{50} values were determined using Sigma Plot analysis (Figure 9B and Figure 16). TDRL-505 was determined to have an IC_{50} value of ~40 μM and cisplatin displayed an IC_{50} of ~4 μM (Figure 9A and Figure 16A, respectively). The IC_{50} value of etoposide was determined to be ~0.15 μM (Figure 16B). Using these values, cells were treated with increasing concentrations of total drug, maintaining a fixed ratio of the agents. AnnexinV/PI flow cytometry was conducted to examine the level of cell death and CI was calculated.

Cisplatin and TDRL-505 induced cell death individually however, when used in combination, cell viability was decreased to a level that was greater than that induced by either agent alone. CI analyses were performed and revealed a synergistic effect between the two compounds with a CI of 0.4 at the highest fraction of cells affected (Figure 17). The interaction between the agents became additive and then antagonistic (revealed from CI values greater than one) at lower fractions of cells affected (Figure 17). These results demonstrate that TDRL-505 is able to potentiate the effect of cisplatin in H460 cells and is consistent with inhibition of the cellular activity of RPA in NER.

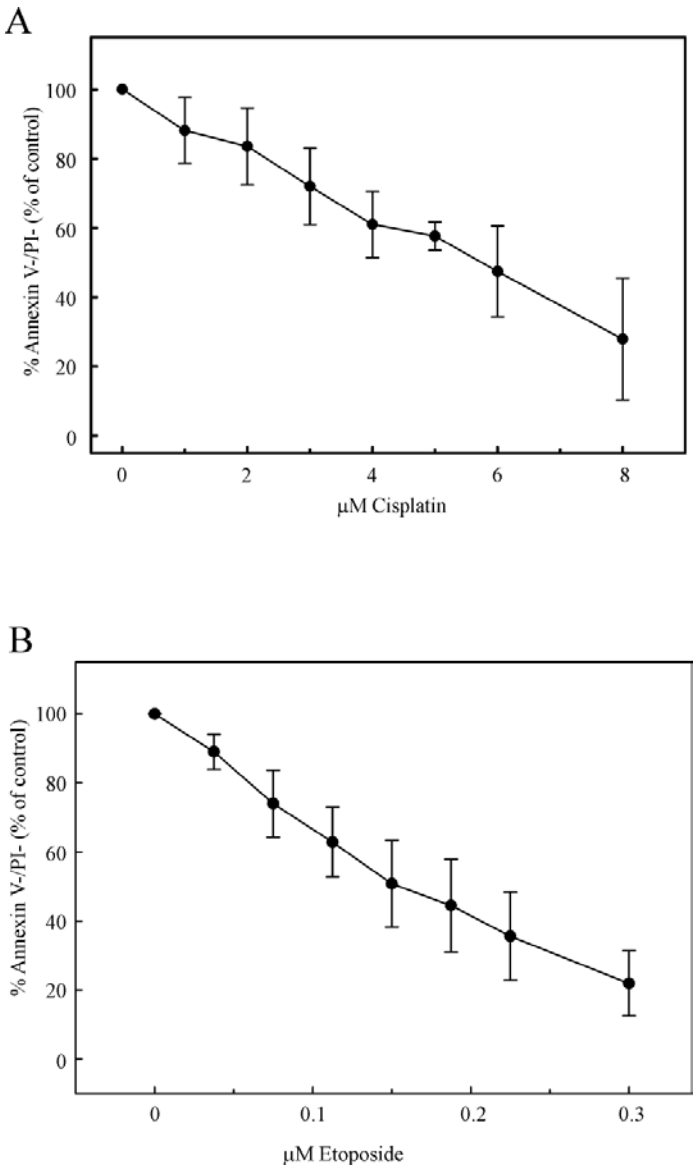

Figure 16. IC_{50} determination of Cisplatin and Etoposide in H460 cells. 16A. H460 cells were treated for 48 hours with increasing concentrations of cisplatin. Following treatment, cells were harvested and stained with PI and Annexin V and analyzed by flow cytometry. Quantification represents the average of 3 individual experiments and an IC_{50} value of ~4 µM was estimated using Sigma Plot analysis. 16B. H460 cells were treated with increasing concentrations of etoposide as indicated. Samples were analyzed and quantified as described in 16A. The IC_{50} value of etoposide was estimated to be 0.15 µM from Sigma Plot analysis.

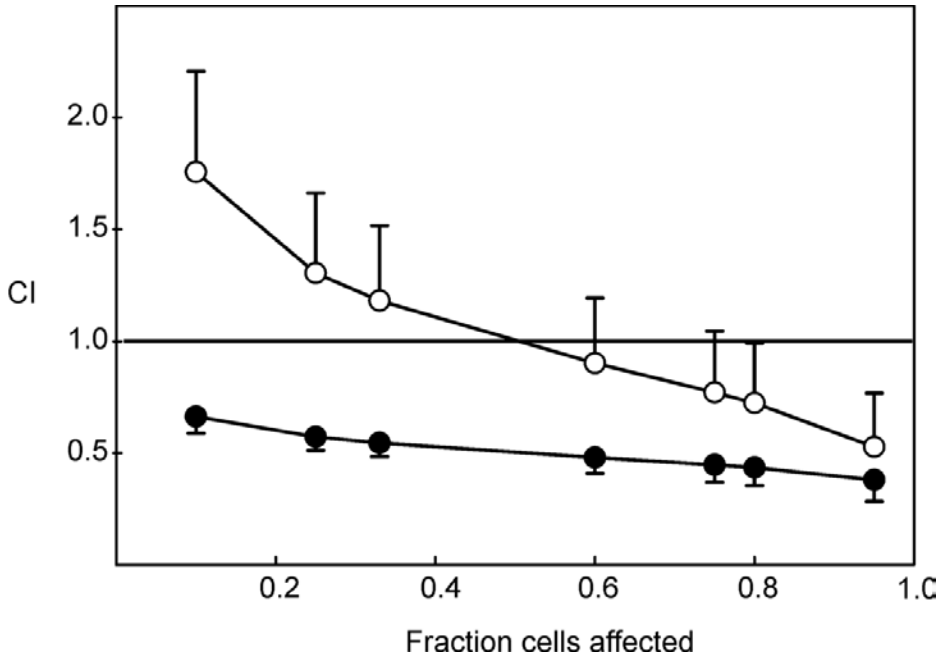

Figure 17. TDRL-505 acts synergistically with cisplatin and etoposide. H460 cells were treated with increasing fractions of the IC_{50} concentration of either cisplatin or etoposide with TDRL-505 for 48 hours. Following treatment, cells were harvested and analyzed for annexin V/PI staining using flow cytometry. Open circles indicate CI analysis of cisplatin with TDRL-505 and closed circles represent etoposide with TDRL-505. The combination index analysis was performed as described in section 2.3. The data are presented as the average ± SD from (N=3).

RPA's role in other DNA metabolic pathways led to us to examine the effect of TDRL-505 on cellular sensitivity to etoposide. Etoposide induces replication fork arrest and is thought to lead to induction of strand breakage DNA damage responses, both cellular processes that require RPA (102). Using the previously determined IC_{50} value of 0.15 μM for etoposide and 40 μM for TDRL-505 in H460 cells, cells were treated with increasing concentrations of total drug, maintaining a fixed ratio of the agents. AnnexinV/PI flow cytometry was conducted to examine the level of cell death and CI was calculated. Interestingly, TDRL-505 was found to have a synergistic effect with etoposide at all fractions of cells affected and suggests that TDRL-505 is able to inhibit the role of RPA in the repair of etoposide induced damage (Figure 17).

We sought to determine the mechanism of inhibition of TDRL-505 in the cellular response to etoposide by measuring the formation of RPA foci in response to etoposide in the presence and absence of TDRL-505. Previous work has demonstrated that RPA forms distinct foci following etoposide treatment and plays a role in the cellular response to this treatment (103). To analyze the effect on foci formation, we treated cells with 50 μM TDRL-505 in the presence or absence of 25 μM etoposide for 4 hours and then processed cells to determine the level of RPA foci formation in response to etoposide. We did not observe a dramatic difference in the formation of etoposide induced RPA foci, however, small differences were observed between TDRL-505 and vehicle treated samples (Figure 18). The overall total number of cells that showed RPA foci did not vary, however, the number of total foci formed in response to etoposide in the presence or absence of TDRL-505 did appear to be slightly different. Further work will expand

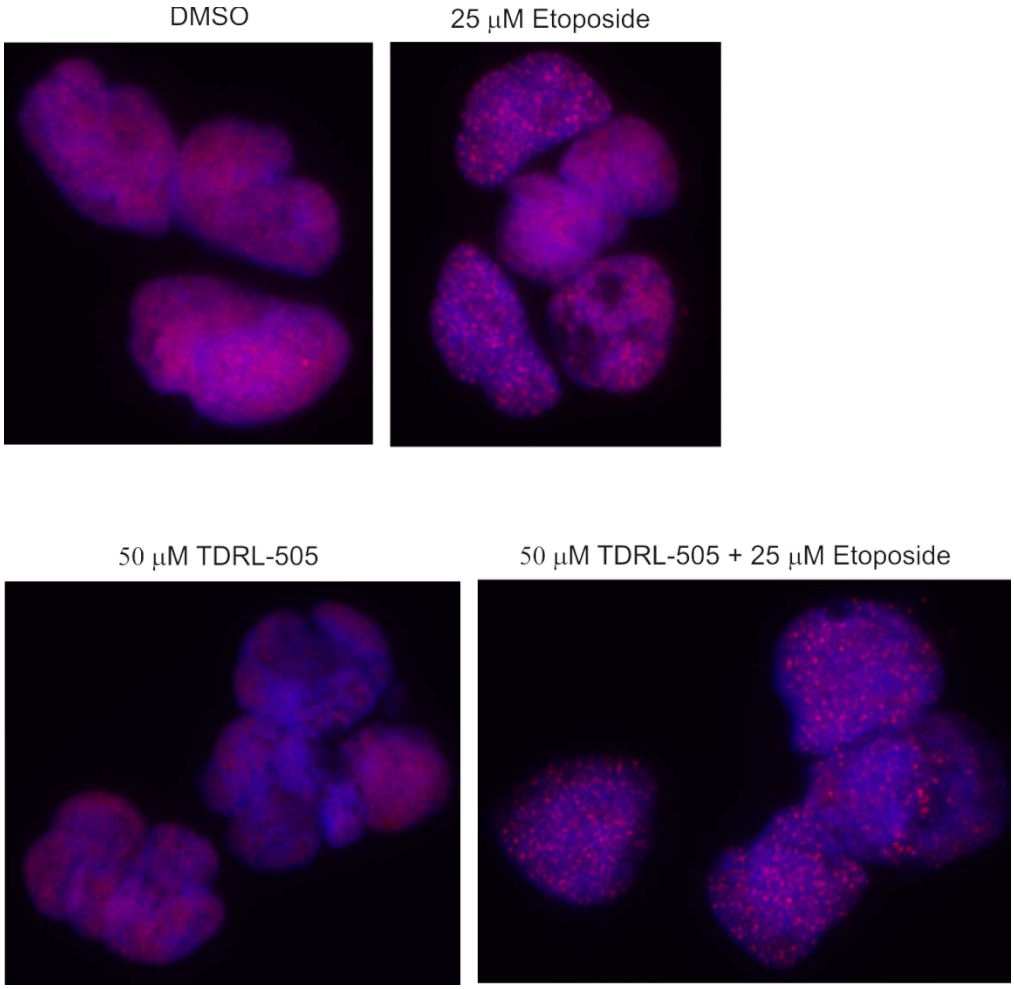

Figure 18. Indirect immunofluoresence of etoposide induced RPA foci. H460 cells were treated with either vehicle or 50 μM TDRL-505 for four hours in the presence or absence of 25 μM etoposide as described in section 2.2.12. Following incubation, cells were stained with anti-RPA p34 antibody (red) and DAPI (blue) and analyzed by microscopy as described in section 2.2.12.

our understanding of how TDRL-505 contributes to the cellular response to etoposide and the role of RPA in this response.

2.4. Discussion

Since the discovery of RPA in the late 1980s, a great deal of mechanistic information has been gained concerning both its structure and ssDNA binding activity (3, 104). In addition, its participation in DNA replication and various DNA repair pathways has been effectively studied in reconstituted *in vitro* systems (28, 105-107). Analysis of RPA function in genetic systems is complicated by the essential nature of the protein, stemming from the three subunits being encoded by separate genes (3). Differences in solubility and expression of the three subunits has also presented problems of the analysis of truncation mutations and trying to analyze each subunit individually (3). Consequently, there has been somewhat limited analysis of RPA mutants in lower eukaryotes and other model systems in addition to limitations in the purification and analysis of mutants and individual subunits. In an effort to develop reagents to probe the cellular activities of RPA, we undertook an *in vitro* high-throughput screen to identify SMIs of RPA's DNA binding activity (92). To date, the identification of inhibitors of DNA binding proteins has lagged behind analysis of inhibitors of the enzymatic activity associated with proteins, presumably due to a lack of a high-throughput protocol for analyzing DNA-binding activity. However, considering the essential role DNA binding proteins play in the progression of cancer and its response to chemotherapy, targeting this activity has the potential for vast applications in cancer treatment (91).

Inhibition of RPA's DNA binding activity in a tumor cell line would be expected to have chemotherapeutic benefits due to RPA's involvement in the essential process of

DNA replication (3). Demonstration that TDRL-505 blocks cell entry into S-phase and results in a cytotoxic/cytostatic response in addition to decreased BrdU incorporation is consistent with inhibition of RPA's role in DNA replication (100). RPA is required both for assembly and firing of pre-replication complexes and elongation, in which it predominantly participates in lagging strand DNA synthesis (108). RPA's role in the early stages of DNA replication would predict a G1-arrest as cells are unable to progress into full DNA replication rather than an intra S-phase arrest, which we have observed. The potential exists that varying the concentration of TDRL-505 and time of treatment will alter the cell cycle distribution that we have observed. While our data demonstrate a G1 block consistent with inhibiting the transition into S-phase, the potential that S-phase cells treated with TDRL-505 have reduced RPA binding and hence blocked elongation and firing of late replication forks cannot be ruled out.

Our data reveals that cells are able to re-enter S-phase following removal of TDRL-505, suggesting that RPA inhibition is reversible or that newly synthesized RPA that is not bound to TDRL-505 is responsible for supporting re-entry into the cell cycle and leading to the initiation of DNA replication. We have also demonstrated that RPA levels are not decreased following treatment with TDRL-505, however, the ability of RPA to associate tightly with DNA appears to be compromised. This presents the possibility that the cytotoxic effects observed following treatment with TDRL-505 are due to inhibition of DNA replication, leading to toxicity in cells actively replicating their DNA, or that cells are unable to fully form replication foci, signaling for cell death. However, the continuation of G1 arrest may also induce cell death after prolonged periods of time, explaining why the degree of cell death after 48 hours of treatment is

greater than the number of cells that are in S-phase. This allows for the possibility of a therapeutic window for specifically targeting actively dividing cells in the context of cancer treatment using SMIs to block the cellular activity of RPA.

The role of RPA in DNA repair also allows for inhibition of its activity to increase the efficacy of chemotherapeutics that induce DNA damage, in the context of combination therapy. Inhibition of DNA repair is anticipated to result in persistent DNA damage which is proposed to increase cytotoxicity. We therefore examined the effect of RPA inhibition in an H460 NSCLC cell line in conjunction with cisplatin and etoposide treatment. The indispensible role of RPA in the recognition and verification steps of NER is well characterized and, in addition, RPA participates in the re-synthesis step following excision of the damaged oligonucleotide (108). Previous studies have shown that cells with decreased levels of NER proteins demonstrate increased sensitivity to cisplatin treatment (39). Consistent with this, our data reveal a synergistic interaction between TDRL-505 and cisplatin at high fractions of cells affected, consistent with cellular inhibition of RPA and its role in NER. Interestingly, at low fractions of cells affected, an antagonistic interaction is observed with combination indices greater than one. This is likely the result of interactions not at the level of repair but at the level of signaling. As cisplatin leads to activation of a G2 checkpoint and induces apoptosis from an extended G2 arrest, the finding that TDRL-505 blocks cells in G1 indicates that fewer cells would be subject to cisplatin induced G2 arrest. Likewise, if TDRL-505 toxicity stems from an extended G1 arrest, the G2 checkpoint induced by cisplatin would result in less cell death as a result of treatment. At high concentrations, this effect is mitigated by the interaction at the level of DNA repair with RPA inhibition increasing cisplatin

toxicity and overcoming the antagonistic signaling interaction. The role of RPA in DNA replication restart and processing of collapsed replication forks also presents opportunities for combination therapy (109, 110). Interestingly, combination index analysis of the activity of etoposide with TDRL-505 showed synergistic activity between the two agents at all fractions of cells affected. Etoposide inhibits the enzymatic activity of topo II resulting in persistent covalent-cleavage complexes on DNA, which leads to replication fork arrest and both single- and double-strand DNA breaks (111). RPA has been demonstrated to respond to and repair these types of lesions and DNA intermediates (102). Therefore, inhibition of RPA would be expected to potentiate the effects seen by inhibiting topo II, which is observed in our analyses. Secondly, due to the asynchronous nature of these cells, at any given time a cell undergoing replication would be expected to be in various stages of replication firing. RPA is required in early replication firing and elongation, while topo II has been shown to be required for later stage replication events (112). Therefore, inhibition of both stages of replication progression would be expected to show a greater effect than inhibiting either one of the steps individually, which would implicate a synergistic relationship between TDRL-505 and etoposide, which was shown using CI analysis. The formation of RPA foci in response to etoposide was not significantly different in the presence or absence of TDRL-505. One explanation may be that although RPA is accumulating into distinct foci in response to etoposide, the exact reason for this and the role that RPA plays in etoposide response is not known (102). For instance, the overall level of direct RPA-DNA binding activity may be altered, but how this activity is involved in the cellular response to etoposide is not known. The potential exists that RPA is unable to bind to DNA but interactions with other proteins contribute

to etoposide-induced foci formation, however the actual repair of these lesions does not occur as a result of decreased RPA-DNA binding. The fact that increased cytotoxicity is observed with concurrent treatment of TDRL-505 and etoposide indicates that RPA inhibition does affect the cellular response to etoposide, however our lack of observation that decreased RPA foci form indicates that further tests examining concurrent vs. sequential treatment and variations in time and dose may tease out the mechanism of increased cellular sensitivity to etoposide treatment that we have observed.

Considering the essential role of RPA in DNA metabolism, SMIs have the potential to elucidate the specific mechanistic roles of DNA binding activity and interaction with other proteins in each of the many DNA metabolic pathways in which RPA participates. Examination of compounds that bind to particular domains within RPA has the potential to increase selectivity as well as allow the assignment of specific RPA-DNA interactions to specific pathways. Although the primary role of RPA is as a ssDNA binding protein, it is unclear how this activity is coordinated to progression of DNA metabolic pathways. For instance, previous studies have shown that mutation of up to five polar residues important for RPA-DNA interactions reduce ssDNA binding activity, but are able to complement the loss of RPA by siRNA knockdown (100). However, mutation of six polar amino acids leads to a cellular profile that is similar to that observed for knockdown of RPA (100). This data indicates that the interaction with ssDNA may be lost to some extent and cellular function of RPA is still conserved. However, the effect of mutations on the level of binding compared to complete inhibition of RPA binding to DNA with a small molecule still leaves the question of the importance of RPA's DNA binding activity on cellular function unanswered. In addition, how

interactions with other proteins are altered following either residue mutation or binding to TDRL-505 is not known, but it is possible that a conformational change induced in mutating residues within RPA or by binding to TDRL-505 can lead to altered protein interactions.

Inhibition of RPA activity and abrogation of pathway function has the potential for widespread utility in cancer treatment. While we focused on a subset of pathways, the role of RPA in several repair pathways opens up other opportunities for combination therapy. Specifically, combining molecularly targeted RPA inhibition with radiation therapy could lead to increased cytotoxicity in tumor cells via inhibition of DNA DSB repair via non-homologous DNA end joining or homology directed repair, both of which have been shown to require RPA (107, 113, 114). While targeting the enzymatic activity of proteins with small molecules is well accepted, the research presented here demonstrates the feasibility and utility of targeting a non-enzymatic protein-DNA interaction. These compounds therefore represent the first SMIs of RPA which display both *in vitro* and cellular activity. The approach of targeting RPA for cancer chemotherapy has several unique advantages including the lack of redundancy. Unlike many signaling pathways, there are no back-up systems to counter act a loss of RPA activity. While similar to oncogene signaling and the potential for oncogene addiction, RPA is essential for the continued proliferation of cancer cells and thus inhibition in rapidly dividing cancer cells provides a therapeutic window for treatment. Additionally, the spectrum of cancers that would benefit from RPA inhibition is also significant as the reliance on RPA for increased cell proliferation and repair of chemotherapeutic DNA damaging agents is not unique to any single cancer. Our targeting of the DNA binding

activity of RPA with a small, drug-like molecule sets the precedent for targeting this class of proteins and thus alters the current drug discovery paradigm to open up an entire new class of targets with potential broad spectrum utility.

3. Determining the Mode of Inhibition of TDRL-505

3.1. Introduction

Inhibition of RPA's DNA binding activity by TDRL-505 is suggestive of an interaction between TDRL-505 and the main ssDNA binding domains (DBD-A and -B) found within p70. This is evidenced by inhibition of RPA's DNA binding activity on a short 12 base substrate as shown in Figure 8C in which binding is largely restricted to DBDs-A and -B (AB region). In order to further define the interaction between TDRL-505 and RPA, we used *in silico* docking to predict where TDRL-505 interacts within the p70 domain of RPA. We purified the AB region of RPA p70 as well as a mutant heterotrimeric form of RPA, both of which were found to be inhibited by TDRL-505. Interestingly, we observed no inhibition of WT heterotrimeric RPA, mutant heterotrimeric RPA, or the AB region of p70 by TDRL-505 on dsDNA containing a 1,2 (dGpG) cisplatin lesion.

The ability of RPA to interact with many proteins found in DNA metabolic processes suggests that its role extends beyond that of a single-strand DNA binding protein and may play a larger role in signaling and ensuring maintenance of the genomic sequence. The potential of SMIs of RPA to further elucidate these actions by blocking protein-protein interactions due to either direct or indirect inhibition has the potential to provide novel biochemical information on the cellular function of RPA. Also, the ability of SMIs to inhibit RPA's role in a pathway specific manner has implications both in a chemotherapeutic context as well as in delineating the biological role of RPA in various DNA metabolic pathways.

3.2. Materials and Methods

3.2.1. Materials

DNA substrates were obtained from IDT (Coralville, IA) and prepared as described in 2.2.3. Sequences can be found in Appendix A. Wildtype RPA p11 plasmid and mutant W361A p11 plasmid were obtained from Dr. Marc Wold from the University of Iowa. Klenow fragment (5′-3′exo-, 3′-5′exo-, 5,000 units/mL) was obtained from New England Biolabs. Phosphocellulose matrix was obtained from Sigma. Goat α-XPA primary antibody was obtained from Santa Cruz Biotechnology and goat α-rabbit secondary antibody was obtained from Biorad.

3.2.2. *In Silico* Docking

In silico docking of TDRL-505 with the central DNA binding domain of RPA p70 (1FGU) was performed using Autodock 4.2 (115). Three independent grids were established 60Å in each dimension to encompass either the interdomain region, DBD-A or DBD-B. Semi-flexible automated ligand docking was performed using the Monte Carlo based simulated annealing and locality search algorithms. The most stable complexes were selected based on binding energies from multiple analyses. Coordinates of the final docked complexes were displayed with PyMOL (DeLano Scientific, LLC). Docking analysis was performed by John Turchi (Indiana University School of Medicine).

3.2.3. Purification of the AB region of RPA

The AB region of RPA p70 was prepared by transforming BL21 competent bacterial cells with pET15b-AB plasmid DNA. The cells were induced with IPTG and incubated at 37°C for two hours. Following induction, cells were harvested by centrifugation at 700 x *g* for 30 minutes at 4°C. The pellet was resuspended in buffer A (20 mM Tris, pH 7.5, 10% glycerol, 500 mM NaCl, 10 mM β-mercaptoethanol (BME) and 1 µg/mL PMSF, leupeptin and pepstatin). Cells were resuspended in 1 mL/gram of cells, sonicated and pelleted at 15,000 x *g* for 30 minutes at 4°C. The supernatant was then loaded onto a 10 mL phosphocellulose column and the flow through collected. Imidazole was added to 5 mM to the flow through which was then loaded onto a 2 mL nickel column at 0.5 mL/minute. The column was then washed with buffer A containing 50 mM imidazole after which protein was eluted from the column using a gradient from 50-500 mM imidazole. Fractions were analyzed for protein content using Bradford and SDS-Page analysis in addition to assessment of DNA binding activity as determined by anisotropy. Fractions were pooled based on those which contained the AB region and dialyzed overnight in buffer B (1 mM Hepes, pH 7.2, 10 mM DTT, 50 mM NaCl and 1 µg/mL PMSF, pepstatin and aprotinin). Aliquots were then stored at -80°C. (Purifications were performed by Sarah Shuck and Victor Anciano, Indiana University School of Medicine).

3.2.4. XPA Purification

$[His]_6$-XPA was expressed by infecting 200 mL of Sf9 cells with recombinant human XPA virus at a multiplicity of infection of 10. After 48 hour infection, cells were sedimented at 4,000 x *g* for 5 minutes at 4°C. Cells were then lysed by dounce homogenization in 30 mL of lysis buffer containing 50 mM Tris, 100 mM NaCl, 0.1% Triton X-100, 10% glycerol, 10 mM BME and 1µg/ml PMSF, pepstatin, leupeptin and aprotinin. The extract was then sonicated at 5 x 0.1s and the lysate was sedimented at 7800 x *g* at 4°C for 15 minutes. Imidazole was added to 1 mM to the supernatant and was loaded onto a 2 mL nickel-NTA agarose column at the rate of 1 mL/min. The column was then washed with nickel buffer (50 mM Tris, pH 8, 100 mM NaCl, 0.01% Triton X-100, 10% glycerol, 10 mM BME, 0.5 mM $ZnCl_2$, 1 mM imidazole and 1 µg/mL PMSF, aprotinin and pepstatin). The protein was then eluted with 20 mL of nickel buffer containing 80 mM imidazole into 1 mL fractions and protein containing fractions were identified by Bradford analysis. Fractions containing more than 50% of the total protein were pooled and applied to a 2 mL heparin-sepharose column and washed with heparin buffer (50 mM Tris, pH 7.5, 1 mM EDTA, 10% glycerol, 100 mM NaCl, 1 mM DTT and 1 µg/mL pepstatin, aprotinin and PMSF). Following column washing, protein was eluted using a gradient from 0.1 M to 1M NaCl. Protein containing fractions were identified by Bradford analysis and XPA containing fractions were identified by SDS-PAGE analysis. XPA containing fractions were pooled and dialyzed overnight in heparin buffer and stored at -80°C.

3.2.5. EMSA Analysis of AB Region of RPA p70

Purified AB region was analyzed for DNA binding activity to a 34-base purine rich ssDNA substrate (SJC 1.5 Xba). Protein was titrated from 1-100 pmol and incubated with 500 fmol of 5′[^{32}P] labeled 34-base DNA for 5 minutes at room temperature in a final reaction volume of 30 µL. Reactions were then loaded onto a 6% native polyacrylamide gel and electrophoresed at 170 volts for 1 hour. Gels were then dried and exposed to a PhosphoImager screen (Molecular Dynamics) for 30 minutes. The screen was then scanned using a Storm 820 (Amersham Biosciences) and quantified using ImageQuant software (Molecular Dynamics). It was determined that 50% of protein was bound at 10 pmol total protein. To determine the effect of TDRL-505 on AB region-DNA interactions, 10 pmol of protein was incubated for 5 minutes with either 1% DMSO or increasing concentrations of TDRL-505 as indicated in the Figure legend. TDRL-505 was diluted from a 10 mM stock into a 0.5 mM dilution in 10% DMSO and 10 µM Hepes, pH 8.0. The reactions were then mixed with 500 fmol of DNA in a final reaction volume of 30µL and incubated for five minutes at room temperature. Samples were then electrophoresed and analyzed as described above. The results indicate the average and standard deviation from at least 3 individual experiments. The IC_{50} values were calculated using Sigma Plot analysis.

3.2.6. Preparation of 1,2 cisplatin damaged DNA

SCS 1.1 and 1.2 substrates (40-nt and 41-nt, respectively) were gel purified as described in section 2.2.3. Sequences may be found in Appendix A. Following gel purification, 1 nmol of SCS 1.1 ssDNA was platinated at a final concentration of 1 pmol/µL DNA with 10 nmol of cisplatin overnight at 37°C in the dark. The 1,2 dGpG

cisplatin damaged DNA was ethanol precipitated with 3:1 volume ratio of 100% EtOH at -20°C:DNA, 0.3 M NaAc, and 20 µg/mL glycogen for 1 hour at -80°C. The DNA was then sedimented at 10,000 x *g* for 45 minutes at 4°C and then resuspended in 20 µL dH_2O and concentration determined by absorbance reading at 260 nm. The 1,2 Pt SCS 1.1 substrate was then annealed to SCS 1.2 at a ratio of 1.5:1 in a 20 µL reaction containing 50 mM Tris, pH 7.5, 10 mM MgAc, and 5 mM DTT with heating at 95°C for 5 minutes followed by cooling to room temperature for 1 hour. SCS 1.1 was then extended by 1 nucleotide (dCTP) in an extension reaction containing 10 mM Tris-HCl, 50 mM NaCl, 10 mM $MgCl_2$, and 1 mM DTT, pH 7.9 with 5 units of Klenow fragment and 0.45 µM of $\alpha[^{32}P]$dCTP by incubating at 37°C for 30 minutes. Following incubation, 200 µM non-radioactive dCTP was added to the reaction and incubated for 5 minutes at 37°C. 20 mM EDTA was then added to the reaction and dH_2O was added to bring the final volume to 50 µL. The concentration of the DNA was then determined using scintillation counting.

3.2.7. EMSA analysis of W361A and WT RPA binding to DNA

W361A mutant heterotrimer RPA was purified as described in section 2.2.4. (Victor Anciano) and analyzed for DNA binding activity. Increasing concentrations of both WT and W361A RPA (as indicated in the Figure legend) were incubated with 500 fmol of SJC 1.5 Xba (Appendix A) 34-base DNA for five minutes at room temperature in 35 µL reactions containing 1x agarose dye (see section 2.2.6). Following incubation, reactions were loaded onto a 6% non-denaturing polyacrylamide gel and electrophoresed at 170 volts for 1 hour. Gels were then dried and exposed to a PhosphoImager screen (Molecular Dynamics) for 30 minutes. The screen was then scanned using a Storm 820

(Amersham Biosciences) and quantified using ImageQuant software (Molecular Dynamics).

3.2.8. EMSA analysis of WT and W361A RPA with TDRL-505

Increasing concentrations of TDRL-505 were incubated with 125 nM WT RPA or 250 nM W361A mutant RPA for five minutes at room temperature as described in section 2.2.6. Following incubation, 12.5 nM 1,2 Pt damaged SCS 1.1/1.2 dsDNA was added to the reactions which were incubated an additional five minutes at room temperature. Samples were then processed and analyzed as described in section 2.2.6. The results indicate the average and standard deviation from at least 3 individual experiments.

3.2.9. ELISA Analysis of RPA-XPA interactions

To determine the effect of TDRL-505 on RPA-XPA interactions, 200 ng of purified XPA (section 3.2.4) was incubated with 100 µL of PBS overnight in a 96-well ELISA plate at 4°C. Following XPA binding, wells were washed 3 x 5 minutes with 200 µL PBS. 200 µL of blocking buffer (PBS + 2% BSA) was added to each well for 2 hours at room temperature with rocking. Following blocking, 300 ng of RPA was pre-incubated with increasing concentrations of TDRL-505 in blocking buffer containing 3% DMSO in 100 µL reactions for 10 minutes at room temperature, following which 50 µL was added to each well, in duplicate, for 1 hour with rocking. Following incubation, wells were washed 3 x 5 minutes with 200 µL blocking buffer after which 50 µL mouse anti-RPA p34 antibody (Neomarkers) (1:500 in blocking buffer) was added to each well for 1 hour with rocking. Wells were then washed 3 x 5 minutes with 200 µL blocking buffer after which 50 µL of goat anti-mouse secondary antibody (Santa Cruz

Biotechnology) (1:2500 in blocking buffer) was added to each well for one hour with rocking. Following the final wash, 100 µL of TMB-ELISA reagent (Thermo Scientific) was added to each well and kinetic analysis was performed with readings at wavelengths 370 and 490 nm at 30 second intervals for 20 minutes on a SpectraMax M5 (Molecular Devices, Silicon Valley, CA). The results indicate the average and standard deviation from at least 3 individual experiments.

3.2.10. ELISA Analysis of XPA-DNA interactions with TDRL-505

ELISAs were performed by binding 200 fmol per well of biotinylated 60-nt single-strand DNA in blocking buffer (2% BSA TBS-Tween) overnight on strepavadin coated plates (Roche Applied Science). Inhibition of protein binding was examined by incubating 10 ng of purified XPA with increasing concentrations of TDRL-505 as indicated in 150 µL reactions containing 5% DMSO and blocking buffer for 10 minutes at room temperature. Following incubation, 100 µL of the reaction was added to each well, in duplicate, and incubated for 1 hour with rocking. The amount of protein bound to DNA was analyzed by incubating 50 µL of goat anti-XPA antibody (Santa Cruz Biotechnology) (1:1000 in blocking buffer) in each well for 30 minutes with rocking. Following incubation with primary antibody, wells were washed 3 x 5 minutes with 200 µL of blocking buffer followed by the addition of 50 µL of goat anti-rabbit secondary antibody (Biorad) (1:2500 in blocking buffer) for 30 minutes. Wells were then washed as described above and 100 µL of TMB-ELISA reagent (Thermo Scientific) was added to each well. Kinetic reads were performed using a SpectraMax M5 spectrophotometer (Molecular Devices, Silicon Valley, CA) for 20 minutes at 30 second intervals at 370 and

490 nm wavelengths. The results indicate the average and standard deviation from at least 3 individual experiments.

3.3. Results

Molecular Modeling of AB Domain of RPA p70

We undertook a molecular modeling approach to determine if the OB-folds of RPA p70 were the potential target of TDRL-505. The crystal structure of RPA p70 181-422 was previously solved in the absence of DNA by Bochkareva et al. (116) and 3-dimensional data obtained from the protein data bank (1FGU). TDRL-505 was prepared as the ligand using Autodock tools 1.5.2 as described in section 3.2.2. A semi-flexible approach was employed maintaining RPA in a rigid conformation and allowing flexibility of the ligand. Docking was performed using Autodock 4.2 with random initial positioning of the ligand and three potential binding sites were identified based on the lowest interaction energies. These sites include each of the OB-folds (DBD-A and -B) and the interdomain region between the two folds (Figure 19). The most stable interaction was with DBD-B and the conformation of TDRL-505 within this site is depicted in green. DBD-A domain (TDRL-505 in blue) ranked second in binding energy and lastly the interdomain region (TDRL-505 in red). The close-up of the interaction presented in the insets reveal that most of the stability is driven via hydrophobic interactions, although the conserved oxo-butyric acid is stabilized via interactions with basic amino acids in each of the three positions. To determine the relative importance of the interaction of TDRL-505 with each domain, docking analysis of TDRL-518 was performed. TDRL-518 shows no inhibition of RPA's DNA binding activity *in vitro* and

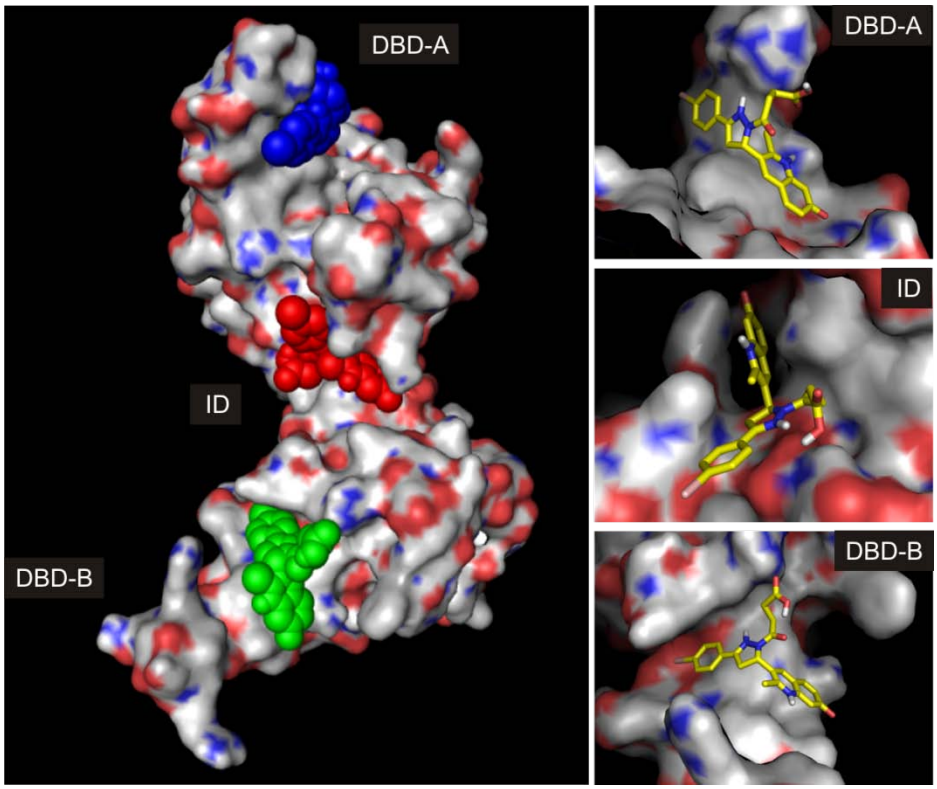

Figure 19. Docking analysis of TDRL-505 in the AB region of RPA. Surface representation of RPA p70 181-422 (1FGU) with TDRL-505 docked in DBD-A (blue), DBA B (green) and the interdomain region (red). Each insert is a close up of the interaction of each respective domain with TDRL-505 as modeled to give the lowest activation energy.

dramatic alterations in binding energies were obtained. Significantly increased ΔG values were obtained for interactions with DBD-B and the interdomain region while only modest increases were calculated for the interaction with DBD-A. These data suggest that the majority of the inhibitory effect of TDRL-505 is manifested through interaction with the DBD-B OB-fold.

TDRL-505 inhibits RPA AB region interactions with DNA

Molecular modeling analysis revealed a thermodynamically favorable interaction between TDRL-505 and regions in the AB domain and we wished to determine the effect of TDRL-505 on the *in vitro* DNA binding activity of the AB region of RPA. This region extends from amino acids 181-432 and has been purified and analyzed for DNA binding activity and displays approximately 1/25 activity compared to WT RPA (117). A subset of this region from amino acids 181-422 was crystallized in complex with a $(dC)_8$ DNA substrate and the structure solved in addition to a DNA-free structure with the entire 181-432 amino acid region (54, 116). In order to examine the effect of TDRL-505 on the AB region alone, we cloned the region of RPA from amino acids 181-432 in the p70 subunit of RPA and expressed it in a pET15b plasmid expression system (Jennifer Earley, Indiana University School of Medicine). The AB region was purified from BL21 *E. coli* cells and analyzed for DNA binding activity (Figure 20A) (Victor Anciano and Sarah Shuck). EMSA analysis revealed binding to a 34-base substrate with 50% of protein bound at 5 pmol total protein (Figure 20B). Examination of TDRL-505 on inhibiting the AB region from binding to DNA revealed a concentration dependent decrease in AB binding with an IC_{50} of 40 μM (Figure 21).

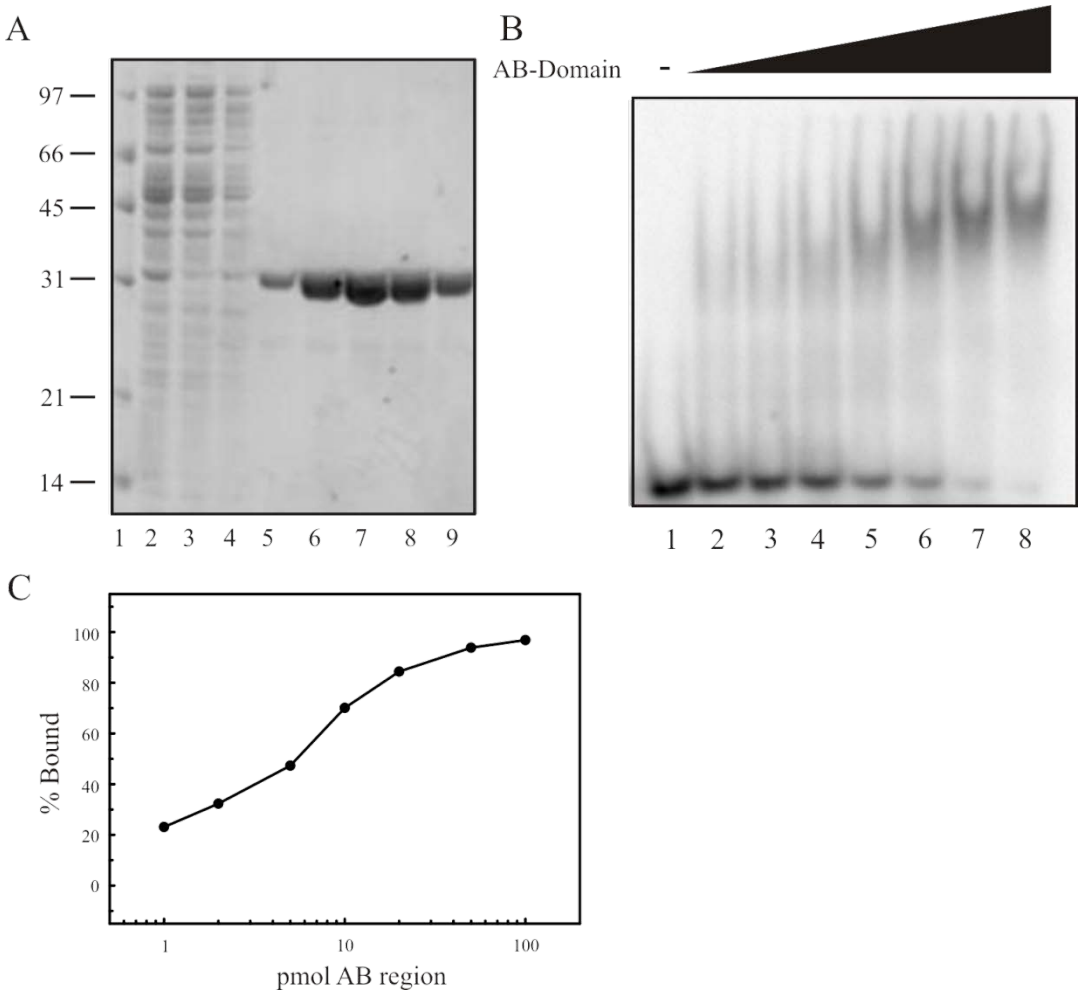

Figure 20. AB region of RPA binding to DNA. 20A. The AB region of RPA was cloned and purified as described in section 3.2.3. Lane 1-Low molecular weight marker, 2-Whole cell extract, 3-Nickel column, flow through, 4-Nickel column, wash, 5-9-Nickel column fractions. 20B. EMSA analysis of the AB region binding to SJC 1.5 Xba dsDNA (Appendix A). Increasing amounts of the AB region were incubated with 500 fmol of DNA and electrophoresed as described in section 3.2.5. The percentage of protein bound relative to the total pmol of protein in each reaction was quantified and displayed in 20C.

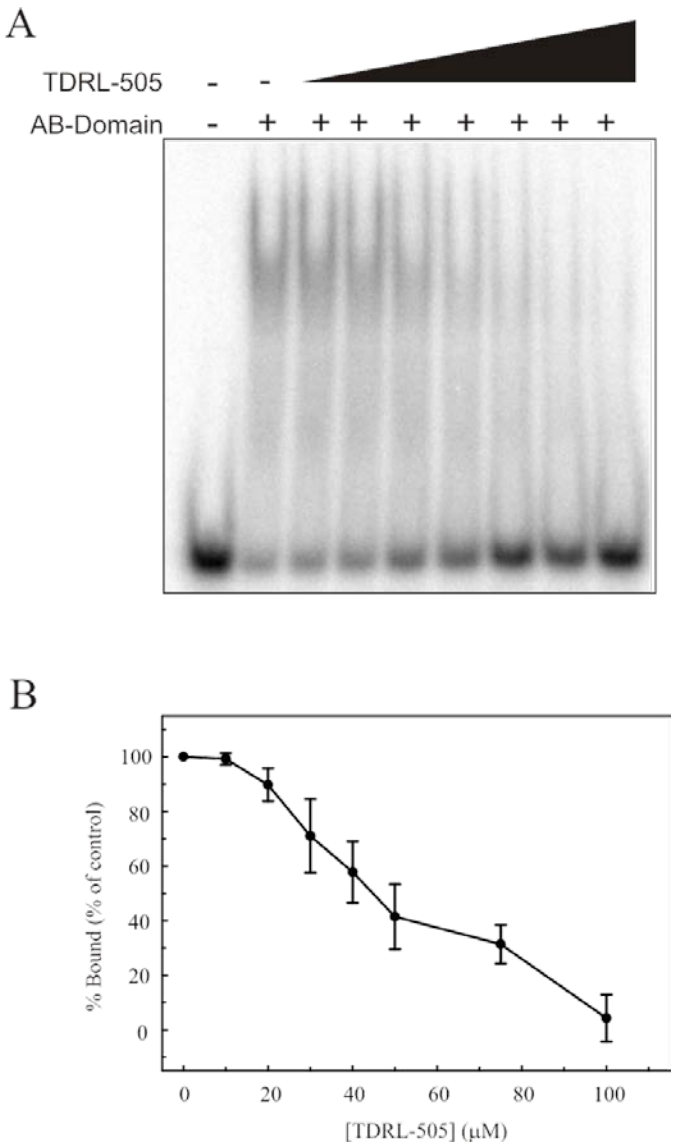

Figure 21. Inhibition of AB region binding to DNA by TDRL-505. 21A. 10 pmol of the AB region was pre-incubated with increasing concentrations of TDRL-505 as described in section 3.2.5. 500 fmol of SJC 1.5 Xba ssDNA (Appendix A) was then added to each reaction and electrophoresed on a native polyacrylamide gel. 21B. Quantification of 21A. The data represent quantification and standard deviation of 4 independent experiments.

Identification of residues potentially important for TDRL-505 interaction with RPA

In order to further discern the mode of interaction between RPA and TDRL-505, we examined the potential sites of interaction between TDRL-505 and the AB region of RPA. We chose to examine amino acids found within DBD-B and the interdomain region that are in close proximity for interaction with TDRL-505 based on the *in silico* docking studies. We examined RPA in the open conformation, as is seen in Figure 4A. Modeling of TDRL-505 is shown in Figure 22 and two residues, W361 and K273 were identified from DBD-B and the interdomain region, respectively, as potential sites of interaction with TDRL-505. Previous work from Dr. Marc Wold's laboratory has identified a W361A mutation that has reduced DNA binding activity, indicating its importance in DNA interactions (118). In order to measure the effect of a residue on TDRL-505 activity, RPA's DNA binding activity must be retained, making W361A an attractive mutation to study due to its preservation, albeit reduced DNA binding activity. In addition to the close proximity between W361 and TDRL-505, this residue is found within the DNA binding domain, which we think is the mode of contact of TDRL-505. In order to measure the contribution of W361 on stabilizing TDRL-505, we obtained the full length RPA p11 plasmid containing the W361A mutation from Dr. Marc Wold (University of Iowa) and purified this protein (Figure 23A, Victor Anciano). We observed approximately a 20% decrease in W361A RPA binding compared to WT RPA when examining binding to SJC 1.5 Xba (sequence in Appendix A), consistent with previous data (118). However, no difference in inhibition by TDRL-505 was observed, indicating that this residue is not required for the stable binding of TDRL-505 (data not shown). Because TDRL-505 was modeled with RPA in the open conformation, the

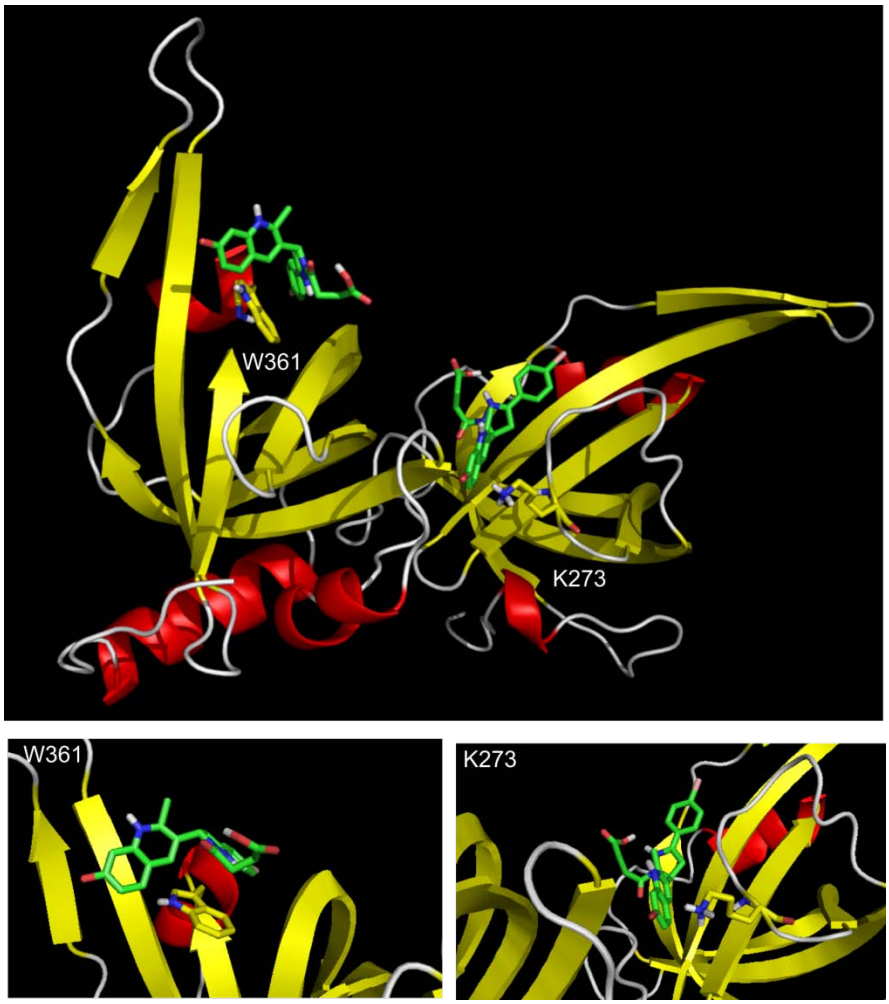

Figure 22. Modeling of TDRL-505 in AB Region. The crystal structure of RPA p70 from residues 181-422 was analyzed using PYMOL analysis of the PBD file 1FGU. TDRL-505 was modeled against DBD-B and the interdomain region. Close up of each region is represented with the DBD-B region on the left panel and the interdomain region on the right. W361 and K273 are displayed as indicated.

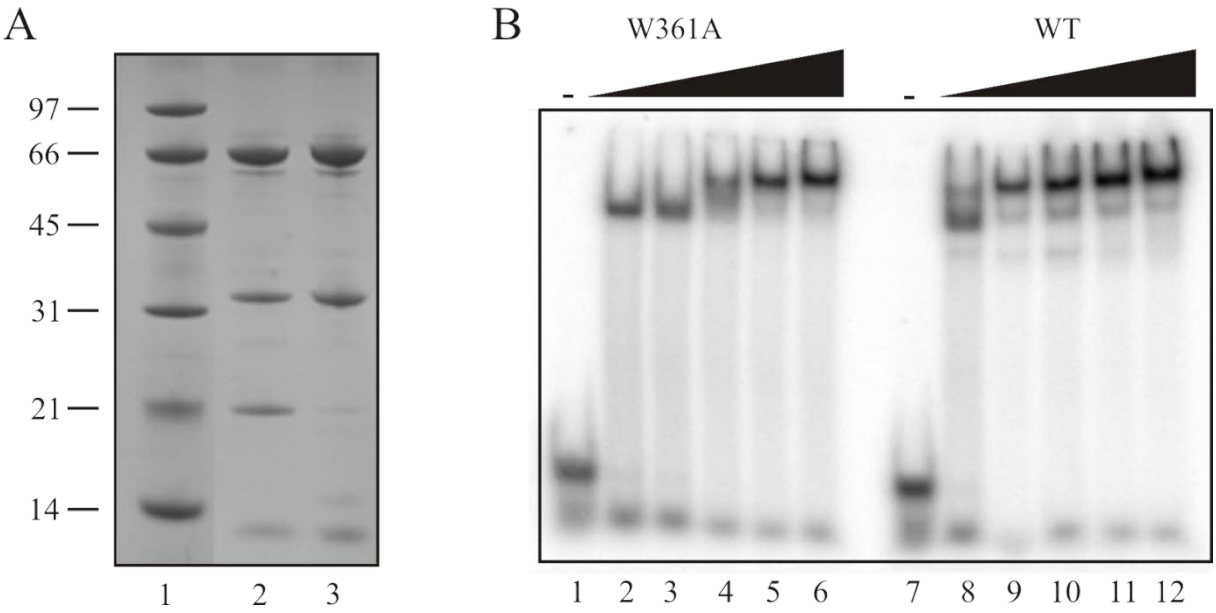

Figure 23. Purification and characterization of RPA W361A mutant. 23A. Mutant W361A RPA was expressed and purified as described in section 2.2.4. Purified protein was analyzed by SDS-Page analysis and was stained with coomassie blue. Lane 1-Low molecular weight marker, 2-W361A, pool A, 3-W361A, pool B. 23B. EMSA analysis of W361A and WT RPA binding to 34-base ssDNA (SJC 1.5 Xba). Lanes 1 and 7 indicate DNA with no RPA. Lanes 2-6 and 8-12 indicate 0.5, 1, 2.5, 5 and 10 pmol of total protein.

potential exists that TDRL-505 interacts with RPA and induces a conformational change that is similar to that seen with DNA. Therefore, W361 may not be within proximity to interact with TDRL-505 if the conformation of this protein is dramatically altered following binding of TDRL-505.

TDRL-505 does not inhibit RPA binding to 1,2 cisplatin damaged DNA

Previous work has shown that RPA has a preference to bind to cisplatin damaged DNA compared to undamaged duplex (60). It was hypothesized that this increase in binding activity is due to RPA recognizing the single-strand DNA character that is introduced in the duplex by the cisplatin adduct (60). However, which OB-folds are important for this binding activity has not been elucidated. After determining that the mode of interaction between TDRL-505 and RPA appears to be within the AB region of RPA, we examined the ability of TDRL-505 to inhibit RPA binding to 1,2 Pt damaged dsDNA (SCS 1.1/1.2, sequences in Appendix A) to determine the contribution of the AB region to binding this type of lesion. We did not observe any significant inhibition of binding with TDRL-505 when tested at 50 μM, indicating the area in which TDRL-505 interacts with RPA is not important for RPA's interaction with 1,2 Pt dsDNA (Figure 24). We also examined the ability of W361A RPA to bind to 1,2 Pt dsDNA to determine its contribution to binding to 1,2 Pt damaged DNA. We observed binding by W361A at half the maximum level of binding for WT RPA, which is similar to that seen for binding to ssDNA (Figure 24A). This result indicates that W361 is not required for interaction with 1,2 Pt damaged 41-nt DNA, although it may contribute to binding to some extent. The ability of TDRL-505 to inhibit binding of W361A RPA to 1,2 Pt damaged DNA was also analyzed and no inhibition of binding was observed, similar to the results obtained for

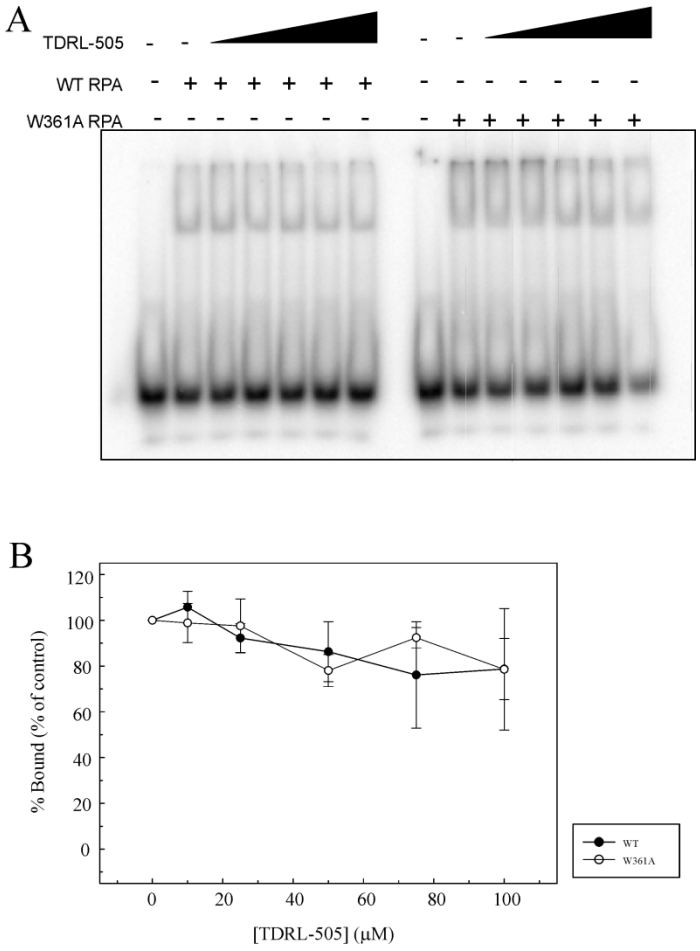

Figure 24. TDRL-505 does not inhibit RPA binding to 1,2 cisplatin damaged DNA. 24A. WT or W361 mutant RPA was pre-incubated with increasing concentrations of TDRL-505 as indicated in 24B. Following pre-incubation, 500 fmol of 1,2 Pt damaged dsDNA was added to each reaction and incubated for an additional 5 minutes. Samples were then electrophoresed on 6% native polyacrylamide gels and analyzed as described in section 3.2.8. 24B. The percentage of RPA bound compared to RPA control was calculated and the average and standard deviation from 3 independent experiments are presented.

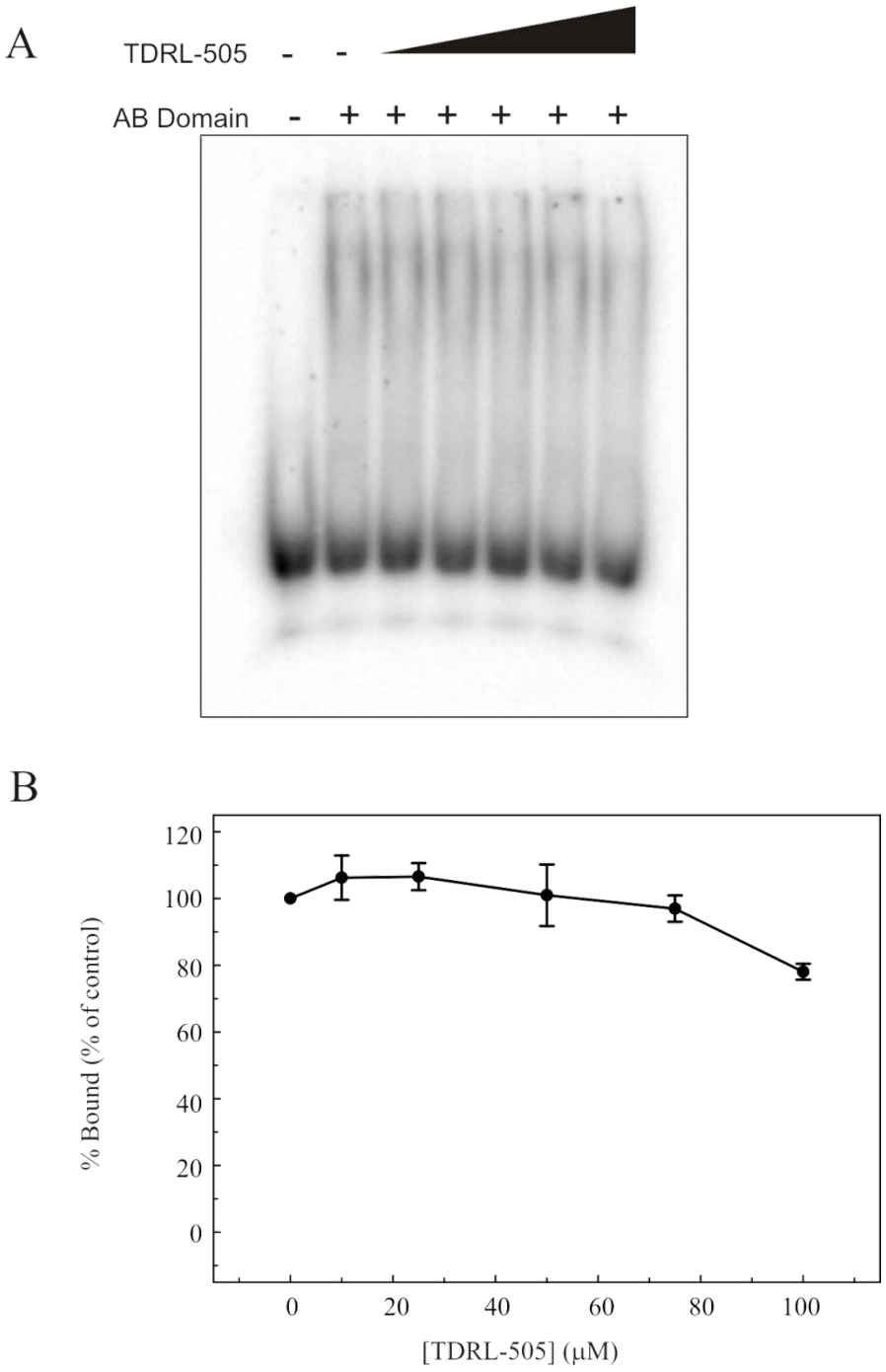

Figure 25. EMSA analysis of the AB region of RPA binding to 1,2 Pt dsDNA. 25A. Increasing concentrations of TDRL-505 were incubated with purified AB region of RPA as described in section 3.2.5. Following incubation, 500 fmol of SJC 1.5 Xba DNA was added to each reaction after which they were electrophoresed on a 6% native gel and visualized as described in section 3.2.5. 25B. Quantification of 26A, the results represent the average and standard deviation from at least 3 independent experiments.

WT RPA (Figure 24). Binding to 1,2 Pt dsDNA by the AB region of RPA was also examined. A significant amount of protein (500 pmol compared to 5 pmol of WT RPA) was required to see ~40% of protein binding but an interaction between the AB region and 1,2 Pt dsDNA was observed. Analysis of this interaction in the presence of TDRL-505 revealed no inhibitory activity on this substrate (Figure 25).

TDRL-505 inhibits the XPA-RPA interaction

Previous studies have shown that RPA interacts with XPA through the p34 and p70 subunits (119). In order to determine if TDRL-505 affects the interaction between RPA and XPA and to further define the mode of interaction between TDRL-505 and RPA, we employed ELISA analysis to examine the RPA-XPA interaction. XPA (10 ng) was bound to an ELISA plate overnight following which 300 ng of RPA pre-incubated with increasing concentrations of TDRL-505 were added to each well containing XPA. Antibody against RPA was then added to each well and the amount of RPA that was bound to XPA was determined. As shown in Figure 26A, the interaction between RPA and XPA is inhibited, albeit with a fairly high concentration of TDRL-505. Immunoprecipitation experiments were performed in order to ascertain if TDRL-505 inhibits the interaction between the p34 antibody and the p34 subunit (data not shown). These experiments indicate that TDRL-505 does not inhibit this interaction, indicating that the observed loss of RPA-XPA binding is due to inhibition of the interaction between the two proteins and is not a result of decreased detection.

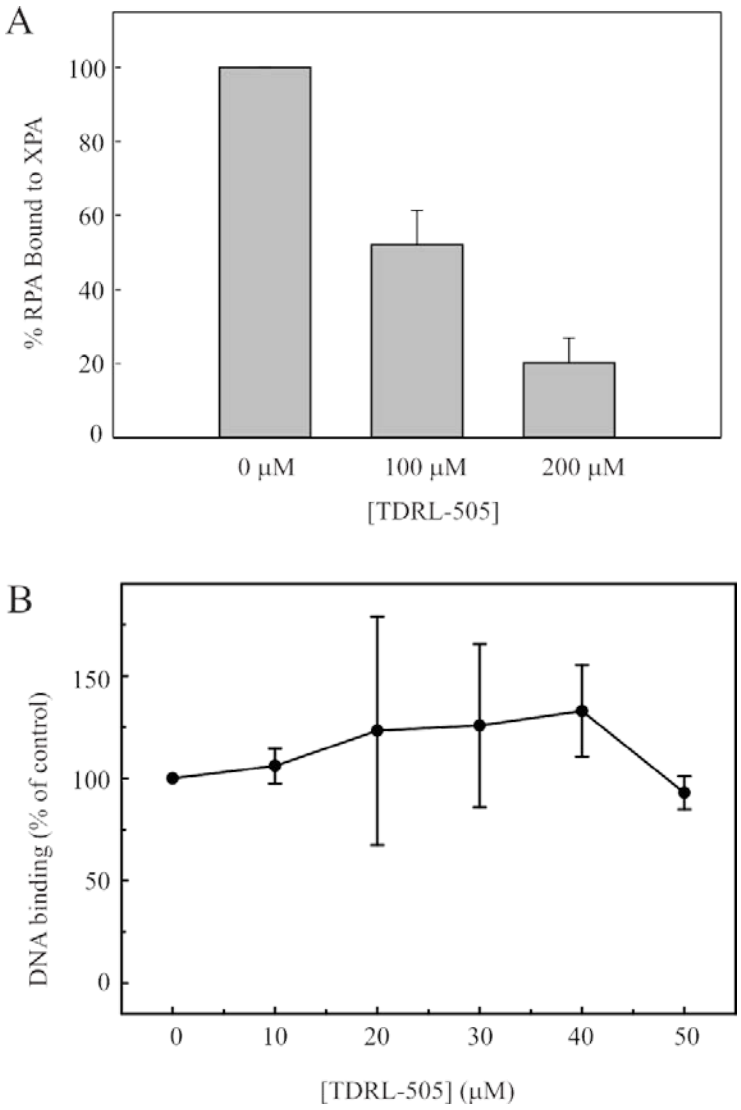

Figure 26. TDRL-505 inhibits the interaction between RPA and XPA but does not inhibit XPA binding to DNA. 26A. XPA was bound to ELISA plates as described in section 3.2.9. Increasing concentrations of TDRL-505 were pre-incubated with RPA and then added in duplicate to the ELISA plate. The ELISA assay was performed as described in section 3.2.9. The graph represents the average and standard deviation of 4 independent experiments. 26B. XPA binding to 60-nt ssDNA was assessed using ELISA analysis as described in section 3.2.10. Increasing concentrations of TDRL-505 were pre-incubated with 10 ng of XPA and then added in duplicate to the ELISA plate. The assay was performed as described in section 3.2.10. The graph represents the average and standard deviation of 5 independent experiments.

TDRL-505 does not inhibit the XPA-DNA interaction

In order to determine the specificity of TDRL-505 for RPA, we measured the ability of the compound to inhibit XPA's DNA binding activity. Although RPA and XPA interact with DNA differently, they both participate in an early step of nucleotide excision repair and are thought to be important for recognizing damaged DNA. XPA shows varying degrees of DNA binding activity when examined using EMSA analysis, prompting us to employ a different method to measure this activity. We therefore used ELISA analysis to measure XPA binding to TMN 1.1 biotinylated 60-nt DNA. TDRL-505 was titrated up to 50 μM as shown in Figure 26B, however no inhibition of XPA binding was observed, indicating some degree of specificity of TDRL-505 for RPA. Analysis of inhibition on an OB-fold containing protein such as Pot1 might give further indication of the specificity of TDRL-505 for RPA.

3.4. Discussion

Considering the complexity of the RPA structure, which is comprised of six OB-folds distributed throughout three subunits, targeting DNA binding activity using a SMI has the potential to elucidate the contribution of these various regions to the numerous activities of RPA in DNA replication, repair and recombination. Targeting a particular OB-fold may allow for pathway-specific targeting of RPA. For instance, one could inhibit RPA's activity in NER and not in replication which would present clinical utility in cancer treatment to allow synergy with other agents while limiting potential toxicity. It has been suggested the OB-folds beyond DBD-A and -B contribute to RPA's interaction with different DNA substrates stemming from the observation that DBD-A and -B can accommodate a $(dC)_8$ DNA substrate, however variations in binding constants

are observed on sequences of various length, indicating a role for additional OB-folds in the RPA-DNA interaction (3). Our observation that TDRL-505 can specifically inhibit the AB region of p70 from binding to DNA supports the molecular modeling data in which energetically favorable binding was observed within DBD-A and -B as well as the interdomain region.

TDRL-505 does not inhibit RPA-DNA interactions when examining a 1,2 dGpG cisplatin lesion on a 41-nt dsDNA susbstrate (SCS 1.1/1.2). Previous data has shown that the binding of RPA to this type of substrate is a result of RPA binding to and separating duplex DNA and the observed gel shift is the result of RPA bound to undamaged ssDNA (120). Our observations indicate that the mode of interaction between RPA and 1,2 Pt damaged dsDNA is not inhibited by TDRL-505. Attempts to measure the strand separation activity of RPA on this substrate have not indicated clear strand separation, however additional work may further define this activity (data not shown). Our results indicate that mode of interaction between heterotrimeric WT RPA is different when comparing ssDNA to 1,2 Pt damaged DNA. The potential exists that TDRL-505 binding to RPA prevents the AB region from interacting with 1,2 Pt damaged DNA and therefore other regions of RPA are important for this interaction. It is also possible that the initial binding step to this substrate does not require the AB region, however it is required to form a stable complex. For instance, if TDRL-505 is transiently binding to RPA, initial binding by another region could bring the AB region into close proximity to the substrate and if TDRL-505 becomes unbound, the AB region is then free to interact with DNA. This is not observed for ssDNA substrates because the AB region is the main domain responsible for ssDNA interactions and TDRL-505 may never become unbound long

enough to permit this interaction. It is also possible that the AB region is not required for binding to this substrate but is required for processing of the cisplatin adducts and/or strand separation activity. Further experiments to determine the effect of TDRL-505 on the binding of other NER proteins and the processing of Pt lesions will result in a clearer understanding of how RPA's ssDNA binding activity is required in DNA metabolic processes.

The fact that no inhibition of the AB region binding to 1,2 Pt dsDNA was observed indicates that this region is sufficient for binding to this substrate. Previous work has identified that RPA binding is correlated to ssDNA that is produced as a result of its strand separation activity (120). We are currently working to elucidate if the AB region has DNA unwinding activity and if this correlates with DNA binding activity that we observe. Observation that TDRL-505 does not inhibit AB region binding to 1,2 Pt DNA indicates that this region is interacting with this DNA substrate differently than that observed for ssDNA and that TDRL-505 does not block this interaction. Because only a short DNA sequence was modeled in the crystal structure of the AB region, it is unclear how this region is interacting with a longer, cisplatin damaged substrate. Also, the large amount of protein it takes to bind ~40% this substrate compared to ssDNA (500 pmol vs. 10 pmol) indicates that the mode of interaction is different, either in the sense of decreased strand separation activity of if there is no strand separation activity, a decrease in the amount of binding to the damaged substrate. The potential also exists in which the on and off rates of the AB region for 1,2 Pt DNA are such that detection of inhibition of binding is not possible using EMSA analysis.

Further analysis examining the effect of TDRL-505 in preventing the XPA-RPA interaction determined that this interaction is prevented at high concentrations, without affecting the ability of XPA to bind to ssDNA. The interaction domain between RPA and XPA is primarily thought to be located within the p34 subunit of RPA, but there is some evidence that p70 can interact as well, although perhaps to a lower extent (119, 121). Therefore, inhibition of the XPA-RPA interaction with TDRL-505 supports targeting of DBD-A and -B, and decreasing the ability of these two subunits to interact. It is unclear if this inhibition is due to direct steric hindrance of TDRL-505 in preventing the XPA-RPA interaction, or if binding of DBD-A and -B to TDRL-505 somehow induces a conformational change that prevents the XPA-RPA interaction. It would be interesting to examine the affect of TDRL-505 on RPA's influence on XPA's DNA binding activity. It is unclear at this point if RPA is required to bind to DNA in order to interact with XPA and/or recruit it to sites of damage. To determine the specificity of TDRL-505 for RPA, we examined its ability to inhibit XPA's DNA binding activity. We did not observe any decrease in XPA binding to ssDNA up to 50 μM of TDRL-505, providing evidence that inhibition of the RPA-XPA interaction is due to specific binding of TDRL-505 to RPA. By targeting DBD-A and -B, we have shown inhibition of RPA's ssDNA binding activity but not inhibition of binding to 1,2 Pt dsDNA, implicating other OB folds in this interaction. Current work is being conducted to crystallize the AB region with TDRL-505 to further determine the sites of interaction. We are also currently working on making additional mutations within RPA to elucidate which residues are important for the interaction between RPA and TDRL-505. The ability to specifically target particular OB-folds within RPA presents the possibility that SMIs can be designed to inhibit

pathway specific roles of RPA, allowing for this protein to be targeted within individual repair pathways and/or within replication. This has the potential to further elucidate the role of RPA within DNA repair pathways and replication and also presents the possibility of targeting RPA's role in a specific pathway in a clinical setting. This inhibition can be coupled with chemotherapeutic treatments and may minimize toxic side effects that might occur from solely inhibiting DNA replication.

4. Small Molecule Inhibition of Xeroderma Pigmentosum Group A

4.1. Introduction

Mutations in XPA account for 90% of the observed phenotype in XP, highlighting the essential nature of this protein for efficient NER (9). In addition to its role in cancer development, XPA has been implicated in chemotherapeutic response to cisplatin treatment (39). As discussed previously, sensitivity to cisplatin treatment has been correlated with protein levels of XPA in testicular cancer, drawing a link between DNA damage repair and chemotherapeutic treatment (38). Attempts to increase sensitivity to cisplatin treatment continue to be pursued as a means to increase efficacy of this treatment. Currently, clinical correlations between DNA repair capacity and chemotherapeutic sensitivity are being investigated and the potential exists that repair capacity may be used as a prognostic indicator for the expected outcome following treatment as well as a means to individually tailor chemotherapeutic treatment.

Using an *in silico* screening assay performed by Dr. J.T. Zhang's laboratory (Indiana University School of Medicine), we have identified a series of small molecules that dock within the DNA binding domain of XPA. *In vitro* analysis of these small molecules by Tracy Neher (Indiana University School of Medicine) has identified a class of compounds that show inhibition of XPA's DNA binding activity. Secondary screening assays have confirmed one of these compounds, 3172-0796 which shows inhibitory activity on ssDNA, dsDNA and 1,2 Pt damaged dsDNA. The effect of 3172-0796 on cisplatin sensitivity on H460 cells has also been examined.

4.2. Materials and Methods

4.2.1. Materials

DNA substrates were obtained from IDT (Coralville, IA) and prepared as described in section 2.2.3. Sequences may be found in Appendix A. Goat α-XPA primary antibody was obtained from Santa Cruz Biotechnology and goat α-rabbit secondary antibody was obtained from BioRad.

4.2.2. *In silic*o screen of small molecule libraries

In silico screening experiments were performed to identify molecules predicted to interact with XPA's DNA binding domain and have the potential to inhibit XPA function. The solution structure of XPA was obtained from the Protein Data Bank (1XPA). Analysis of this structure allowed for grids to be made to specifically target the DNA binding domain of XPA. *In silico* screnning of the ChemDiv small molecule libraries was performed by Jianyuan Liu (Indiana University School of Medicine). More than 200,000 compounds were docked, screened and then scored using a DOCK GRID scoring function, following which the top 2000 compounds were rescored by AMBER score function (to determine solvation free energy) incorporated in DOCK 6. The top 1000 compounds were then clustered and the docked compounds were visually examined using the UCSF Chimera ViewDock function. Approximately 100 compounds were determined for each library based on GRID and AMBER scores, drug likeness (Lipinski's Rule of Five), and with consideration of diversifying representative compounds and visual examination of the docked protein-compound complexes.

4.2.3. ELISA analysis of XPA binding to DNA

ELISAs were performed by binding 200 fmol per well of biotinylated 60-nt single-strand DNA in blocking buffer (2% BSA TBS-Tween) overnight on strepavadin coated plates (Roche Applied Science). Ten ng of purified XPA was then incubated with increasing concentrations of compound as indicated for 10 minutes at room temperature in blocking buffer and then added to wells containing DNA for 1 hour. Wells were then washed 3 x 5 minutes with blocking buffer after which primary anti-XPA antibody (Santa Cruz Biotechnology) (1:1000 in blocking buffer) was added for 30 minutes. Following incubation with primary antibody, wells were washed 3 x 5 minutes with blocking buffer followed by the addition of goat anti-rabbit secondary antibody (Biorad) (1:2500 in blocking buffer) for 30 minutes. Wells were then washed as described above and 100 µL TMB-ELISA reagent (Thermo Scientific) was added to each well. Kinetic reads were performed using a SpectraMax M5 spectrophotometer for 20 minutes at 30 second intervals at wavelengths 490 and 370 nm. The maximum mAbs/sec absorbance value was determined for each sample and represented as a percentage of the absorbance value obtained for the control treated sample. The averages represent the results of duplicate samples from 4 independent experiments. The IC_{50} and standard deviation were calculated by fitting the curve to a standard 2-parameter hyperbolic curve (equation f=(a*b)/(b+x)). ELISA assays for the cisplatin damaged and undamaged double-strand substrates were performed as described above, however, 10 and 50 ng of XPA were used, respectively.

4.2.4. Crystal violet analysis

H460 NSCLC cells were plated at a density of at 1 x 10^4 cells/cm^2 and incubated for 24 hours at 37°C and then treated with increasing concentrations of 3172-0796 or vehicle in the presence or absence of 2 µM cisplatin as indicated for 48 hours. Cells were also plated and treated with increasing concentrations of cisplatin with 100 µM 3172-0796 or vehicle for 48 hours. Following treatment, wells were washed with PBS and stained with crystal violet solution (0.75% Crystal Violet in 50% EtOH with 0.125% NaCl and 0.88% Formaldehyde) for 10 minutes. Following staining, cells were washed in dH_2O and the dye resolubilized with 1% SDS in PBS. Absorbance was read at 595 nm using a SpectraMax M5 spectrophotometer (Molecular Devices).

4.3. Results

Identification of inhibitors of XPA-DNA interactions

A high-throughput screen using fluorescence anisotropy as described for RPA was performed to identify SMIs of XPA (92). From screening 35,200 compounds, 58 were identified as positive hits (92). However, none of these compounds were verified in FP based secondary screening assays. We therefore chose to employ an *in silico* screen to identify potential SMIs of XPA in collaboration with Dr. J.T. Zhang's laboratory (Indiana University School of Medicine). The DNA binding domain of XPA (residues 98-219), was divided into regions including clefts consisting of residues 138-142, 165-171, 174 and 177-181 to be used as the targeted area for small molecule docking. Following the virtual screen, 63 identified compounds which may putatively inhibit XPA's DNA binding activity were examined by Dr. Tracy Neher using a secondary *in vitro* FP screening assay to test the ability of each compound to interact with XPA and

prevent DNA binding (data not shown). From this screen, 3 compounds were found to inhibit XPA's DNA binding activity, 3172-0796, 0917-0097 and 1080-0542 (Figure 27).

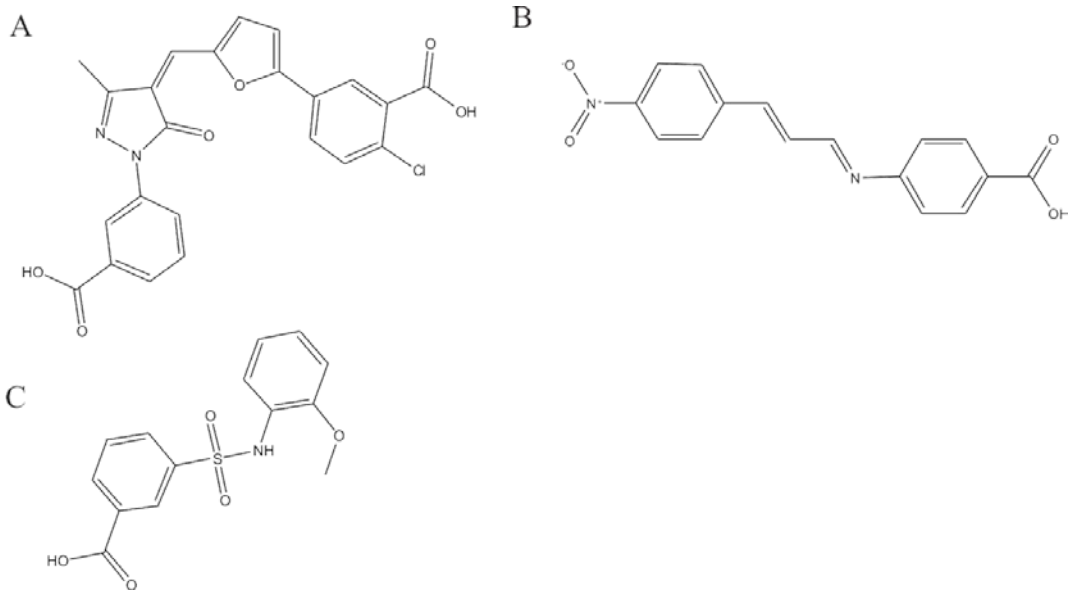

Figure 27. Structure of SMIs of XPA identified from fluorescence anisotropy. 27A. 3172-0796. 27B. 1080-0542. 27C. 0917-0097.

In vitro analysis of SMIs of XPA

In order to examine the *in vitro* activity of the 3 lead SMIs, an ELISA based assay was used to assess the ability of these compounds to inhibit XPA from binding DNA. ELISA analysis was employed in order to reduce the spectroscopic effects observed for some of the small molecules and as another assay to verify *in vitro* inhibitory activity. In order to determine the optimal concentration to measure inhibition of XPA's DNA binding activity, 500 fmol of biotin conjugated 60-nt ssDNA (TMN 1.1B) was bound to streptavidin coated ELISA plates and the binding activity of 10 and 100 ng of XPA was analyzed. Ten ng of purified XPA was found to result in ~50% of maximum XPA-DNA binding activity and this amount was used to examine inhibition of the XPA-DNA interaction. Ten ng of XPA was pre-incubated with either vehicle or each compound for ten minutes and then incubated with DNA for one hour. Following incubation, the plates were probed with α-XPA polyclonal antibody followed by goat α-rabbit secondary antibody. TMB ELISA reagent was then added to each well and kinetic reads were performed to quantify the amount of XPA bound to DNA (see section 4.2.3). Compound 3172-0796 was shown to have the highest *in vitro* inhibitory activity of XPA's DNA binding activity with an IC_{50} value of 20.9 ± 2.7 μM on ssDNA (Figure 29A). Compounds 0917-0097 and 1080-0542 were also examined to determine their ability to inhibit XPA's DNA binding activity, however, neither of these compounds showed *in vitro* inhibitory activity when examined by this assay, when tested up to 200 μM (Figure 28). The ability of 3172-0796 to inhibit XPA's DNA binding activity on undamaged 60-nt dsDNA (TMN 1.1B/1.2) was also examined revealing an IC_{50} value of 38.82 ± 14.24 μM (Figure 29B).

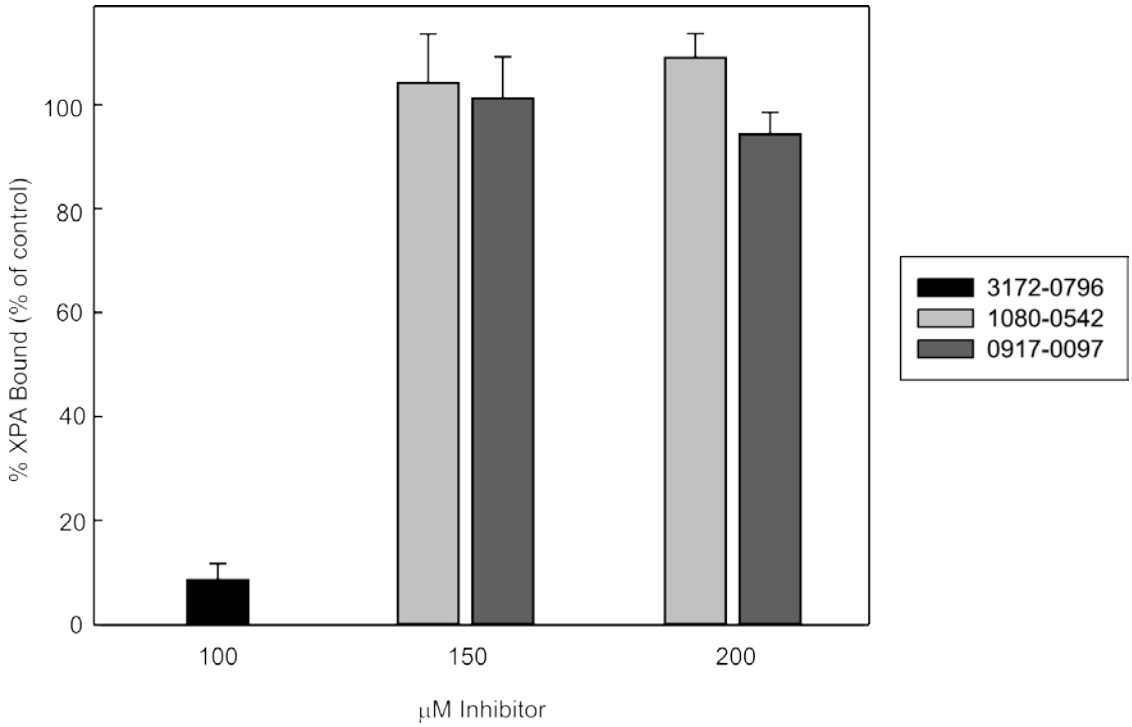

Figure 28. ELISA analysis of SMIs of XPA. Increasing concentrations of 0917-0097 and 1080-0542 and 100 μM 3172-0796 were incubated with 10 ng of XPA and then added to strepavidin coated ELISA plates prebound with biotinylated TMN 1.1 60-nt DNA as described in section 4.2.3. The amount of XPA bound to DNA was detected using an anti-XPA antibody and the results represent the average and standard deviation from at least 3 independent experiments.

Similarly, XPA was also found to be inhibited on a 60-nt double-strand substrate containing a single 1,2 cisplatin adduct (TMN 1.1B+Pt/1.2) with an IC_{50} value of 28.25 ± 7.85 μM (Figure 29C). T-test analysis of these IC_{50} values did not reveal a significant difference between them, indicating that 3172-0796 is interacting with XPA in a way that prevents its binding to various types of DNA substrates and also presents the possibility that XPA is interacting in the same way with these different substrates. XPA has been shown previously to bind to damaged DNA (122), however, the mode of interaction between XPA and damaged DNA has yet to be determined. Our results indicate that 3172-0796 is preventing XPA from binding to various DNA substrates in a similar way, which points to an attribute of XPA that is important for binding to ssDNA, dsDNA and 1,2 Pt damaged dsDNA. Identification of the interaction domain between 3172-0796 and XPA has the potential to identify the mode in which XPA is interacting with the DNA substrates examined.

Examination of XPA residues potentially important for interaction with 3172-0796

Examination of the structure of XPA docked with 3172-0796 reveals several amino acids that may contribute to the stable binding of this compound to XPA to result in inhibition of XPA's DNA binding activity. Among the amino acids examined within the DNA binding domain, four were identified as having putative interactions with 3172-0796 (Figure 30). Lysine 167 is in close proximity to the chlorine residue protruding from the benzoic acid and has the potential to have polar interactions with the compound at this position. Threonines 140 and 142 are positioned near the pyrazole and furan ring of 3172-0796 with the potential for hydrogen bonding activity.

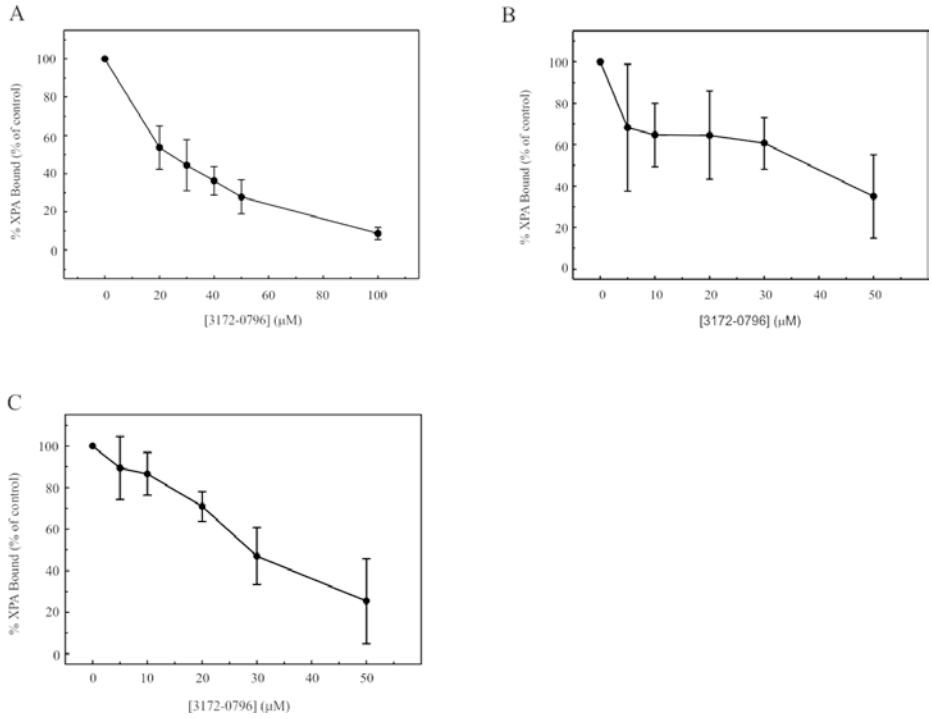

Figure 29. ELISA analysis of 3172-0796 on various DNA substrates. 29A. XPA was incubated with increasing concentrations of TDRL-505 as indicated and then added to strepavidin plates containing 500 fmol of ssDNA (TMN 1.1B). 29B. XPA was incubated with increasing concentrations of TDRL-505 as indicated and then added to strepavidin plates containing 500 fmol of dsDNA (TMN 1.1B/1.2). 29C. XPA was incubated with increasing concentrations of TDRL-505 as indicated and then added to strepavidin coated ELISA plates containing 500 fmol of dsDNA containing a 1,2 Pt lesion (TMN 1.1B+Pt/1.2). The results display the average and standard deviation of at least 3 independent experiments.

The fourth amino acid examined which may putatively stabilize the interaction between the XPA DNA binding domain and 3172-0796 is histidine 171. The potential interaction between this histidine and 3172-0796 is may be a hydrophobic interaction that occurs via ring stacking. Identification of potential sites of interaction allows for the design of more specific and potent inhibitors of XPA's DNA binding activity.

Cellular analysis of 3172-0796

The exclusive role of XPA in NER predicts that single-agent cellular inhibition of this protein would not display signal agent activity in the absence of agents that induce damage repaired by NER. However, the necessity of XPA in repairing cisplatin induced DNA damage indicates that its inhibition has the potential to increase cellular sensitivity to cisplatin. In order to examine if 3172-0796 increases cellular sensitivity to cisplatin, H460 cells were treated with a fixed concentration of cisplatin and increasing concentrations of 3172-0796. Following 48 hour incubation, cells were stained with crystal violet as described in section 4.2.4 to analyze cytotoxicity (Figure 31B). Interestingly, 3172-0796 did not increase cellular sensitivity to cisplatin as would be expected with inhibition of XPA. Cisplatin was also titrated with a fixed concentration of 3172-0796 which did not affect cell viability (Figure 31A). The lack of increased cytotoxicity indicates that under the conditions tested, 3172-0796 does not affect cellular processing and/or repair of cisplatin, which may be due to an ability of the compound to be taken up into cells or other cellular factors.

A

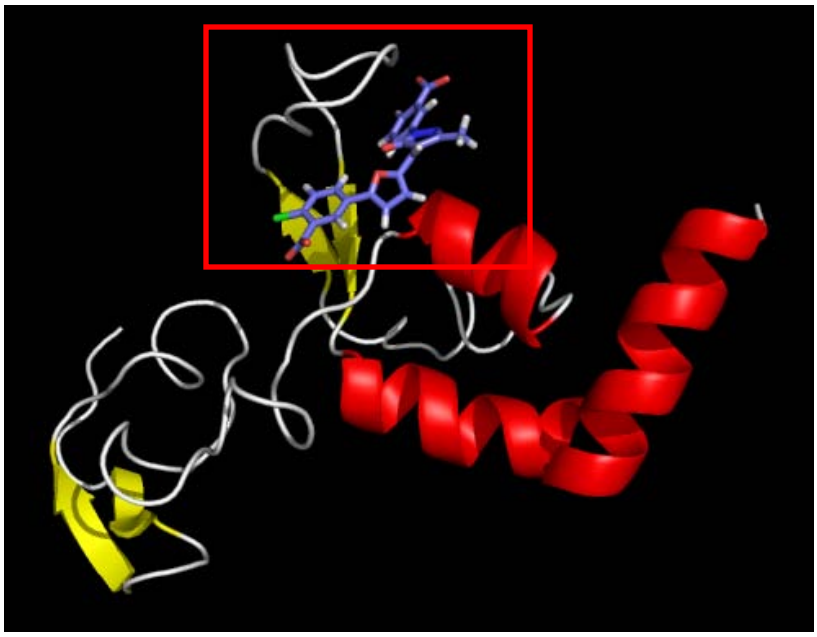

B

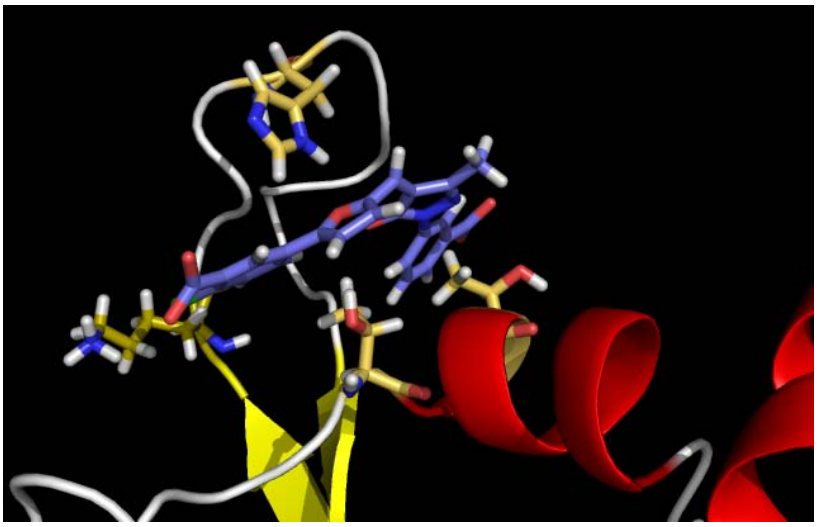

Figure 30. Modeling of 3172-0796 with XPA. 30A. The solution structure of XPA was modeled with 3172-0796 as described in section 4.2.2. The region of XPA that is blown up in 31B is outlined by the red square. 30B. A close up representation of XPA modeled with 3172-0796. Residues that are shown are, clockwise from far left, lysine 167, histidine 171 and threonines 140 and 142.

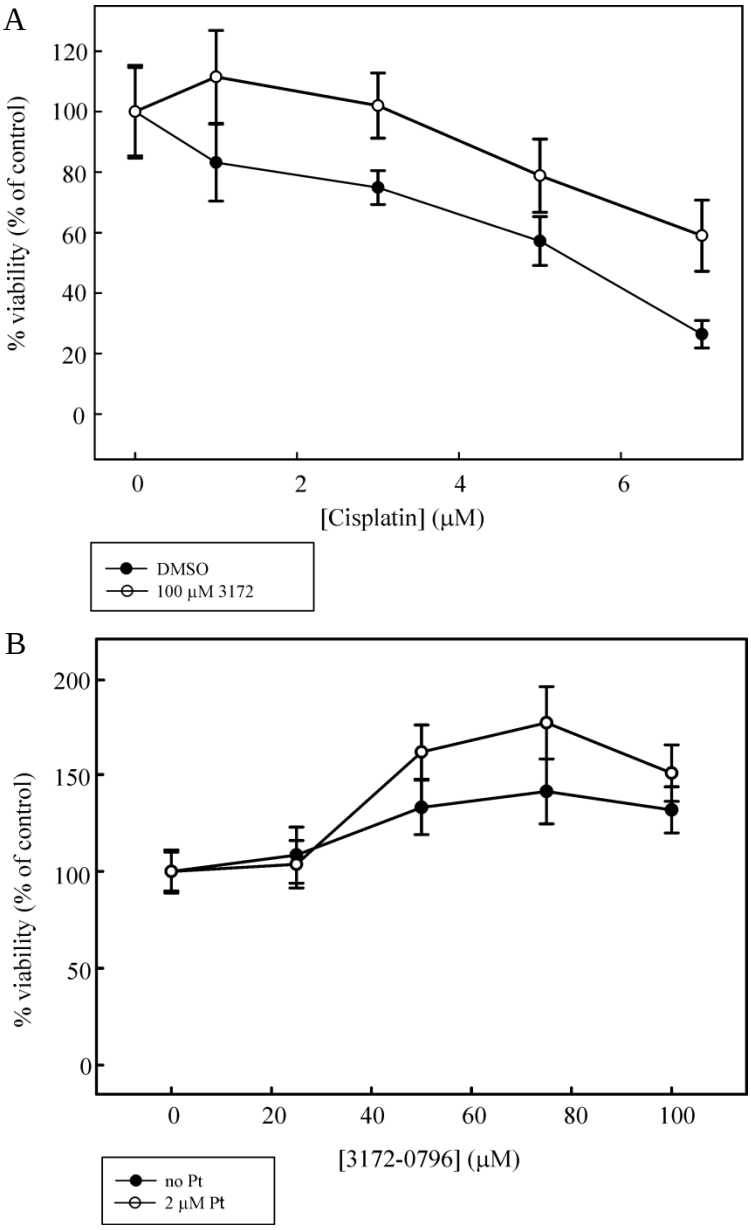

Figure 31. H460 cells treated with cisplatin in the presence and absence of 3172-0796. 31A. Cells were treated for 48 hours with increasing concentrations of cisplatin in the presence or absence of 100 μM 3172-0796. The results represent the average and standard deviation from at least 3 independent experiments. 31B. Cells were treated for 48 hours with increasing concentrations of 3172-0796 in the presence or absence of 2 μM cisplatin (IC_{30} value).

4.4. Discussion

Targeting proteins essential for DNA repair has been the goal of several lab groups in recent years. One of the drawbacks of targeting proteins active in DNA repair pathways is inhibition of the repair of normally incurred DNA damage such as that induced by ROS. Inhibition of these pathways has the potential to result in the development of secondary cancers and lead to high toxicity in non-malignant cells. Targeting XPA with SMIs presents an attractive approach for increasing cancer cell sensitivity to DNA damaging agents such as cisplatin due to the exclusive role of XPA in NER. Also, NER is an essential pathway for the repair of bulky DNA damage, the majority of which is induced by exposure to UV-light. Treatment of cancer patients with a drug targeting XPA is predicted to have few off-target cytotoxic effects when examining single-agent activity, a major advance and divergence from current chemotherapeutic treatment. Also, unlike targeted inhibition of other pathways, there is no known redundancy of NER, meaning that inhibition of this pathway will prevent the removal the majority of cisplatin-DNA lesions. One negative aspect to this approach is that global cellular sensitivity to cisplatin will increase, resulting in enhancement of the side-effects typically observed with cisplatin treatment including nephrotoxicity, ototoxicity, and gastrointestinal toxicities (123). However, the advantage of decreasing cancer cell growth may be worth the risk of generating these side-effects. Another advantage of inhibiting XPA is the lack of redundancy of this protein, preventing other cellular mechanisms from compensating for its loss. The identification of 3172-0796 allows for the investigation and development of additional XPA inhibitors in cellular and mouse models and a novel target for increasing cisplatin sensitivity.

Identification of residues potentially important for stabilizing the interaction of 3172-0796 with XPA has may allow us to elucidate how 3172-0796 is interacting with XPA and also allow us to further understand how XPA interacts with DNA. In addition, modeling of 3172-0796 within the DNA binding domain of XPA allows for the design of other SMIs that can inhibit XPA's DNA binding activity, leading to a library of SMIs to examine for *in vitro*, cellular, and *in vivo* activity.

5. Conclusion

The global application of inhibiting the repair of cisplatin lesions, both by targeting XPA and RPA is appealing due to the lack of the successful development of a protein inhibitor that is widespread for many cancer treatments. The interest in examining DNA repair both in the context of cancer development and response to chemotherapy has ascended to new levels, presumably because the underlying theme in all cancers is a change in genomic DNA that leads to mutant protein production and eventual uncontrolled cell proliferation. This coupled with the lack of novel effective chemotherapeutics has shifted the focus of the field somewhat to "get back to basics" and remember that although cancers develop as a result of various protein mutations, they all share the common theme of deleterious mutations that result in uncontrolled cell growth and proliferation. Bruce Alberts, the current editor-in-chief of *Science* magazine, recently commented on the importance of DNA repair in cancer: "…we can expect all cancer cells to be defective in some aspect of DNA repair that makes them unusually mutable. In principle, this weakness can be exploited by finding a drug that makes the original defect lethal to the cancerous cell instead of just destabilizing it, without causing harm to normal cells. The recent discovery of the strong therapeutic benefit of so-called

PARP inhibitors, when used on tumors with defects in one type of DNA repair pathway, provides a proof of principle for organizing a major new attack on cancer." (91). This statement highlights the direction that some individuals feel the field of cancer research should be moving and this shift has the potential to have a vast effect on cancer treatment.

Targeted inhibition, while successful in a small percentage of cancers such as chronic myeloid leukemia (CML), is limiting due to wide diversity of mutations that result in cancer development. CML is characterized by a chromosomal rearrangement that results in a constitutively active BCR-ABL kinase and successful remission of this cancer has been observed following treatment with imitanib, a potent and specific inhibitor of BCR-ABL kinase (124). For patients suffering with CML, the development of imitanib provides a treatment option that will allow for remission of their cancer and the ability to continue with their lives. However, for the thousands of patients that develop other cancers, imitanib is not an option for successful treatment.

The bulk of the development of novel chemotherapeutics has focused on targeted inhibition of proteins shown to play a role in cancer development. However, the ability of cancer cells to adapt and continue to thrive despite this inhibition limits the usefulness of approaching cancer therapy in this manner. Until cancer profiles have been clearly elucidated and physicians are able to consider inter-individual variations when choosing chemotherapeutic treatment, global cell killing seems to be the most effective way of stopping cancer growth, albeit with very undesirable side effects. Combination therapy to enhance the efficacy of current chemotherapeutics such as cisplatin may prove to be an

essential innovation in cancer treatment that will reduce the number of mortalities attributable to cancer.

APPENDIX A. DNA OLIGONUCLEOTIDES

dT_{12} (12-mer)

5′-TTTTTTTTTTTT-3′

SJC 1.5CXba (34-mer)

5′-CTAGAAAGGGGGAAGAAAGGGAAGAGGCCAGAGA-3′

SCS 1.1 (40-mer)

5′-TCATTACTACTCACTCTGTCGGCCATCGCTCTCTATTCCC-3′

SCS 1.2 (41-mer)

5′-GGGGAATAGAGAGCGATGGCCGACAGAGTGAGTAGTAATGA-3′

TMN 1.1B (60-mer)

5′-/5Biotin/CCCTTCTTTCTCTTCCCCCTCTCCTTCTTGGCCTCTTCCTTCC

CCTTCCCTTTCCTCCCC-3′

TMN 1.2 (60-mer)

5′-GGGGAGGAAAGGGAAGGGGAAGGAAGAGGCCAAGAAGGAGAGGG

GGAAGAGAAAGAAGG-3′

*Underlined bases indicate sites to induce cisplatin damage.

REFERENCE LIST

1 Collins,K., Jacks,T. and Pavletich,N.P. The cell cycle and cancer, Proc.Natl.Acad.Sci.U.S.A, *94:* 2776-2778, 1997.

2 Hanahan,D. and Weinberg,R.A. The hallmarks of cancer, Cell, *100:* 57-70, 2000.

3 Wold,M.S. Replication protein A: a heterotrimeric, single-stranded DNA- binding protein required for eukaryotic DNA metabolism. [Review] [190 refs], Annual Review of Biochemistry, *66:* 61-92, 1997.

4 Shuck,S.C., Short,E.A. and Turchi,J.J. Eukaryotic nucleotide excision repair: from understanding mechanisms to influencing biology, Cell Res., *18:* 64-72, 2008.

5 Hanna,N., Neubauer,M., Yiannoutsos,C., McGarry,R., Arseneau,J., Ansari,R., Reynolds,C., Govindan,R., Melnyk,A., Fisher,W., Richards,D., Bruetman,D., Anderson,T., Chowhan,N., Nattam,S., Mantravadi,P., Johnson,C., Breen,T., White,A. and Einhorn,L. Phase III study of cisplatin, etoposide, and concurrent chest radiation with or without consolidation docetaxel in patients with inoperable stage III non-small-cell lung cancer: the Hoosier Oncology Group and U.S. Oncology, J.Clin.Oncol., *26:* 5755-5760, 2008.

6 Sandler,A., Gray,R., Perry,M.C., Brahmer,J., Schiller,J.H., Dowlati,A., Lilenbaum,R. and Johnson,D.H. Paclitaxel-carboplatin alone or with bevacizumab for non-small-cell lung cancer, N.Engl.J.Med., *355:* 2542-2550, 2006.

7 Knudson,A.G., Jr. Mutation and cancer: statistical study of retinoblastoma, Proc.Natl.Acad.Sci.U.S.A, *68:* 820-823, 1971.

8 Badano,J.L. and Katsanis,N. Beyond Mendel: an evolving view of human genetic disease transmission, Nat.Rev.Genet., *3:* 779-789, 2002.

9 Stary,A. and Sarasin,A. The genetics of the hereditary xeroderma pigmentosum syndrome, Biochimie, *84:* 49-60, 2002.

10 David,S.S., O'Shea,V.L. and Kundu,S. Base-excision repair of oxidative DNA damage, Nature, *447:* 941-950, 2007.

11 Zegerman,P. and Diffley,J.F. DNA replication as a target of the DNA damage checkpoint, DNA Repair (Amst), *8:* 1077-1088, 2009.

12 Bell,S.P. and Dutta,A. DNA replication in eukaryotic cells, Annu.Rev.Biochem., *71:* 333-374, 2002.

13 Diffley,J.F. Regulation of early events in chromosome replication, Curr.Biol., *14:* R778-R786, 2004.

14 Cook,J.G. Replication licensing and the DNA damage checkpoint, Front Biosci., *14:* 5013-5030, 2009.

15 Waga,S. and Stillman,B. The DNA replication fork in eukaryotic cells, Annu.Rev.Biochem., *67:721-751:* 721-751, 1998.

16 Burgers,P.M.J. Eukaryotic DNA polymerases in DNA replication and DNA repai r, Chromosoma, *107:* 218-227, 1998.

17 Wang,J.C. Cellular roles of DNA topoisomerases: a molecular perspective, Nat.Rev.Mol.Cell Biol., *3:* 430-440, 2002.

18 Aladjem,M.I. Replication in context: dynamic regulation of DNA replication patterns in metazoans, Nat.Rev.Genet., *8:* 588-600, 2007.

19 Bruce Alberts,A.J.J.L.M.R.K.R.P.W. DNA Replication, Repair, and Recombination. *In*: AnonymousMolecular Biology of the Cell, Taylor and Francis Group: New York, 2007.

20 Zhou,B.B. and Elledge,S.J. The DNA damage response: putting checkpoints in perspective, Nature, *408:* 433-439, 2000.

21 Braun,K., Lao,Y., He,Z., Ingles,C. and Wold,M. Role of protein-protein interactions in the function of replication protein A (RPA): RPA modulates the activity of DNA polymerase alpha by multiple mechanisms, Biochemistry, *36:* 8443-8454, 1997.

22 Kinsella,T.J. Coordination of DNA mismatch repair and base excision repair processing of chemotherapy and radiation damage for targeting resistant cancers, Clin.Cancer Res., *15:* 1853-1859, 2009.

23 Horton,J.K. and Wilson,S.H. Hypersensitivity phenotypes associated with genetic and synthetic inhibitor-induced base excision repair deficiency, DNA Repair (Amst), *6:* 530-543, 2007.

24 Hitomi,K., Iwai,S. and Tainer,J.A. The intricate structural chemistry of base excision repair machinery: implications for DNA damage recognition, removal, and repair, DNA Repair (Amst), *6:* 410-428, 2007.

25 Ratnam,K. and Low,J.A. Current development of clinical inhibitors of poly(ADP-ribose) polymerase in oncology, Clin.Cancer Res., *13:* 1383-1388, 2007.

26 Francklyn,C.S. DNA polymerases and aminoacyl-tRNA synthetases: shared mechanisms for ensuring the fidelity of gene expression, Biochemistry, *47:* 11695-11703, 2008.

27 Li,G.M. Mechanisms and functions of DNA mismatch repair, Cell Res., *18:* 85-98, 2008.

28 Ramilo,C., Gu,L.Y., Guo,S.L., Zhang,X.P., Patrick,S.M., Turchi,J.J. and Li,G.M. Partial reconstitution of human DNA mismatch repair in vitro: Characterization of the role of human replication protein A, Mol.Cell Biol., *22:* 2037-2046, 2002.

29 Peltomaki,P. and Vasen,H.F. Mutations predisposing to hereditary nonpolyposis colorectal cancer: database and results of a collaborative study. The International Collaborative Group on Hereditary Nonpolyposis Colorectal Cancer, Gastroenterology, *113:* 1146-1158, 1997.

30 Fishel,R., Lescoe,M.K., Rao,M.R., Copeland,N.G., Jenkins,N.A., Garber,J., Kane,M. and Kolodner,R. The human mutator gene homolog MSH2 and its association with hereditary nonpolyposis colon cancer, Cell, *77:* 1, 1994.

31 Fishel,R. and Kolodner,R.D. Identification of mismatch repair genes and their role in the development of cancer, Curr.Opin.Genet.Dev., *5:* 382-395, 1995.

32 Laghi,L., Bianchi,P. and Malesci,A. Differences and evolution of the methods for the assessment of microsatellite instability, Oncogene, *27:* 6313-6321, 2008.

33 de la,C.A. Microsatellite instability, N.Engl.J.Med., *349:* 209-210, 2003.

34 Sancar,A. Excision repair in mammalian cells. [Review] [67 refs], J.Biol.Chem., *270:* 15915-15918, 1995.

35 Cleaver,J. DNA repair in Chinese hamster cells of different sensitivities to ultra-violet light, International Journal of Radiation Biology & Related Studies in Physics, Chemistry & Medicine, *16:* 277-285, 1969.

36 Cleaver,J. Defective repair replication of DNA in xeroderma pigmentosum, Nature, *218:* 652-656, 1968.

37 Einhorn,L.H. Curing metastatic testicular cancer, Proceedings of the National Academy of Sciences of the United States of America, *99:* 4592-4595, 2002.

38 Koberle,B., Masters,J.R.W., Hartley,J.A. and Wood,R.D. Defective repair of cisplatin-induced DNA damage caused by reduced XPA protein in testicular germ cell tumours, Current Biology, *9:* 273-276, 1999.

39 Welsh,C., Day,R., McGurk,C., Masters,J.R.W., Wood,R.D. and Koberle,B. Reduced levels of XPA, ERCC1 and XPF DNA repair proteins in testis tumor cell lines, Int.J.Cancer, *110:* 352-361, 2004.

40 Weterings,E. and Chen,D.J. The endless tale of non-homologous end-joining, Cell Res., *18:* 114-124, 2008.

41 Jeggo,P. and Lavin,M.F. Cellular radiosensitivity: how much better do we understand it?, Int.J.Radiat.Biol., *85:* 1061-1081, 2009.

42 Huertas,P. DNA resection in eukaryotes: deciding how to fix the break, Nat.Struct.Mol.Biol., *17:* 11-16, 2010.

43 Yun,M.H. and Hiom,K. CtIP-BRCA1 modulates the choice of DNA double-strand-break repair pathway throughout the cell cycle, Nature, *459:* 460-463, 2009.

44 Rose,P.G. Concurrent cisplatin-based radiotherapy and chemotherapy for locally advanced cervical cancer., N.Engl.J.Med., *341:* 708, 1999.

45 Boeckman,H.J., Trego,K.S. and Turchi,J.J. Cisplatin sensitizes cancer cells to ionizing radiation via inhibition of nonhomologous end joining, Mol.Cancer Res., *3:* 277-285, 2005.

46 Lees-Miller,S.P., Godbout,R., Chan,D.W., Weinfeld,M., Day,R.S., Barron,G.M. and Allalunis-Turner,J. Absence of p350 subunit of DNA-activated protein kinase from a radiosensitive human cell line, Science, *267:* 1183-1185, 1995.

47 Peralta-Leal,A., Rodriguez-Vargas,J.M., guilar-Quesada,R., Rodriguez,M.I., Linares,J.L., de Almodovar,M.R. and Oliver,F.J. PARP inhibitors: new partners in the therapy of cancer and inflammatory diseases, Free Radic.Biol.Med., *47:* 13-26, 2009.

48 Ashworth,A. A synthetic lethal therapeutic approach: poly(ADP) ribose polymerase inhibitors for the treatment of cancers deficient in DNA double-strand break repair, J.Clin.Oncol., *26:* 3785-3790, 2008.

49 Quinn,J.E., Carser,J.E., James,C.R., Kennedy,R.D. and Harkin,D.P. BRCA1 and implications for response to chemotherapy in ovarian cancer, Gynecol.Oncol., *113:* 134-142, 2009.

50 Wang,W. and Figg,W.D. Secondary BRCA1 and BRCA2 alterations and acquired chemoresistance, Cancer Biol.Ther., *7:* 1004-1005, 2008.

51 Bolderson,E., Richard,D.J., Zhou,B.B. and Khanna,K.K. Recent advances in cancer therapy targeting proteins involved in DNA double-strand break repair, Clin.Cancer Res., *15:* 6314-6320, 2009.

52 Bochkarev,A. and Bochkareva,E. From RPA to BRCA2: lessons from single-stranded DNA binding by the OB-fold, Current Opinion in Structural Biology, *14:* 36-42, 2004.

53 Fanning,E., Klimovich,V. and Nager,A.R. A dynamic model for replication protein A (RPA) function in DNA processing pathways, Nucleic Acids Res., *34:* 4126-4137, 2006.

54 Bochkarev,A., Pfuetzner,R.A., Edwards,A.M. and Frappier,L. Structure of the single-stranded-DNA-binding domain of replication protein A bound to DNA, Nature, *385:* 176-181, 1997.

55 Bastin-Shanower,S.A. and Brill,S.J. Functional analysis of the four DNA binding domains of replication protein A - The role of RPA2 in ssDNA binding, J.Biol.Chem., *276:* 36446-36453, 2001.

56 Henricksen,L.A., Umbricht,C.B. and Wold,M.S. Recombinant replication protein A: expression, complex formation, and functional characterization [published erratum appears in J Biol Chem 1994 Jun 10;269(23):16519], J.Biol.Chem., *269:* 11121-11132, 1994.

57 Georgaki,A., Strack,B., Podust,V. and Hubscher,U. DNA unwinding activity of replication protein A, FEBS Lett., *308:* 240-244, 1992.

58 Georgaki,A. and Hubscher,U. DNA unwinding by replication protein A is a property of the 70 kDa subunit and is facilitated by phosphorylation of the 32 kDa subunit, Nucleic Acids Res., *21:* 3659-3665, 1993.

59 Clugston,C.K., McLaughlin,K., Kenny,M.K. and Brown,R. Binding of human single-stranded DNA binding protein to DNA damaged by the anticancer drug cis-diamminedichloroplatinum (II), Cancer Res., *52:* 6375-6379, 1992.

60 Patrick,S.M. and Turchi,J.J. Human Replication Protein A Preferentially Binds Duplex DNA Damaged with Cisplatin, Biochemistry, *37:* 8808-8815, 1998.

61 Li,L., Lu,X., Peterson,C.A. and Legerski,R.J. An interaction between the DNA repair factor XPA and replication protein A appears essential for nucleotide excision repair, Mol.Cell Biol., *15:* 5396-5402, 1995.

62 Lee,S.H., Kim,D.K. and Drissi,R. Human xeroderma pigmentosum group A protein interacts with human replication protein A and inhibits DNA replication, J.Biol.Chem., *270:* 21800-21805, 1995.

63 He,Z., Henricksen,L.A., Wold,M.S. and Ingles,C.J. RPA involvement in the damage-recognition and incision steps of nucleotide excision repair, Nature, *374:* 566-569, 1995.

64 Matsunaga,T., Park,C.H., Bessho,T., Mu,D. and Sancar,A. Replication protein A confers structure-specific endonuclease activities to the XPF-ERCC1 and XPG subunits of human DNA repair excision nuclease, J.Biol.Chem., *271:* 11047-11050, 1996.

65 de Laat,W.L., Appeldoorn,E., Sugasawa,K., Weterings,E., Jaspers,N.G. and Hoeijmakers,J.H. DNA-binding polarity of human replication protein A positions nucleases in nucleotide excision repair, Genes & Development, *12:* 2598-2609, 1998.

66 Dornreiter,I., Erdile,L.F., Gilbert,I.U., Vonwinkler,D., Kelly,T.J. and Fanning,E. Interaction of DNA polymerase-alpha primase with cellular replication protein-A and SV40-T antigen, EMBO J., *11:* 769-776, 1992.

67 Asahina,H., Kuraoka,I., Shirakawa,M., Morita,E.H., Miura,N., Miyamoto,I., Ohtsuka,E., Okada,Y. and Tanaka,K. The XPA protein is a zinc metalloprotein with an ability to recognize various kinds of DNA damage, Mutat.Res., *315:* 229-237, 1994.

68 Jones,C.J. and Wood,R.D. Preferential binding of the xeroderma pigmentosum group A complementing protein to damaged DNA, Biochemistry, *32:* 12096-12104, 1993.

69 Camenisch,U., Dip,R., Vitanescu,M. and Naegeli,H. Xeroderma pigmentosum complementation group A protein is driven to nucleotide excision repair sites by the electrostatic potential of distorted DNA, DNA Repair (Amst), 2007.

70 Ikegami,T., Kuraoka,I., Saijo,M., Kodo,N., Kyogoku,Y., Morikawa,K., Tanaka,K. and Shirakawa,M. Solution structure of the DNA- and RPA-binding domain of the human repair factor XPA, Nature Structural Biology, *5:* 701-706, 1998.

71 Morita,E.H., Ohkubo,T., Kuraoka,I., Shirakawa,M., Tanaka,K. and Morikawa,K. Implications of the zinc-finger motif found in the DNA-binding domain of the human XPA protein, Genes to Cells, *1:* 437-442, 1996.

72 Camenisch,U., Dip,R., Schumacher,S.B., Schuler,B. and Naegeli,H. Recognition of helical kinks by xeroderma pigmentosum group A protein triggers DNA excision repair, Nat.Struct.Mol.Biol., *13:* 278-284, 2006.

73 Hermanson-Miller,I.L. and Turchi,J.J. Strand-specific binding of RPA and XPA to damaged duplex DNA, Biochemistry, *41:* 2402-2408, 2002.

74 Patrick,S.M. and Turchi,J.J. Xeroderma pigmentosum complementation group A protein (XPA) modulates RPA-DNA interactions via enhanced complex stability and inhibition of strand separation activity, J.Biol.Chem., *277:* 16096-16101, 2002.

75 Rajski,S.R. and Williams,R.M. DNA Cross-Linking Agents as Antitumor Drugs, Chem.Rev., *98:* 2723-2796, 1998.

76 Chalmers,A.J. The potential role and application of PARP inhibitors in cancer treatment, Br.Med.Bull., *89:* 23-40, 2009.

77 Calabrese,C.R., Almassy,R., Barton,S., Batey,M.A., Calvert,A.H., Canan-Koch,S., Durkacz,B.W., Hostomsky,Z., Kumpf,R.A., Kyle,S., Li,J., Maegley,K., Newell,D.R., Notarianni,E., Stratford,I.J., Skalitzky,D., Thomas,H.D., Wang,L.Z., Webber,S.E., Williams,K.J. and Curtin,N.J. Anticancer chemosensitization and radiosensitization by the novel poly(ADP-ribose) polymerase-1 inhibitor AG14361, J.Natl.Cancer Inst., *96:* 56-67, 2004.

78 Pommier,Y. DNA topoisomerase I inhibitors: chemistry, biology, and interfacial inhibition, Chem.Rev., *109:* 2894-2902, 2009.

79 Liu,L.F. DNA topoisomerase poisons as antitumor drugs, Annu.Rev.Biochem., *58:* 351-375, 1989.

80 Nichols,C.R., Breeden,E.S., Loehrer,P.J., Williams,S.D. and Einhorn,L.H. Secondary leukemia associated with a conventional dose of etoposide: review of serial germ cell tumor protocols, J.Natl.Cancer Inst., *85:* 36-40, 1993.

81 Rosenberg,B., Vancamp,L. and KRIGAS,T. INHIBITION OF CELL DIVISION IN ESCHERICHIA COLI BY ELECTROLYSIS PRODUCTS FROM A PLATINUM ELECTRODE, Nature, *205:* 698-699, 1965.

82 Rosenberg,B., Vancamp,L., Trosko,J. and Mansour,V. Platinum compounds: a new class of potent antitumour agents, Nature, *222:* 385-386, 1969.

83 Rosenberg,B. and Vancamp,L. The successful regression of large solid sarcoma 180 tumors by platinum compounds, Cancer Res., *30:* 1799-1802, 1970.

84 Jamieson,E.R. and Lippard,S.J. Structure, Recognition, and Processing of Cisplatin-DNA Adducts, Chem.Rev., *99:* 2467-2498, 1999.

85 Kartalou,M. and Essigmann,J.M. Mechanisms of resistance to cisplatin, Mutation Research-Fundamental and Molecular Mechanisms of Mutagenesis, *478:* 23-43, 2001.

86 Zlatanova,J., Yaneva,J. and Leuba,S.H. Proteins that specifically recognize cisplatin-damaged DNA: a clue to anticancer activity of cisplatin, FASEB J., *12:* 791-799, 1998.

87 Zamble,D.B. and Lippard,S.J. Cisplatin and DNA repair in cancer chemotherapy. [Review] [33 refs], Trends Biochem.Sci., *20:* 435-439, 1995.

88 Sandler,A., Gray,R., Perry,M.C., Brahmer,J., Schiller,J.H., Dowlati,A., Lilenbaum,R. and Johnson,D.H. Paclitaxel-carboplatin alone or with bevacizumab for non-small-cell lung cancer, N.Engl.J.Med., *355:* 2542-2550, 2006.

89 Blum,R. and Kloog,Y. Tailoring Ras-pathway--inhibitor combinations for cancer therapy, Drug Resist.Updat., *8:* 369-380, 2005.

90 Davies,H., Bignell,G.R., Cox,C., Stephens,P., Edkins,S., Clegg,S., Teague,J., Woffendin,H., Garnett,M.J., Bottomley,W., Davis,N., Dicks,E., Ewing,R., Floyd,Y., Gray,K., Hall,S., Hawes,R., Hughes,J., Kosmidou,V., Menzies,A., Mould,C., Parker,A., Stevens,C., Watt,S., Hooper,S., Wilson,R., Jayatilake,H., Gusterson,B.A., Cooper,C., Shipley,J., Hargrave,D., Pritchard-Jones,K., Maitland,N., Chenevix-Trench,G., Riggins,G.J., Bigner,D.D., Palmieri,G., Cossu,A., Flanagan,A., Nicholson,A., Ho,J.W., Leung,S.Y., Yuen,S.T., Weber,B.L., Seigler,H.F., Darrow,T.L., Paterson,H., Marais,R., Marshall,C.J., Wooster,R., Stratton,M.R. and Futreal,P.A. Mutations of the BRAF gene in human cancer, Nature, *417:* 949-954, 2002.

91 Alberts,B. Redefining cancer research, Science, *325:* 1319, 2009.

92 Turchi,J.J., Shuck,S.C., Short,E.A. and Andrews,B.J. Targeting Nucletode Exicsion Repair as a Mechanism to Increase Cisplatain Efficacy. *In*: A. Bonetti, R. Leone, F. M. Muggia and S. B. Howell (eds.), Platinum and Other Heavy Metal Compounds in Cancer Chemotherapy, pp. 177-188. Humana Press: New York, 2009.

93 Jin,Z., Dicker,D.T. and el-Deiry,W.S. Enhanced sensitivity of G1 arrested human cancer cells suggests a novel therapeutic strategy using a combination of simvastatin and TRAIL, Cell Cycle, *1:* 82-89, 2002.

94 Dodson,G.E., Shi,Y. and Tibbetts,R.S. DNA replication defects, spontaneous DNA damage, and ATM-dependent checkpoint activation in replication protein A-deficient cells, J.Biol.Chem., *279:* 34010-34014, 2004.

95 Patrick,S.M., Oakley,G.G., Dixon,K. and Turchi,J.J. DNA Damage Induced Hyperphosphorylation of Replication Protein A. 2. Characterization of DNA Binding Activity, Protein Interactions, and Activity in DNA Replication and Repair, Biochemistry, *44:* 8438-8448, 2005.

96 Patrick,S.M. and Turchi,J.J. Stopped-flow kinetic analysis of replication protein A-binding DNA - Damage recognition and affinity for single-stranded DNA reveal differential contributions of k(on) and k(off) rate constants, J.Biol.Chem., *276:* 22630-22637, 2001.

97 Dispersyn,G., Nuydens,R., Connors,R., Borgers,M. and Geerts,H. Bcl-2 protects against FCCP-induced apoptosis and mitochondrial membrane potential depolarization in PC12 cells, Biochim.Biophys.Acta, *1428:* 357-371, 1999.

98 Palermo,C.M., Bennett,C.A., Winters,A.C. and Hemenway,C.S. The AF4-mimetic peptide, PFWT, induces necrotic cell death in MV4-11 leukemia cells, Leuk.Res., *32:* 633-642, 2008.

99 Van,S.S., Kyula,J., Kelly,D.M., Karaiskou-McCaul,A., Stokesberry,S.A., Van,C.E., Longley,D.B. and Johnston,P.G. Chemotherapy-induced epidermal growth factor receptor activation determines response to combined gefitinib/chemotherapy treatment in non-small cell lung cancer cells, Mol.Cancer Ther., *5:* 1154-1165, 2006.

100 Haring,S.J., Mason,A.C., Binz,S.K. and Wold,M.S. Cellular functions of human RPA1. Multiple roles of domains in replication, repair, and checkpoints, J.Biol.Chem., *283:* 19095-19111, 2008.

101 Chou,T.C., Talalay,P. and . Quantitative-analysis of dose-effect relationships - the combined effects of multiple-drugs or enzyme-inhibitors, Advances in Enzyme Regulation, *22:* 27-55, 1984.

102 Robison,J.G., Bissler,J.J. and Dixon,K. Replication protein A is required for etoposide-induced assembly of MRE11/RAD50/NBS1 complex repair foci, Cell Cycle, *6:* 2408-2416, 2007.

103 Robison,J.G., Dixon,K. and Bissler,J.J. Cell cycle-and proteasome-dependent formation of etoposide-induced replication protein A (RPA) or Mre11/Rad50/Nbs1 (MRN) complex repair foci, Cell Cycle, *6:* 2399-2407, 2007.

104 Iftode,C., Daniely,Y. and Borowiec,J. Replication protein A (RPA): the eukaryotic SSB, Crit.Rev.Biochem.Molec.Biol., *34:* 141-180, 1999.

105 Araujo,S.J., Tirode,F., Coin,F., Pospiech,H., Syvaoja,J.E., Stucki,M., Hubscher,U., Egly,J.M. and Wood,R.D. Nucleotide excision repair of DNA with recombinant human proteins: definition of the minimal set of factors, active forms of TFIIH, and modulation by CAK, Genes & Development, *14:* 349-359, 2000.

106 Sancar,A., Lindsey-Boltz,L.A., Unsal-Kacmaz,K. and Linn,S. Molecular mechanisms of mammalian DNA repair and the DNA damage checkpoints, Annual Review of Biochemistry, *73:* 39-85, 2004.

107 Perrault,R., Cheong,N., Wang,H.C., Wang,H.Y. and Iliakis,G. RPA facilitates rejoining of DNA double-strand breaks in an in vitro assay utilizing genomic DNA as substrate, Int.J.Radiat.Biol., *77:* 593-607, 2001.

108 Dip,R., Camenisch,U. and Naegeli,H. Mechanisms of DNA damage recognition and strand discrimination in human nucleotide excision repair, Dna Repair, *3:* 1409-1423, 2004.

109 Wang,L.C., Stone,S., Hoatlin,M.E. and Gautier,J. Fanconi anemia proteins stabilize replication forks, DNA Repair (Amst), *7:* 1973-1981, 2008.

110 Manthey,K.C., Opiyo,S., Glanzer,J.G., Dimitrova,D., Elliott,J. and Oakley,G.G. NBS1 mediates ATR-dependent RPA hyperphosphorylation following replication-fork stall and collapse, J.Cell Sci., *120:* 4221-4229, 2007.

111 Baldwin,E.L. and Osheroff,N. Etoposide, topoisomerase II and cancer, Curr.Med.Chem.Anticancer Agents, *5:* 363-372, 2005.

112 Ishimi,Y., Sugasawa,K., Hanaoka,F., Eki,T. and Hurwitz,J. Topoisomerase II plays an essential role as a swivelase in the late stage of SV40 chromosome replication in vitro, J.Biol.Chem., *267:* 462-466, 1992.

113 Wang,X. and Haber,J.E. Role of Saccharomyces single-stranded DNA-binding protein RPA in the strand invasion step of double-strand break repair, Plos Biology, *2:* 104-112, 2004.

114 Stauffer,M.E. and Chazin,W.J. Physical interaction between replication protein A and Rad51 promotes exchange on single-stranded DNA, J.Biol.Chem., *279:* 25638-25645, 2004.

115 Goodsell,D.S., Morris,G.M. and Olson,A.J. Automated docking of flexible ligands: applications of AutoDock, J.Mol.Recognit., *9:* 1-5, 1996.

116 Bochkareva,E., Belegu,V., Korolev,S. and Bochkarev,A. Structure of the major single-stranded DNA-binding domain of replication protein A suggests a dynamic mechanism for DNA binding, EMBO J., *20:* 612-618, 2001.

117 Wyka,I.M., Dhar,K., Binz,S.K. and Wold,M.S. Replication protein A interactions with DNA: Differential binding of the core domains and analysis of the DNA interaction surface, Biochemistry, *42:* 12909-12918, 2003.

118 Walther,A., Gomes,X., Lao,Y., Lee,C. and Wold,M. Replication protein A interactions with DNA. 1. Functions of the DNA-binding and zinc-finger domains of the 70-kDa subunit, Biochemistry, *38:* 3963-3973, 1999.

119 Stigger,E., Drissi,R. and Lee,S.H. Functional analysis of human replication protein a in nucle otide excision repair, J.Biol.Chem., *273:* 9337-9343, 1998.

120 Patrick,S.M. and Turchi,J.J. Replication Protein A (RPA) Binding to Duplex Cisplatin-damaged DNA Is Mediated through the Generation of Single-stranded DNA, J.Biol.Chem., *274:* 14972-14978, 1999.

121 Matsuda,T., Saijo,M., Kuraoka,I., Kobayashi,T., Nakatsu,Y., Nagai,A., Enjoji,T., Masutani,C., Sugasawa,K., Hanaoka,F., Yasui,A. and Tanaka,K. DNA repair protein XPA binds replication protein A (RPA), J.Biol.Chem., *270:* 4152-4157, 1995.

122 Gunz,D., Hess,M. and Naegeli,H. Recognition of DNA adducts by human nucleotide excision repair. Evidence for a thermodynamic probing mechanism, J.Biol.Chem., *271:* 25089-25098, 1996.

123 Muggia,F. Platinum compounds 30 years after the introduction of cisplatin: implications for the treatment of ovarian cancer, Gynecol.Oncol., *112:* 275-281, 2009.

124 Druker,B.J., Guilhot,F., O'Brien,S.G., Gathmann,I., Kantarjian,H., Gattermann,N., Deininger,M.W., Silver,R.T., Goldman,J.M., Stone,R.M., Cervantes,F., Hochhaus,A., Powell,B.L., Gabrilove,J.L., Rousselot,P., Reiffers,J., Cornelissen,J.J., Hughes,T., Agis,H., Fischer,T., Verhoef,G., Shepherd,J., Saglio,G., Gratwohl,A., Nielsen,J.L., Radich,J.P., Simonsson,B., Taylor,K., Baccarani,M., So,C., Letvak,L. and Larson,R.A. Five-year follow-up of patients receiving imatinib for chronic myeloid leukemia, N.Engl.J.Med., *355:* 2408-2417, 2006.

CURRICULUM VITAE

Sarah C. Shuck

EDUCATION

Indiana University, Bloomington, IN
1999-2003
B.S. in Biology

Indiana University, Indianapolis IN
2003-2005
M.S. in Cellular and Integrative Physiology
Advisor – Frank A. Witzmann

Indiana University, Indianapolis IN
2005-2010
Ph.D. in Biochemistry and Molecular Biology
Dissertation: Identification of novel small molecule inhibitors of proteins required for genomic maintenance and stability.
Chair/Advisor – John J. Turchi
Committee Members – Frank A. Witzmann, Mark E. Kelley, Tom D. Hurley

PUBLICATIONS (Peer-Reviewed)

1) **Shuck SC**, Short EA, Turchi JJ. (2008) Eukaryotic nucleotide excision repair: from understanding mechanisms to influencing biology. *Cell Res.* 2008 Jan;18(1):64-72.

2) Turchi JJ, **Shuck SC**, Short EA, and Andrews BJ. (2009) Targeting nucletode excision repair as a mechanism to increase cisplatin efficacy, in *Platinum and Other Heavy Metal Compounds in Cancer Chemotherapy*, A.Bonetti, R.Leone, F.M.Muggia, and S.B.Howell, eds. (New York: Humana Press), pp. 177-188.

3) **Shuck SC** and Turchi JJ. (2010) Targeted inhibition of RPA reveals cytotoxic activity, synergy with chemotherapeutic DNA damaging agents and insight into cellular function. *Cancer Research.* 2010 Apr 15;70(8):3189-98.

4) **Shuck SC***, Neher TM*, Liu J, Zhang JT, and Turchi JJ. (2010) Molecular modeling, *in vitro*, and cellular analysis of small molecule inhibitors of XPA. *Submitted* *Authors contributed equally

ABSTRACTS (NON-PEER REVIEWED) (*Presenting author)

National/International

1) **Shuck SC***, Short EA, and Turchi JJ. (2007) Inhibition of Nucleotide Excision Repair Leads to Cell Cycle Arrest and Decreased Cell Survival in Lung and Ovarian Cancer Cell Lines. The 9th Annual Midwest DNA Repair Symposium. Columbus, OH

2) **Shuck SC***, Short EA, and Turchi JJ. (2007) Targeting Nucleotide Excision Repair as a Mechanism to Increase Cisplatin Efficacy. The 10th International Symposium on Platinum Coordinating Compounds. Verona, Italy

3) Turchi JJ*, **Shuck SC**, Jalal, SI and Short EA. (2008) DNA Repair Capacity to Predict and Target Chemoresistant Small Cell Lung Cancer. Flight Attendants Medical Research Institute. Boston, MA

4) **Shuck SC*** and Turchi JJ. (2009) The Effect of a Small Molecule Inhibitor of Replication Protein A (TDRL-505) on DNA Binding, Cellular Function and Platinum Sensitivity. The American Association for Cancer Research 100th Annual Meeting. Denver, CO

5) Jalal SI*, **Shuck SC** and Turchi JJ. (2009) Determination of Mechanisms of Chemotherapy Synergy in Small Cell Lung Cancer Cell Lines. The American Association for Cancer Research 100th Annual Meeting. Denver, CO

6) **Shuck SC*** and Turchi JJ. (2009) The Effect of a Small Molecule Inhibitor of Replication Protein A (TDRL-505) on DNA Binding, Cellular Function and Platinum Sensitivity. The 11th Annual Midwest DNA Repair Symposium. Ann Arbor, MI.

7) **Shuck SC*** and Turchi JJ. (2009) Small Molecule Inhibition of Replication Protein A Induces Cell Cycle Arrest, Decreased Viability, and Synergizes with Cisplatin. The American Society for Microbiology 4th International DNA Repair and Mutagenesis Symposium. Whistler, British Columbia

8) Turchi JJ* and **Shuck SC**. (2010) Small molecule inhibition of Replication Protein A blocks cellular proliferation, induces cell death and enhances sensitivity to chemotherapeutic DNA-damaging agents. 8th International Symposium on Targeted Anticancer Therapies. Bethesda, MD

9) Turchi JJ* and **Shuck SC**. (2010) Small molecule inhibition of Replication Protein A blocks cellular proliferation, induces cell death and enhances sensitivity to chemotherapeutic DNA-damaging agents. icBEST 2010. Beijing, China

University Affiliated

1) **Shuck SC***, Andrews BJ and Turchi JJ. (2006) Inhibition of Replication Protein A Leads to Cell Cycle Arrest and Decreased Cell Survival in Lung and Ovarian Cancer Cell Lines. Biochemistry Retreat. Indianapolis, IN.

2) **Shuck SC***, Short EA and Turchi JJ. (2007) Inhibition of Replication Protein A Leads to Cell Cycle Arrest and Decreased Cell Survival in Lung and Ovarian Cancer Cell Lines. IU School of Medicine Cancer Research Day. Indianapolis, IN.

3) **Shuck SC***, Short EA and Turchi JJ. (2007) Inhibition of Replication Protein A Leads to Cell Cycle Arrest and Decreased Cell Survival in Lung and Ovarian Cancer Cell Lines. Biochemistry Retreat. Indianapolis, IN.

4) **Shuck SC***, Short EA, Montgomery JS and Turchi JJ. (2008) The Effect of Small Molecule Inhibitors of Replication Protein A on DNA Binding, Cellular Function and Platinum Sensitivity. Biochemistry Retreat. Indianapolis, IN.

5) **Shuck SC***, Short EA, Montgomery JS and Turchi JJ. (2008) The Effect of Small Molecule Inhibitors of Replication Protein A on DNA Binding, Cellular Function and Platinum Sensitivity. IU School of Medicine Cancer Research Day. Indianapolis, IN.

RESEARCH ORAL PRESENTATIONS (^Selected from Abstracts)

1) **Shuck SC*** and Turchi JJ. (2007) Inhibition of Replication Protein A Leads to Cell Cycle Arrest and Decreased Cell Survival in Lung and Ovarian Cancer Cell Lines. Hematology/Oncology Conference. Indianapolis, IN

2) **Shuck SC***^ and Turchi JJ. (2008) The Effect of Small Molecule Inhibitors of Replication Protein A on DNA Binding, Cellular Function and Platinum Sensitivity. 10^{th} annual Midwest DNA Repair Symposium. Pittsburgh, PA

PROFESSIONAL MEMBERSHIPS AND ACTIVITIES

Indiana University School of Medicine Lung Cancer Working Group	2006 - Present
American Association for the Advancement of Science	2006 - Present
American Society of Microbiology	2008 - Present

Invited and hosted IUSOM Department of Biochemistry Student Invited Speaker, 2008
Joanna Groden, Professor, The Ohio State University
Genetic Stability and Cancer Predisposition

TEACHING EXPERIENCE

Undergraduate Teaching Instructor, Indiana University, Bloomington, IN
Evolution and Diversity, 2000-2001

AWARDS

Indiana University School of Medicine Student Travel Award, 2007
The 10th International Symposium on Platinum Coordinating Compounds.
Verona, Italy